

AD-A270 150



WL-TR-93-3068



**PROCEDURES AND DESIGN DATA FOR THE
FORMULATION OF AIRCRAFT CONFIGURATIONS**

**THOMAS R. SIERON
DUDLEY FIELDS
A. WAYNE BALDWIN
DAVID W. ADAMCZAK**

**AEROTHERMODYNAMICS AND FLIGHT
MECHANICS RESEARCH BRANCH
AEROMECHANICS DIVISION**



August 1993

FINAL REPORT FOR THE PERIOD JANUARY 1992 - JUNE 1993

APPROVED FOR PUBLIC RELEASE; DISTRIBUTION UNLIMITED

**FLIGHT DYNAMICS DIRECTORATE
WRIGHT LABORATORY
AIR FORCE MATERIEL COMMAND
WRIGHT PATTERSON AFB, OHIO 45433-7913**

93-23106




93 10 1 2 14

NOTICE

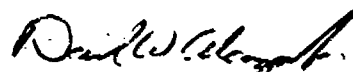
WHEN GOVERNMENT DRAWINGS, SPECIFICATIONS, OR OTHER DATA ARE USED FOR ANY PURPOSE OTHER THAN IN CONNECTION WITH A DEFINITELY GOVERNMENT-RELATED PROCUREMENT, THE UNITED STATES GOVERNMENT INCURS NO RESPONSIBILITY OR ANY OBLIGATION WHATSOEVER, THE FACT THAT THE GOVERNMENT MAY HAVE FORMULATED OR IN ANY WAY SUPPLIED THE SAID DRAWINGS, SPECIFICATIONS, OR OTHER DATA, IS NOT TO BE REGARDED BY IMPLICATION, OR OTHERWISE IN ANY MANNER CONSTRUED, AS LICENSING THE HOLDER, OR ANY OTHER PERSON OR CORPORATION; OR AS CONVEYING ANY RIGHTS OR PERMISSION TO MANUFACTURE, USE, SELL ANY PATENTED INVENTION THAT MAY IN ANY WAY BE RELATED THERETO.


THIS TECHNICAL REPORT HAS BEEN REVIEWED AND IS APPROVED FOR PUBLICATION.


THOMAS R. SIERON
Technical Manager
Flight Mechanics Research Group


DUDLEY FIELDS
Senior Aerospace Specialist
Aerodynamics Group


A. WAYNE BALDWIN
Senior Aerospace Engineer
Aerodynamics Group


DAVID W. ADAMCZAK
Aerospace Engineer
Flight Mechanics Research Group


VALENTINE DAHLEM
Chief, Aerothermo & Flight Mechanics Branch
Aeromechanics Division

IF YOUR ADDRESS HAS CHANGED, IF YOU WISH TO BE REMOVED FROM OUR MAILING LIST, OR IF THE ADDRESSEE IS NO LONGER EMPLOYED BY YOUR ORGANIZATION PLEASE NOTIFY WL/FIMH, WRIGHT-PATTERSON AFB, OH 45433-7913 TO HELP MAINTAIN A CURRENT MAILING LIST.

COPIES OF THIS REPORT SHOULD NOT BE RETURNED UNLESS RETURN IS REQUIRED BY SECURITY CONSIDERATIONS, CONTRACTUAL OBLIGATIONS, OR NOTICE ON A SPECIFIC DOCUMENT.

REPORT DOCUMENTATION PAGE

Form Approved
OMB No. 0704-0188

Public reporting burden for this collection of information is estimated to average 1 hour per response, including the time for reviewing instructions, searching existing data sources, gathering and maintaining the data needed, and completing and reviewing the collection of information. Send comments regarding this burden estimate or any other aspect of this collection of information, including suggestions for reducing this burden, to Washington Headquarters Services, Directorate for Information Operations and Reports, 1215 Jefferson Davis Highway, Suite 1204, Arlington, VA 22202-4302, and to the Office of Management and Budget, Paperwork Reduction Project (0704-0188), Washington, DC 20503.

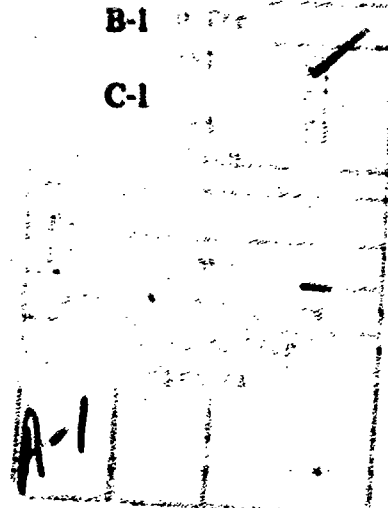
1. AGENCY USE ONLY (Leave blank)		2. REPORT DATE Aug 1993		3. REPORT TYPE AND DATES COVERED Final report Jan 92- Jun 93	
4. TITLE AND SUBTITLE PROCEDURES AND DESIGN DATA FOR THE FORMULATION OF AIRCRAFT CONFIGURATIONS				5. FUNDING NUMBERS PE: 62201F PR: 2404 TA: 240416 WU: 67	
6. AUTHOR(S) THOMAS R. SIERON, DUDLEY FIELDS, A. WAYNE BALDWIN, DAVID W. ADAMCZAK					
7. PERFORMING ORGANIZATION NAME(S) AND ADDRESS(ES) WRIGHT LABORATORY, AFMC FLIGHT DYNAMICS DIRECTORATE AEROMECHANICS DIVISION, WL/FIMH WRIGHT-PATTERSON AFB OH 45433-7936				8. PERFORMING ORGANIZATION REPORT NUMBER WL-TR-93-3068	
9. SPONSORING / MONITORING AGENCY NAME(S) AND ADDRESS(ES) WRIGHT LABORATORY, AFMC FLIGHT DYNAMICS DIRECTORATE AEROMECHANICS DIVISION, WL/FIMH WRIGHT-PATTERSON AFB OH 45433-7936				10. SPONSORING / MONITORING AGENCY REPORT NUMBER WL-TR-93-3068	
11. SUPPLEMENTARY NOTES					
12a. DISTRIBUTION / AVAILABILITY STATEMENT Approved for public release; distribution unlimited.				12b. DISTRIBUTION CODE	
13. ABSTRACT (Maximum 200 words) This report contains design data and rapid analysis methods to assist in establishing an initial aircraft configuration to begin the conceptual design process. It is based on an array of data acquired over many years for fighter, bomber and transport aircraft. The data is compiled to estimate the gross take-off weight and physical size of a representative configuration for various range, payload and speed requirements. Other data and procedures are included to define the general dimensions of the fuselage, wing, vertical and horizontal stabilizers. Aerodynamic methods and data are provided to rapidly estimate the drag and lift characteristics at subsonic, transonic and supersonic speeds for the this class of aircraft. Performance data has been assembled to show the impact of range, payload, speed, maneuverability, take-off and landing requirements on the physical and geometric characteristics of these configurations. A sample problem is presented to illustrate the use of this design data in formulating an aircraft configuration.					
14. SUBJECT TERMS AIRCRAFT CONFIGURATIONS, CONCEPTUAL DESIGN, AERODYNAMIC PREDICTION METHODS, AIRCRAFT DESIGN				15. NUMBER OF PAGES 151	
				16. PRICE CODE	
17. SECURITY CLASSIFICATION OF REPORT UNCLASSIFIED	18. SECURITY CLASSIFICATION OF THIS PAGE UNCLASSIFIED	19. SECURITY CLASSIFICATION OF ABSTRACT UNCLASSIFIED	20. LIMITATION OF ABSTRACT UNLIMITED		

NSN 7540-01-280-5500

TABLE OF CONTENTS

		<u>PAGE</u>
1.	INTRODUCTION	1-1
2.	AIRCRAFT CONCEPTUAL DESIGN	2-1
3.	IMPACT OF PERFORMANCE REQUIREMENTS ON CONFIGURATION SHAPE	3-1
4.	DESIGN DATA FOR INITIAL SIZING AND SHAPING OF CONFIGURATIONS	4-1
5.	METHODS AND DATA TO ESTIMATE PRELIMINARY AERODYNAMIC CHARACTERISTICS	5-1
6.	INFLUENCE OF AERODYNAMIC AND CONFIGURATION PARAMETERS ON PERFORMANCE	6-1
7.	PROCEDURES FOR THE FORMULATION AND ANALYSIS OF AN AIRCRAFT CONFIGURATION	7-1
8.	CONCLUSIONS	8-1
9.	REFERENCES	9-1
APPENDIX A	REPRESENTATIVE OPERATIONAL AND ADVANCED CONFIGURATIONS	A-1
APPENDIX B	VOLUME AND AREA RELATIONSHIPS	B-1
APPENDIX C	WINGS IN SUPERSONIC FLOW	C-1

DTIC QUALITY INSPECTED 2



LIST OF FIGURES

Figure	Title	Page
2-1	Concept Formulation	2-2
3-1	Impact of Speed on Configuration Features	3-2
3-2	Subsonic Aircraft Pressure Drag	3-3
3-3	Supersonic Aircraft Wave Drag	3-4
3-4	Aircraft Thrust and Wing Loadings	3-6
3-5	Parametric Performance Trade-Off Study	3-7
4-1	Payload-Range Capability for Transports	4-2
4-2	Payload-Range Capability for Supersonic Fighters	4-3
4-3	Length of Transports	4-4
4-4a	Length of Supersonic Fighters	4-5
4-4b	Length of Supersonic Fighters	4-5
4-5	Empty Weight Fraction for Bombers and Transports	4-8
4-6	Empty Weight Fraction for Fighters	4-9
4-7	Fuel and Payload Fraction for Transports	4-10
4-8	Fuel and Payload Fraction for Fighters	4-11
4-9	Wetted Area for Transports and Bombers	4-13
4-10	Wetted Area for Fighters	4-14
4-11	Aircraft Volume	4-15
4-12	Aircraft Dry Weight Density Parameter	4-16

4-13	Wing Area and Wetted Area	4-18
4-14	Span Loading and Wing Loading	4-19
4-15	Fighter Aspect Ratio and Wing Sweepback	4-20
4-16	Wing Sweepback Angle	4-21
4-17	Aspect Ratio and Wing Thickness Ratio	4-23
4-18	Wing Characteristics	4-24
4-19	Horizontal Tail Sizing Guideline	4-25
4-20	Vertical Tail Sizing Guideline	4-27
5-1	Dynamic Pressure	5-2
5-2	Reynolds Number	5-3
5-3	Drag Prediction/Definition	5-5
5-4	Turbulent Skin Friction	5-7
5-5	Drag Build-up and Mach Number Effects	5-8
5-6	Fighter Drag Polar-Lift Efficiency	5-10
5-7	Drag-Due-to-Lift	5-11
5-8	Wing Efficiency Factor	5-12
5-9	Trim Lift and Drag Procedure	5-14
5-10	Aerodynamic Cleanness of Aircraft	5-15
5-11	Minimum Wave Drag Bodies of Revolution	5-18
5-12	Supersonic Area Rule Concept	5-20
5-13	Transonic Drag Rise at Mach 1.2	5-22
5-14	Transonic Drag Correlation	5-23

5-15	Parasite Drag Area Correlation at Mach 2	5-24
5-16	Variation of C_{D0} with Mach Number	5-25
5-17	Subsonic Lift Curve Slope	5-27
5-18	Supersonic Lift Curve Slope	5-28
5-19	Maximum Lift-to-Drag Ratio	5-30
5-20	Subsonic Maximum L/D Correlation	5-32
5-21	Subsonic Maximum L/D Variation with Aspect Ratio	5-33
5-22	Variation of Maximum L/D with Mach Number	5-34
5-23	Maximum L/D at Subsonic Cruise and Maximum Speed	5-35
6-1	FLAPS Down $C_{L\text{ MAX}}$	6-2
6-2	Stall Velocity Versus Wing Loading	6-3
6-3	Take-Off Velocity	6-4
6-4	Take-Off Distance	6-5
6-5	Cruise Altitude	6-7
6-6	Impact of Cruise Fuel on Transport Range	6-9
6-7	Impact of Cruise Fuel on Fighter Range	6-10
6-8	Impact of Supersonic Speed on Fighters	6-11
6-9	Specific Excess Power, $G = 1.0$	6-16
6-10	Specific Excess Power, $G = 5.0$	6-17
6-11	Maximum Sustained "G" Contours, $M = 0.6$	6-19
6-12	Maximum Sustained "G" Contours, $M = 0.9$	6-20
6-13	Maximum Sustained "G" Contours, $M = 1.5$	6-21

6-14	Thrust Variation for a Modern Fighter	6-22
6-15	Aircraft Turn Rate, $V = 200 - 800$ Knots	6-25
6-16	Aircraft Turn Rate, $V = 700 - 1400$ Knots	6-26
6-17	Landing Ground Distance	6-28
6-18	Descent Distance Over 50 feet	6-29
A-1	A-7D Fighter Configuration	A-2
A-2	F-106 Fighter Configuration	A-3
A-3	F-15 Fighter Configuration	A-4
A-4	F-16 Fighter Configuration	A-5
A-5	Advanced Supersonic Fighter Configuration	A-6
A-6	C-141 Transport Configuration	A-7
A-7	C-5 Transport Configuration	A-8
A-8	Advanced Transport Configuration	A-9
A-9	B-52 Bomber Configuration	A-10
C-1	Arrowhead Wings with Double Wedge at Zero Incidence	C-5

Nomenclature

a	Acceleration, ft/sec ²
α	Angle of attack, deg
A_x	Frontal projected area, ft ²
AR	Aspect ratio b^2/S_{Ref}
A_{WET}	Wetted area, ft ²
b	Wing span, ft
β	$\beta = \sqrt{M^2 - 1} \quad \text{for } M > 1$ $= \sqrt{1 - M^2} \quad \text{for } M < 1$
c	Chord length, ft
\bar{c}	Wing mean aerodynamic chord, ft
C_D	Drag coefficient
C_{D0}	Drag coefficient at zero lift
C_{DP}	Pressure drag coefficient
C_{DTr}	Trim drag coefficient
C_{DW}	Supersonic wave drag coefficient
C_f	Friction coefficient
C_{fe}	Equivalent friction coefficient
C_L	Lift coefficient
C_{La}	Lift curve slope, 1/deg or 1/rad
C_{LMAX}	Maneuver lift coefficient
C_{LMAX}	Maximum useable lift coefficient

C_{LTO}	Lift coefficient at take-off
C_R	Wing root chord length, ft
C_T	Wing tip chord length, ft
d	Diameter, ft
d_e	Fuselage equivalent diameter, ft ²
δ	Deflection angle, deg
δ_h	Horizontal tail deflection angle, deg
DLF	Design load factor, g's
e	Wing efficiency factor
f	Equivalent parasite area, ft ²
FF	Form factor
g	Acceleration due to gravity, ft/sec ²
γ	Glide slope angle, deg
GTOW	Gross take-off weight, lb
h	Altitude, ft
IF	Interference factor
K	Drag due to lift factor, $K = \frac{1}{\pi A R e}$
L	Fuselage Length, ft or Lift, lbs
LE	Leading edge
λ	Wing taper ratio, C_T/C_R
Λ, Λ_{LE}	Wing leading edge sweep angle, deg

Λ_{qc}	Wing quarter chord sweep angle, deg
L/D	Lift to drag ratio
l_{HT}	Horizontal tail arm, ft
l_{VT}	Vertical tail arm, ft
M, M_∞	Mach number
n	Load factor, g's
q	Dynamic pressure, lb/ft ²
R	Radius, ft or Range, nm
Re/ft	Reynolds number per foot
ρ	Air Density, slugs/ft ³
SFC	Specific fuel consumption lb _{fuel} /(lb _{thrust} hr)
S_{GROUND}	Landing/Take-off ground roll distance, ft
S_{HT}	Horizontal tail area, ft ²
σ	Density Ratio, $\frac{\rho_{ALT}}{\rho_{SL}}$
SL	Sea level
S_R	Reference area based on frontal projected area, ft ²
S_{Ref}	Wing reference area, ft ²
S_{VT}	Vertical tail area, ft ²
S_W, S_{WING}	Wing area, ft ²
S_{WET}	Wetted area, ft ²
t	Wing thickness, ft

T	Thrust, lb
t/c	Wing thickness to chord ratio
$\dot{\theta}$	Turn rate, deg/sec
T/W	Thrust to weight ratio
ULF	Ultimate load factor, g's
V	Velocity, knots
V, V_0	Volume, ft ³
V_{APP}	Landing approach velocity, knots
V_{STALL}	Stall velocity, knots
V_{TO}	Take-off velocity, knots
W	Weight, lb
W/b^2	Span loading, lb/ft ²
W_{EMPTY}	Empty weight, lb
$W_{FC}, W_{FCRUISE}$	Cruise fuel weight, lb
W_{FUEL}	Fuel weight, lb
W_{PL}	Payload weight, lb
W/S	Wing loading, lb/ft ²
W_{TO}	Take-off weight, lb
$()_\infty$	Freestream conditions

FOREWORD

This report was prepared in-house by Thomas R. Sieron, Dudley Fields, A. Wayne Baldwin, and David W. Adamczak of the Aeromechanics Division, Flight Dynamics Directorate, Wright Laboratory at Wright-Patterson Air Force Base, Ohio 45433-7913. It presents a compilation of design data acquired over many years in the development and analysis of advanced aircraft configuration concepts. The work was accomplished under Project 2404, Task 16, and Work Unit 67. It was prepared during the period January 1992 to June 1993.

The report is composed of eight sections with a sample problem contained in section seven. The sample problem presents a procedure for using the design data and aerodynamic prediction methods in the formulation and analysis of an aircraft configuration. Appendix A provides a handy reference to obtain geometry information on current and advanced aircraft. Appendix B contains mathematical equations to compute the volume of simple shapes, such as, cones, bodies of revolution, and cylinders. Appendix C contains fundamentals of wing wave drag in supersonic flow.

1. INTRODUCTION

The development of aircraft configurations is both an art and a science. Most beginning designers start out with a background in aeronautics and learn to understand the basic functions of airplane components. These include the fuselage, canopy, wing, engine, inlets, nozzles, horizontal and vertical stabilizers and control surfaces. Instructions in a text book are then used to configure an airplane and evaluate its basic performance capabilities. As the designer acquires experience the formal process tends to diminish and is replaced with knowledge and skills learned in the practical design of airplanes.

This report provides design data and procedures in an attempt to fill a gap between the seasoned designer and inexperienced designer. It is based on an array of data acquired over many years in the design and analysis of various types of aircraft configurations. This empirical data base can be used in the initial sizing and shaping of a configuration to meet some specified performance requirements. These performance requirements generally consist of cruise range, maximum speed, payload, maneuverability, loiter and take-off/landing field distances. Other requirements may be imposed but these are the primary ones for most military aircraft configurations.

The report is intended to augment aircraft design textbooks such as Nicholai and Raymer (References 1 & 2). These textbooks contain a systematic approach to the preliminary design of aircraft configurations. They are very valuable to engineers in understanding the airplane design process.

The rapid advancement in computer technology has created a revolution in the design and analysis of aircraft configuration. It is not unusual to have a workstation for each engineer with

access to numerous computer aided design (CAD) programs. Computer analysis programs are available in the government and industry for each technical discipline, such as, aerodynamics, structures and propulsion. In addition, design synthesis programs are available which combine these single discipline programs into a completely integrated program (Reference 3 and 4). These design programs contain geometry development subroutines as well as subroutines for each of the technical disciplines. These subroutines are controlled by a central executor. The executor controls the problem and routes the information to the various subroutines, as required to solve the problem. These design synthesis programs can be used to perform rapid configuration trade-off studies and converge the design to meet specified performance requirements.

The continued advancement in computer size, speed and storage capacity should drastically reduce the time required in the design cycle and permit the development of more optimum configurations with higher performance. The emergence of computational fluid dynamics (CFD) as a design tool will expedite the design cycle by reducing the amount of time required to validate and verify the airplane design. Today the configuration is defined using a combination of linear theories, semi-empirical methods, CFD and wind tunnels testing. In the long term (10 to 15 years) it is envisioned CFD will be used throughout the design, and wind tunnels will be used only to spot-check the final airplane design. These developments will all enhance the design process and produce a higher quality airplane ...in less time...and at reduced costs.

2. AIRCRAFT CONCEPTUAL DESIGN

The evolution of a new aircraft concept is generally based on a set of performance requirements. The design engineer must depend on background and experience to formulate the initial configuration in search of satisfying these performance requirements. The cycle between the initial concept formulation and the final configuration, which satisfies the requirements, is known as the design process.

This report is intended to assist in establishing the initial configuration concept in the design process. Past data are provided to estimate a gross weight based on range, payload and speed requirements. The gross weight can be used to determine the physical size of a representative configuration. Other data and procedures are included to define the general dimensions of the fuselage, wing, vertical and horizontal stabilizers. These inputs are required to begin the analysis and design process.

The process was previously performed by individual analysis programs, but with the advent of personal computers and workstations it has become fully automated. Today, vehicle synthesis programs are available which perform the entire conceptual design process. This process is depicted in Figure 2-1. Major features consist of sizing algorithms, aerodynamic, weights, propulsion and performance subroutines which iterate until the concept meets the specified performance requirements.

A program used extensively by the Aeromechanics Division is called the Combat Aircraft Synthesis Program (CASP), a robust program applicable to a wide variety of aircraft. CASP is a computer code for the conceptual design of military fighters, bombers and transports, plus their variants. It uses a basic geometric description of a vehicle to generate a detailed aerodynamic

Configuration Concept Formulation

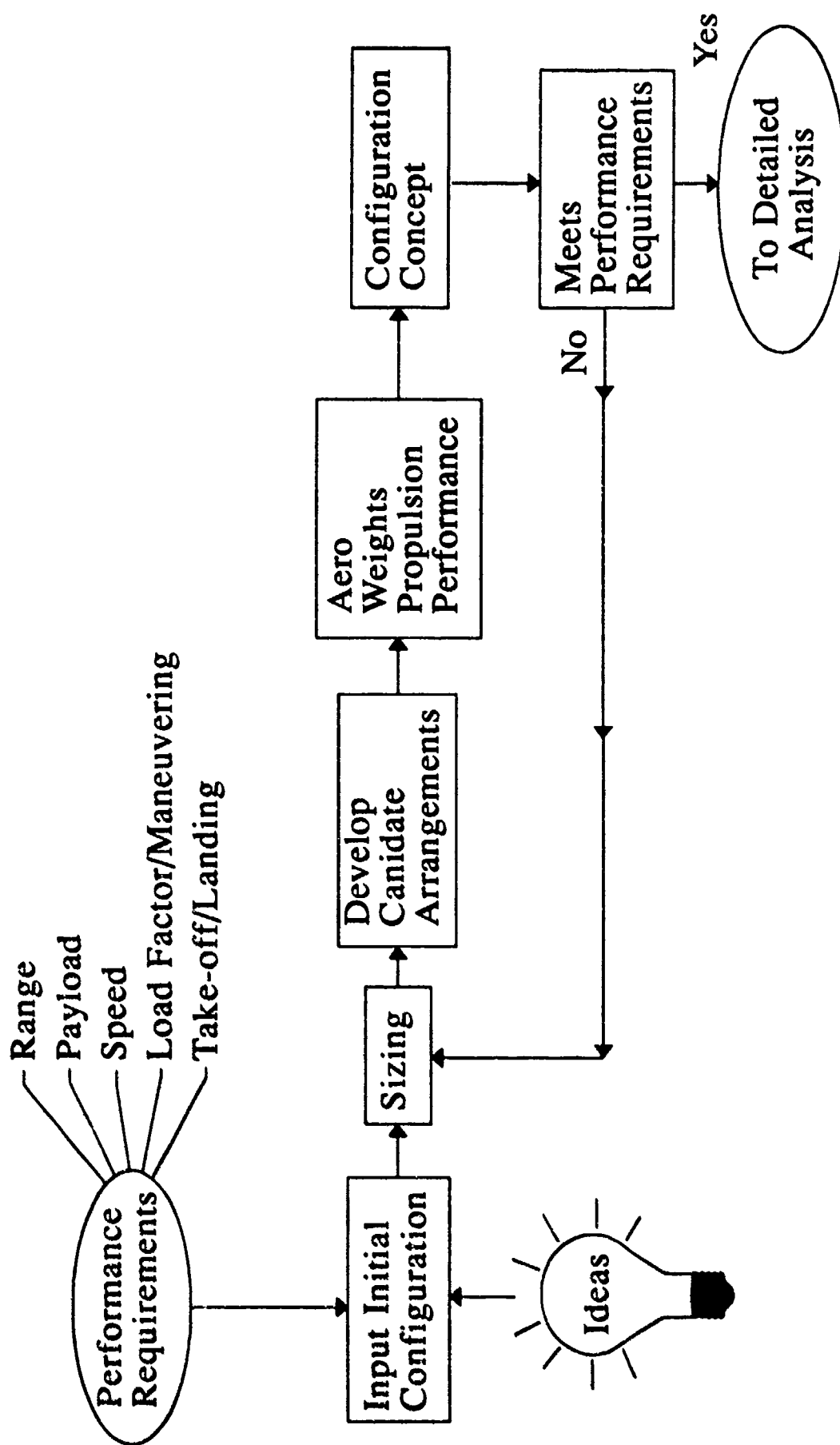


FIGURE 2-1 Concept Formulation

and weight analysis using Datcom type methods. (References 5 and 6).

The aerodynamic analysis is a first level calculation for lift and drag based on the Air Force Datcom handbooks. The calculations include lift curve slope, lift at zero angle of attack, maximum lift and maximum angle of attack. Drag calculations include skin friction drag, wave drag, camber drag, drag due to lift and trim drag.

The weights analysis is a first level mass properties methodology which outputs estimates for structure, propulsion system, and useful loads, plus systems and equipment weights. Methods in the analysis are based on the specific type of aircraft being studied, a user input, and additional inputs of payload weight, basic engine weight, maximum dynamic pressure, ultimate load factor, and gross weight estimate. These inputs are used with the geometric description to calculate mass properties, fuel weight and a check of volume available versus volume required. A mission analysis subroutine uses the calculated aerodynamics and weights from the input geometry. The user has to supply a mission using different segment options (Acceleration, Climb, Cruise, Combat, Landing, Loiter) and the engine propulsion deck (thrust and fuel flows). CASP will then run the given mission and output the mission segments in a detailed printout. In addition to basic mission profile results, CASP can also be tasked to optimize the overall mission for specific payoff functions. The user may choose to maximize loiter time, radius, or number of combat turns, or to minimize the aircraft gross weight. CASP runs on an IRIS workstation and takes less than 30 seconds to run a basic aerodynamic and weight analysis, while a complete mission and optimization of a mission takes only several minutes of computer time.

The arrangement and blending of the configuration components is still a challenging task, even with the assistance of rapid computers and friendly software. The designer needs to have

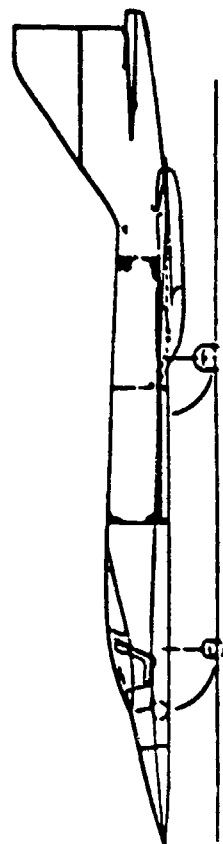
a thorough understanding of the impact of performance requirements on the configuration size and shape. This knowledge and experience permits the injection of innovative ideas into the vehicle design.

3. IMPACT OF PERFORMANCE REQUIREMENTS ON CONFIGURATION DESIGN

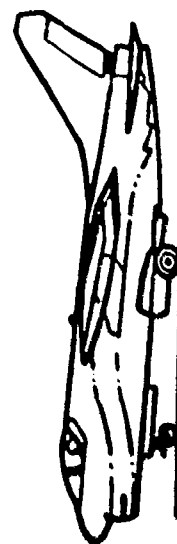
An experienced designer can view a new aircraft and make a reasonably accurate evaluation of its performance capability. This ability is based on an extensive background in aeronautics and indicates that individual configuration features are related to the performance requirements of an aircraft. A thorough understanding of fluid mechanics, performance and propulsion coupled with general knowledge of structures and subsystems is therefore a prerequisite to being a seasoned designer. The most important performance parameters are speed, maneuverability, range, take-off and landing distances and useful payload. (References 7, 8 and 9)

The speed of an aircraft determines the primary appearance of a configuration. A subsonic fighter and a conceptual supersonic interceptor are illustrated in figure 3-1. A number of other aircraft are also displayed in Appendix A as a convenient reference. Subsonic airplanes are characterized by low fuselage fineness ratios, blunt nose and wing leading edges, short fuselage nose sections and large protruding cockpits. Subsonic aircraft typically, have fineness ratios in the range of 5 to 7 to minimize subsonic pressure drag and maximize internal volume as shown in Figure 3-2. There is only a minimal decrease in pressure drag beyond these fineness ratio values. Supersonic cruise airplanes have high fuselage fineness ratios, sleek nose sections with the canopy blended into the fuselage, high wing sweepback with low thickness ratios and low wing aspect ratios. These features are dictated by the need to keep profile drag at the lowest possible level. Figure 3-3 displays transonic wave drag as a function of fineness ratio. Fineness ratios of 8 or higher are required to avoid large wave drag increases.

The maneuverability requirements of an aircraft are very dependent on its application.



Supersonic Interceptor



Subsonic Attack

FIGURE 3-1 Impact of Speed on Configuration Features

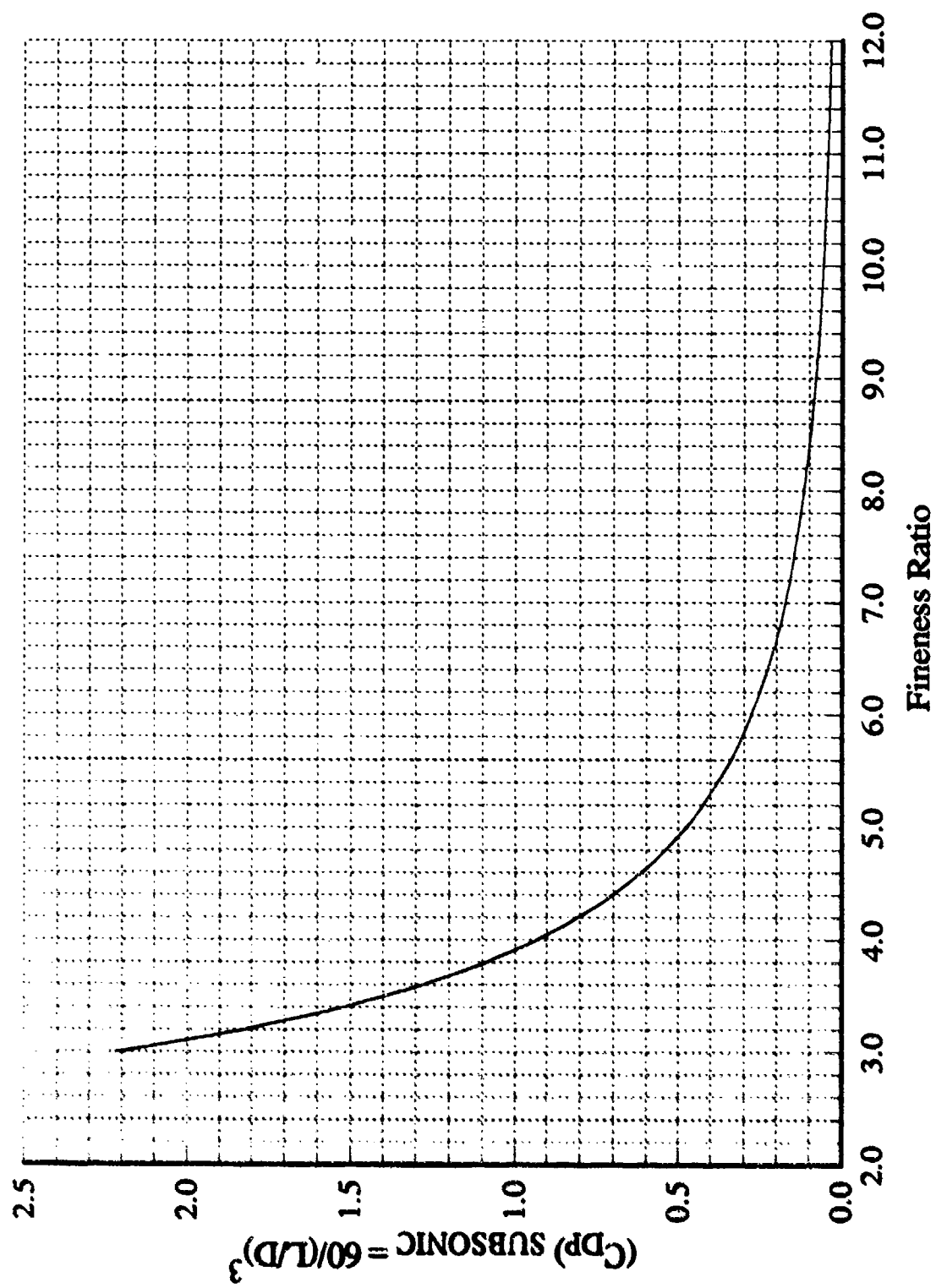
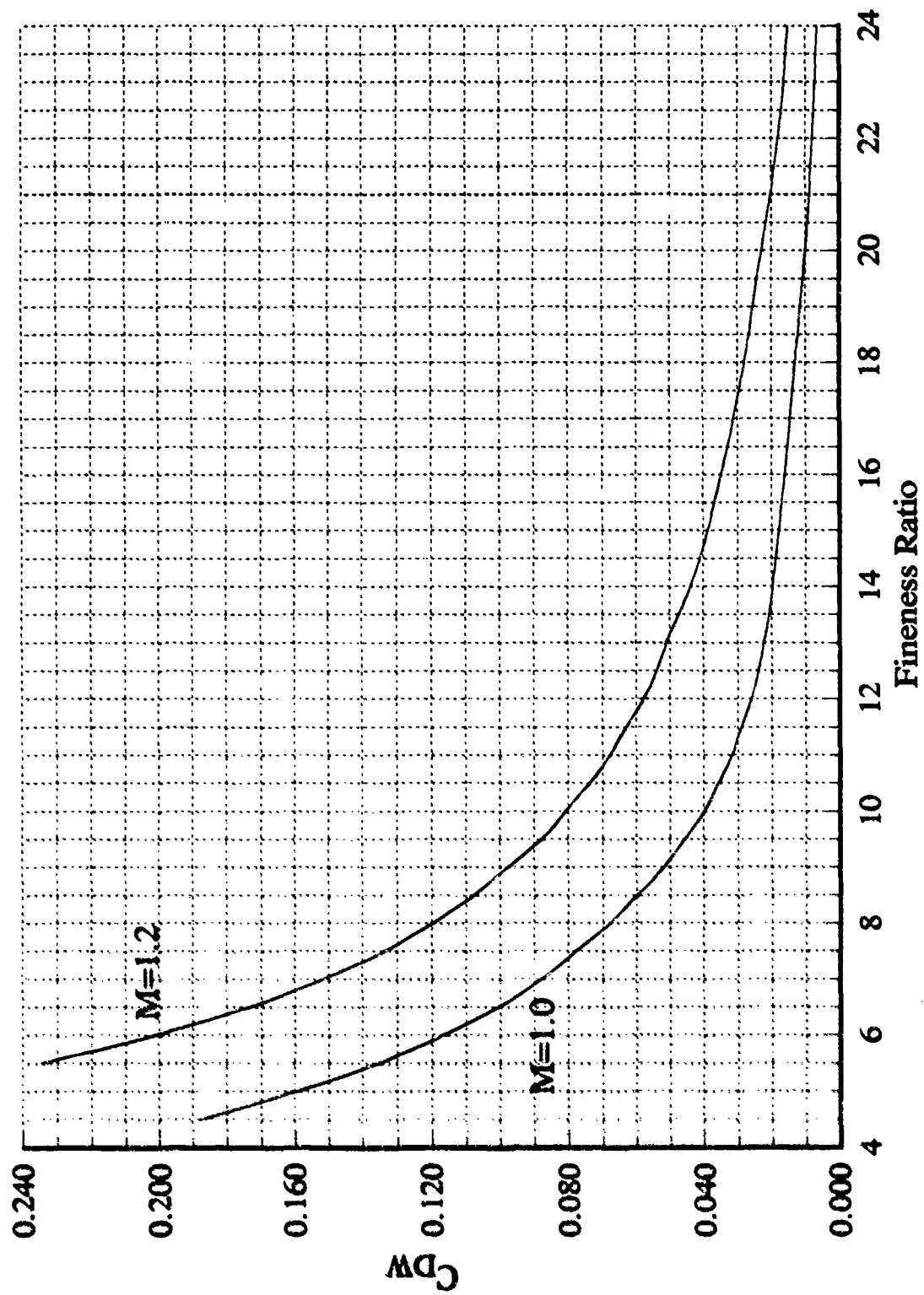


FIGURE 3-2 Subsonic Aircraft Pressure Drag



3-4

FIGURE 3-3 Supersonic Aircraft Wave Drag

Transports and bombers generally have very low maneuver requirements. Representative maximum load factor values are between 2.0 and 3.0. This permits these aircraft to have relatively high wing loadings dictated by fuel load and take-off and landing. Typical ranges of thrust and wing loadings are presented in figure 3-4. A typical transport has a $T/W = 0.25$ and $W/S = 110$, in contrast to modern day fighters of $T/W = 1.10$ and $W/S = 75$. Fighters are designed to engage in air-to-air combat and require a very high maneuver capability. The maximum load factor is 7.33 for the F-15 and 9.0 for the F-16. Parametric trade studies of performance characteristics are conducted early in the design cycle to arrive at nominal values of T/W and W/S for each airplane. Figure 3-5 shows the impact of maneuver, acceleration and take-off distance on the gross take-off weight as a function of T/W and W/S for an advanced supersonic fighter. Each individual requirement imposes a different set of T/W and W/S values and these type of trade studies assist in establishing a final set of configuration requirements at minimum gross take-off weight.

The range or radius capability of aircraft is directly dependent on the lift-to-drag ratio (L/D). This is the true aerodynamic efficiency measure for aircraft. The L/D is directly proportional to the wing aspect ratio and the cleanliness of a configuration. The drag must be kept to a minimum in all speed regimes, and the configuration shaped to avoid flow separation at cruise conditions. Wing sweepback angle is generally a compromise between range, speed, and maneuverability. The advent of supercritical wing technology permits higher lift for the same aspect ratio wing and thus higher L/D 's. The range requirement also influences the fuselage size since fuel is generally carried in fuselage tanks as well as the wing.

Another performance parameter which influences the configuration shape is take-off and

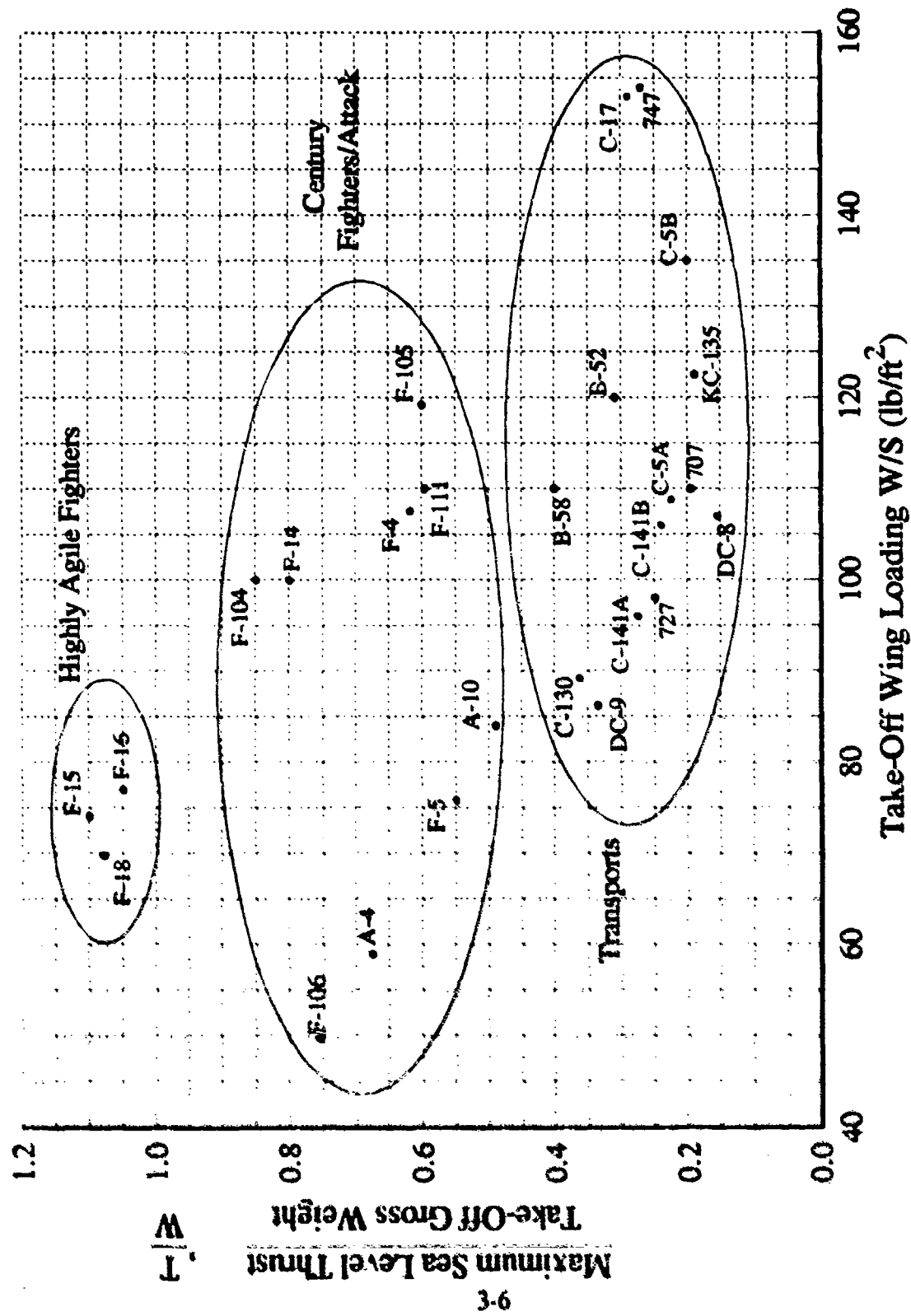


FIGURE 3-4 Aircraft Thrust And Wing Loadings

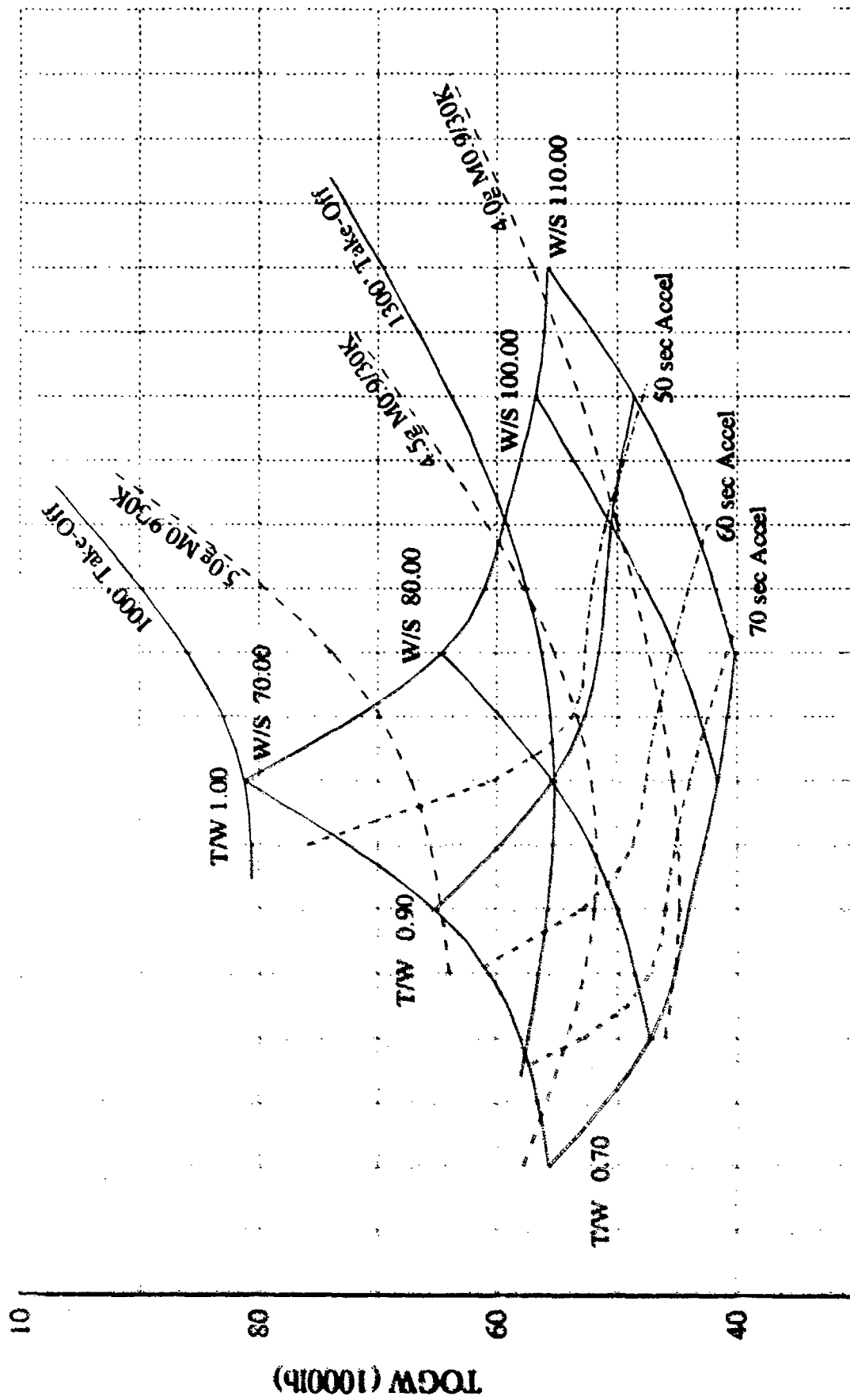


FIGURE 3-5 Parametric Performance Trade-Off Study

landing. The speed at take-off is directly proportional to wing loading and inversely proportional to the lift coefficient. Thus the designer must also consider the length of runways in determining the size and geometry of the wing. High lift devices can be used to augment the lift of the basic wing during take-off and landing.

Payload is the useful load an airplane can carry and deliver. This is perhaps the most meaningful performance requirement since it is the ultimate reason aircraft are built. Payload consists of crew, passengers, cargo, guns, bombs, missiles, etc. Cargo weight and density drive the payload bay size and are directly related to the fuselage length and diameter. If air drop of equipment is a mission requirement, this strongly influences the aft fuselage design. In fighters, the primary payload is missiles, bombs, and guns. These weapons may be carried either internally or externally on the aircraft. External weapons need to be fully integrated with the underside of the airplane, if low drag is a goal. Internal weapons require larger internal volumes. Internal versus external weapons carriage assessments involve many factors such as mission, speed, vehicle size and cost, and typically require design details beyond the level addressed in this report.

The above discussion illustrates the impact of various mission requirements on the aircraft geometry. It also is to be noted that some components are influenced by two or more requirements. This mandates that the component be optimized considering all requirements. This is the task of the airplane designer in developing the most efficient design.

4. DESIGN DATA FOR INITIAL SIZING AND SHAPING OF CONFIGURATIONS

The physical size and shape of an aircraft configuration is dependent on the performance goals established by the customer or using organization. Appendix A displays pertinent features and dimensions of several past, present and advanced aircraft configurations. A parameter which can be used to correlate the size of an aircraft is known as ton-miles and combines range and payload requirements. It can be used for both military and commercial aircraft. The gross take-off weights of numerous subsonic aircraft are shown as a function of ton-miles in Figure 4-1 (References 10 - 13). The payload of the aircraft is divided by 2000 to obtain tons. This is next multiplied by the range of the aircraft to obtain ton-miles. A large increase in ton-mile capability can be seen as the gross take-off weight exceeds 500,000 pounds. This same parameter can be used to correlate fighter aircraft, as depicted in Figure 4-2. A band is used for this type of aircraft since fighters tend to have more diverse performance requirements. These design curves provide a rapid method to estimate aircraft initial gross take-off weights based on payload and range requirements. The gross take-off weight is defined as:

$$W_{TO} = W_{EMPTY} + W_{FUEL} + W_{PAYLOAD}$$

The length of an aircraft is very critical and depends on gross take-off weight as shown in Figures 4-3 and 4-4a. The driving performance requirement is cargo size and weight for transports and maximum speed and maneuverability for fighters. A factor which must also be considered in aircraft length is the size of available maintenance hangers and protective shelters to maintain and protect the aircraft. There is excellent correlation with gross take-off weight for transports and moderate agreement with fighters. The fighter correlation can be improved if the empty weight is known as shown in figure 4-4b. In either case, the data provides an initial

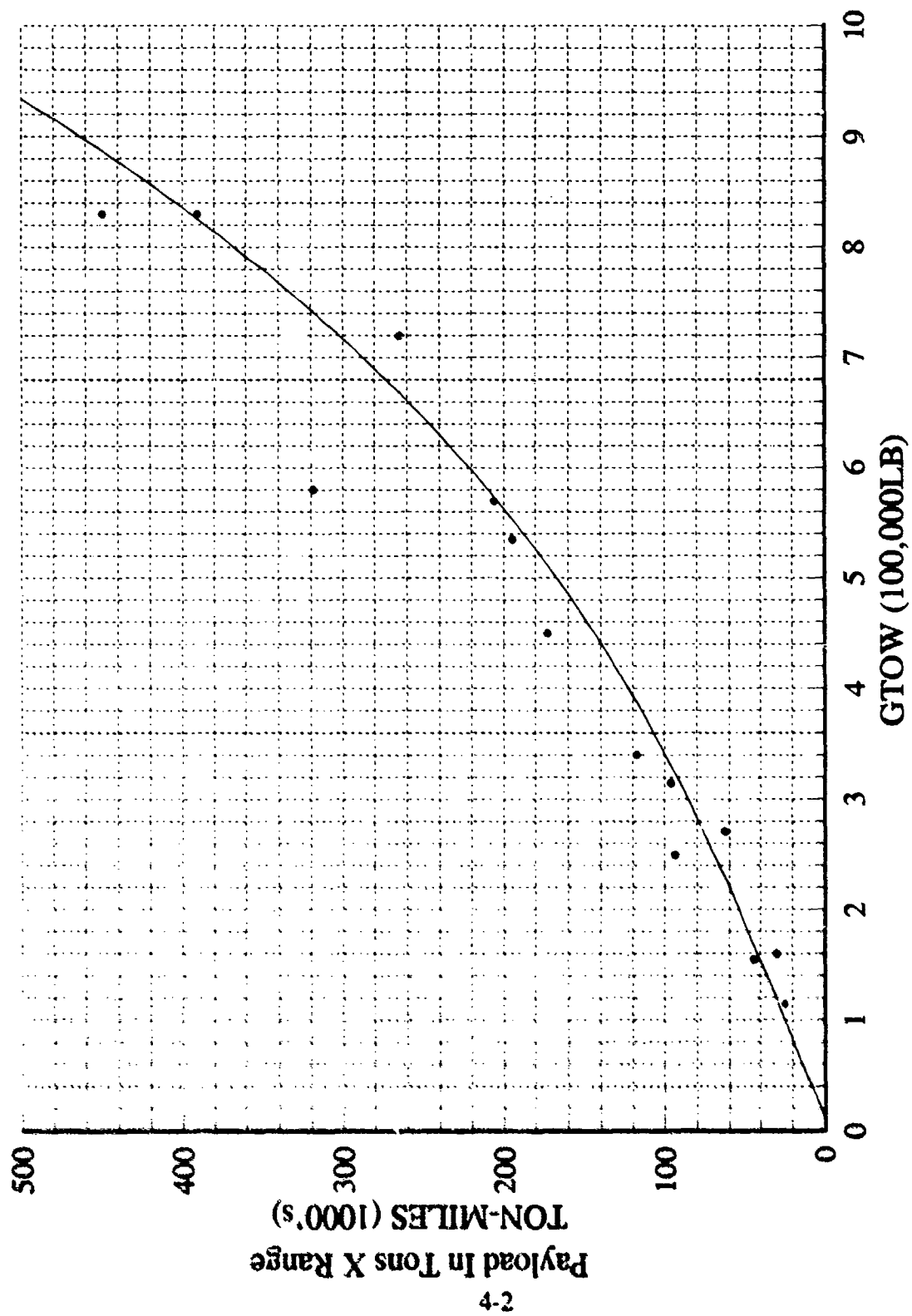


FIGURE 4-1 Payload-Range Capability For Transports

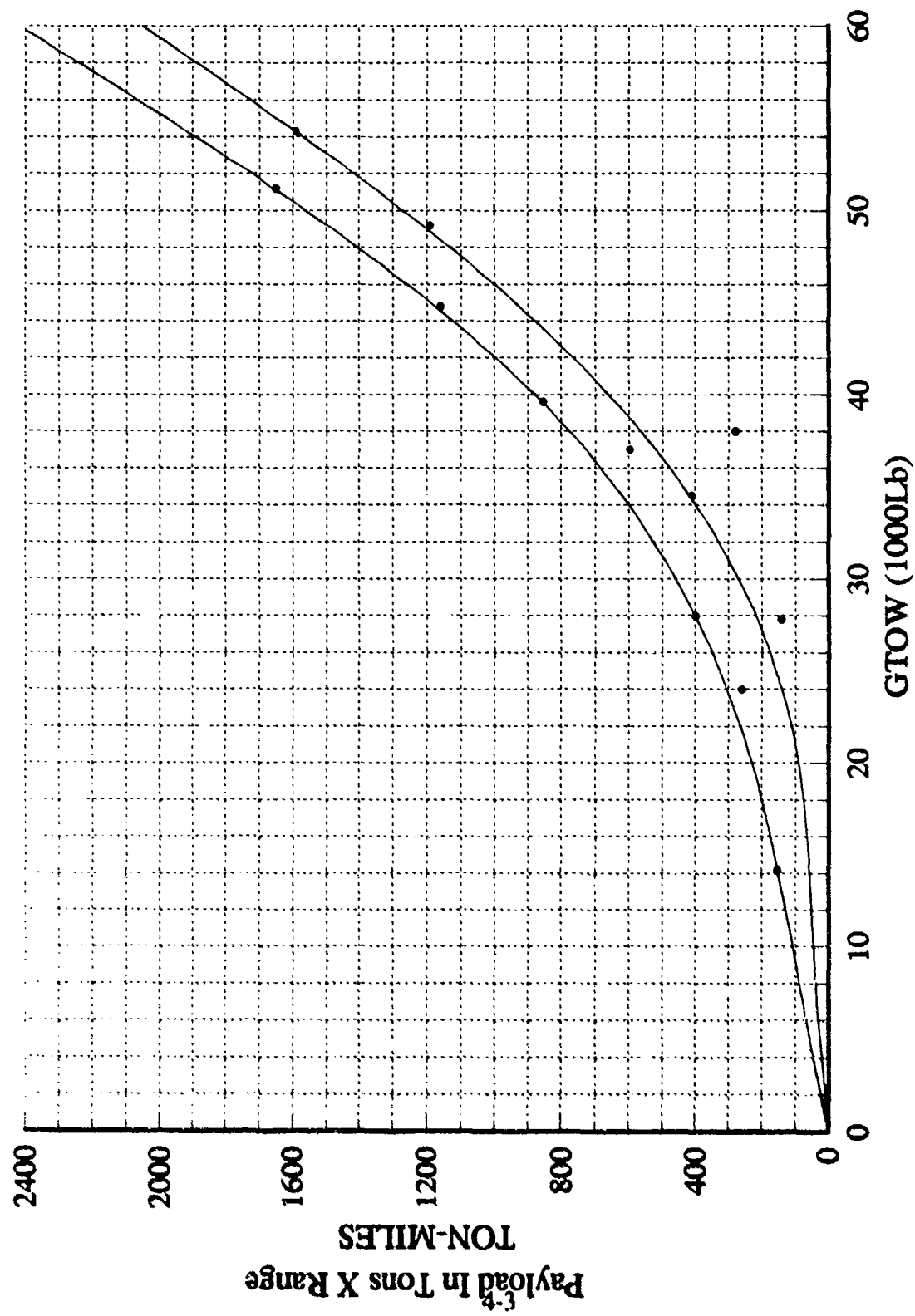


FIGURE 4-2 Payload-Range For Supersonic Fighters

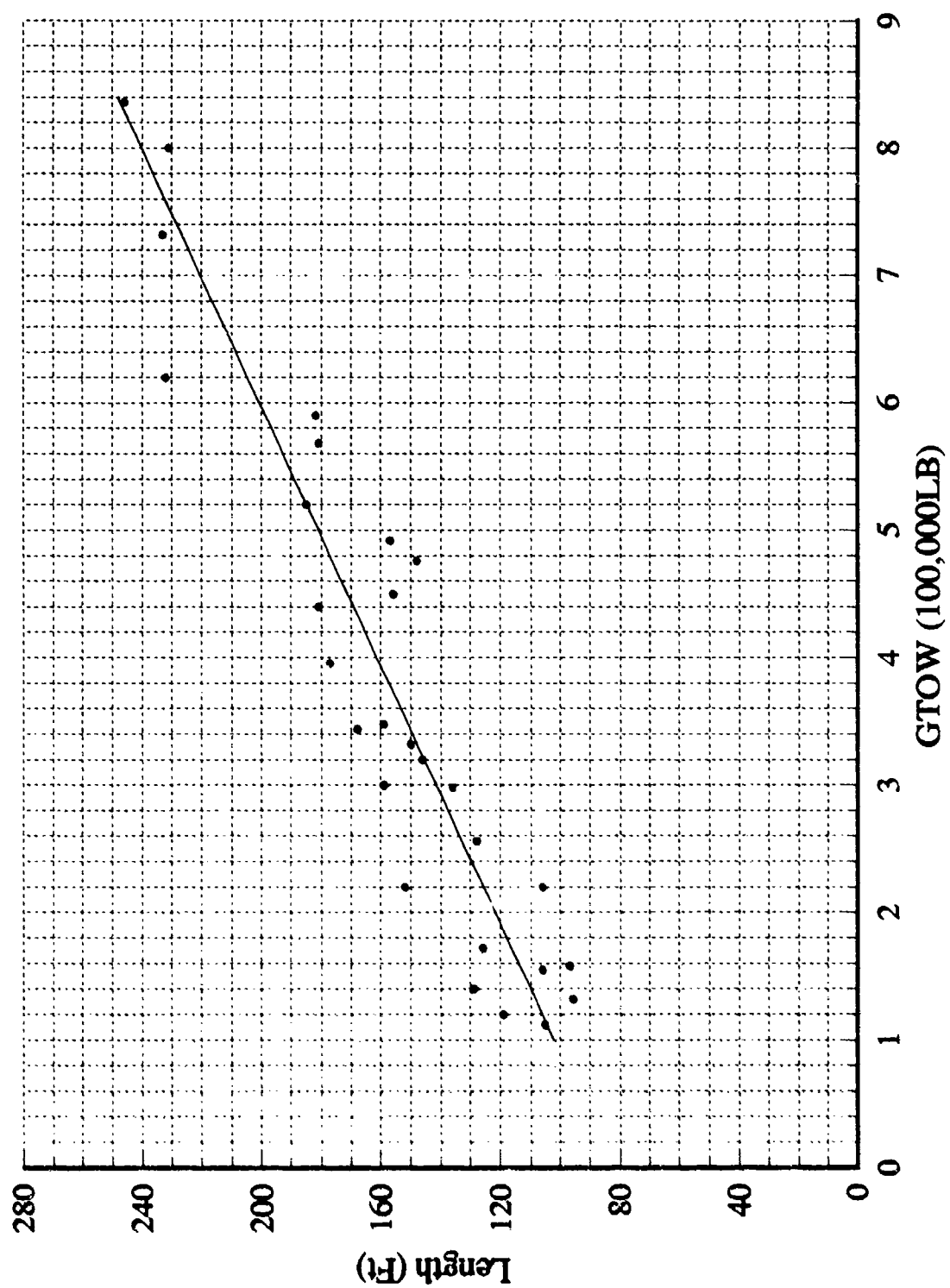


FIGURE 4-3 Length Of Transports

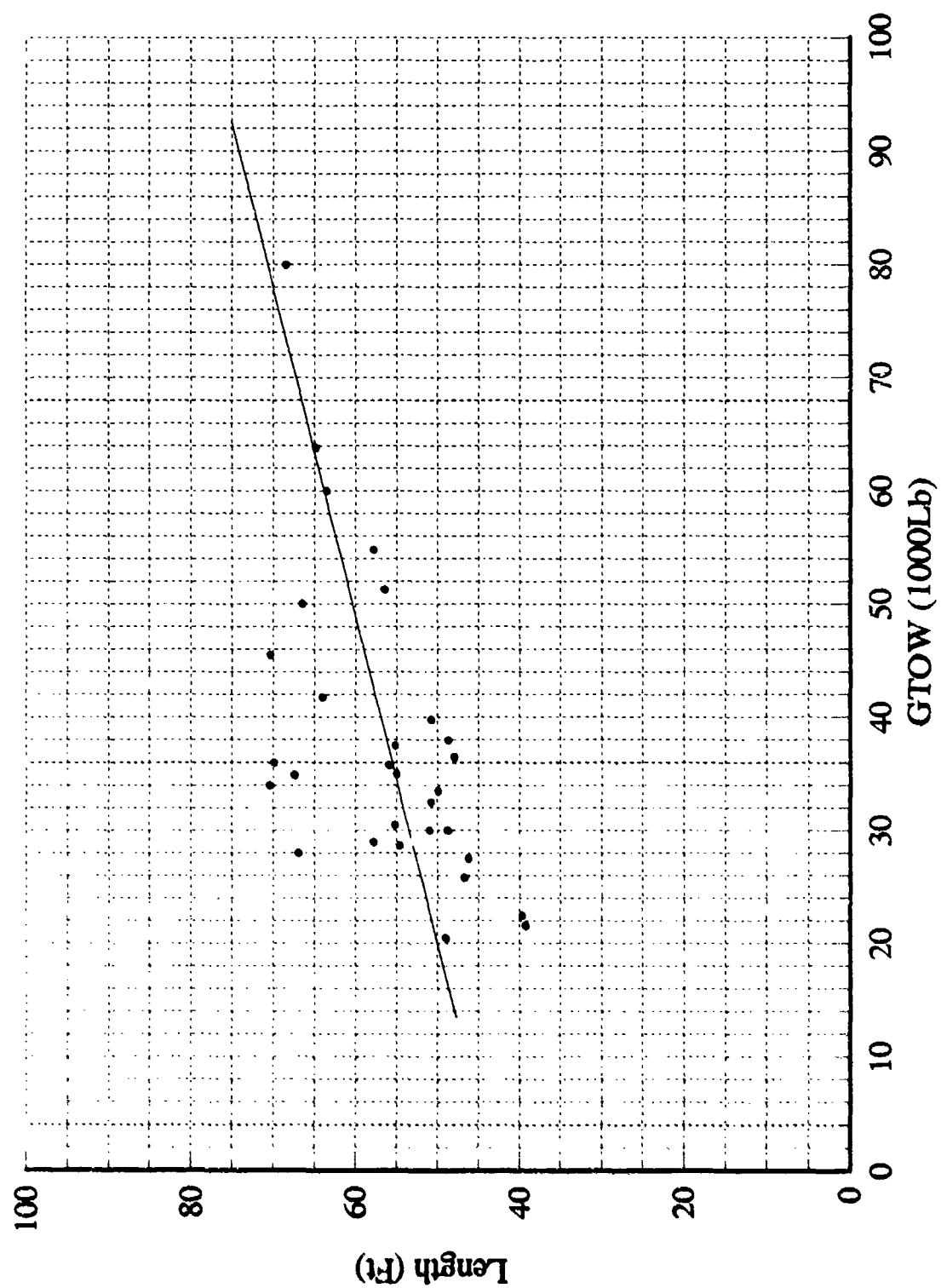


FIGURE 4-4a Length Of Supersonic Fighters

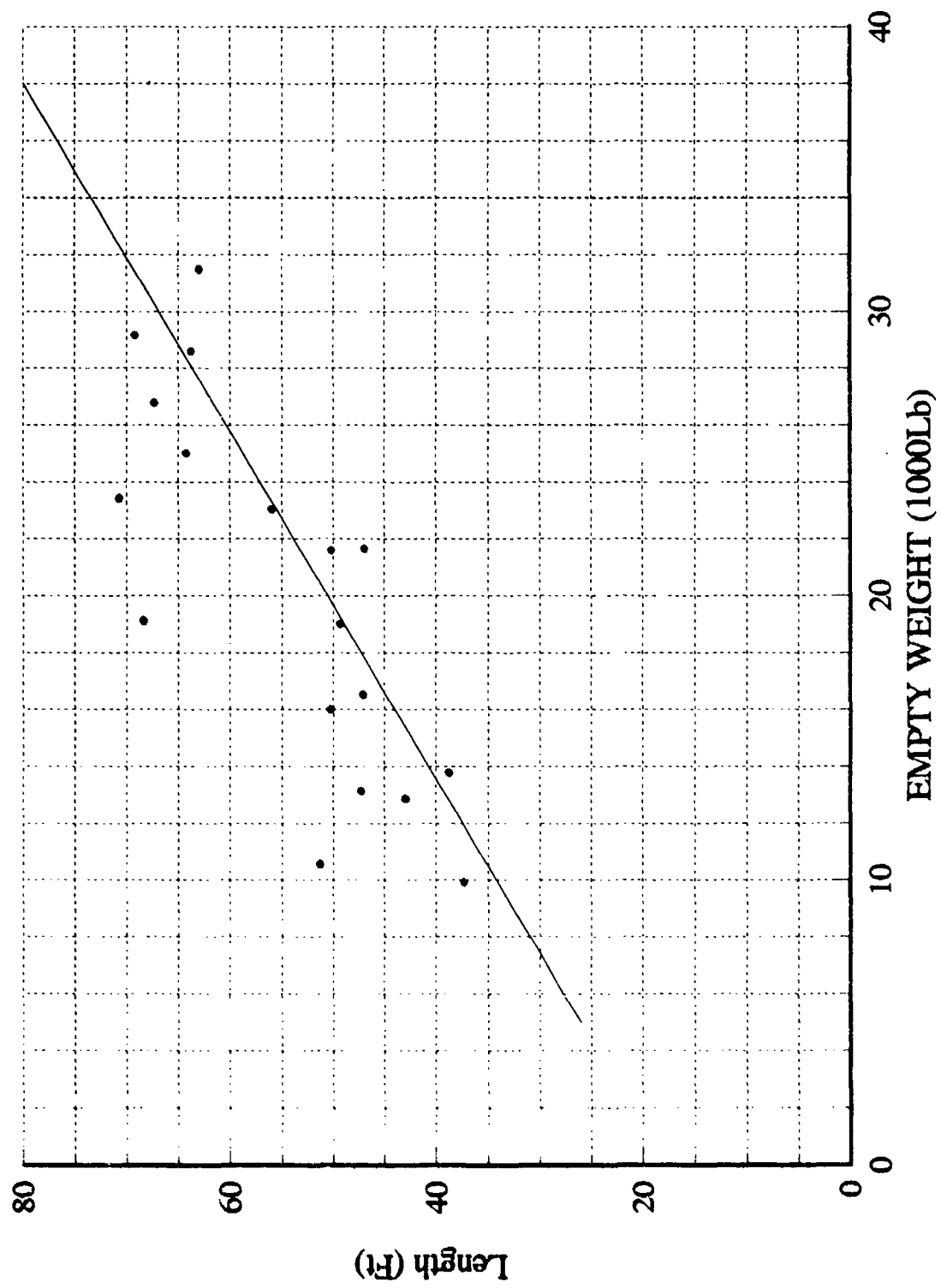


FIGURE 4-4b Length Of Supersonic Fighters

starting point and may be changed as the analysis progresses.

Empty aircraft weight is often considered more important than gross take-off weight in estimating cost. The majority of cost estimating relationships use empty weight for Research, Development, Test and Evaluation costs. In general, empty weight includes all aircraft weight except fuel and payload.

Empty weight fractions are presented in Figure 4-5 for transports and bombers. Empty weight fractions decrease from 0.55 for transport aircraft weighing 100,000 pounds to 0.44 for aircraft weighing 800,000 pounds. Bombers show a similar trend with GTOW with a nominal value of 0.35. In general, bombers are designed for very long ranges and require more fuel than transports. Also the payload requirements are small in comparison to transports. Typical payloads may range from 20,000 to 40,000 pounds.

Empty weight fractions for fighters are higher than transports because of maneuverability requirements. As noted earlier, fighters are designed to fly up to 9 g's. This requires a much heavier structural weight to withstand the flight loads. Fighter empty weight fractions are presented in Figure 4-6 and range from 0.72 at low GTOW's to 0.65 at GTOW approaching 60,000 pounds. The agreement of the design data for past and current aircraft is surprisingly good and may be used with a high degree of confidence.

A corollary to the empty weight fraction is the fuel fraction and payload fraction. It can be seen from Figure 4-7 that the fuel fraction and payload fraction increase with gross-take-off weight for transports. In transport design, many times more fuel will be carried in exchange for payload depending on specific mission needs. In fighter designs, the fuel fraction varies from 0.25 to 0.30 depending on gross weight as illustrated in Figure 4-8. The payload fraction steadily

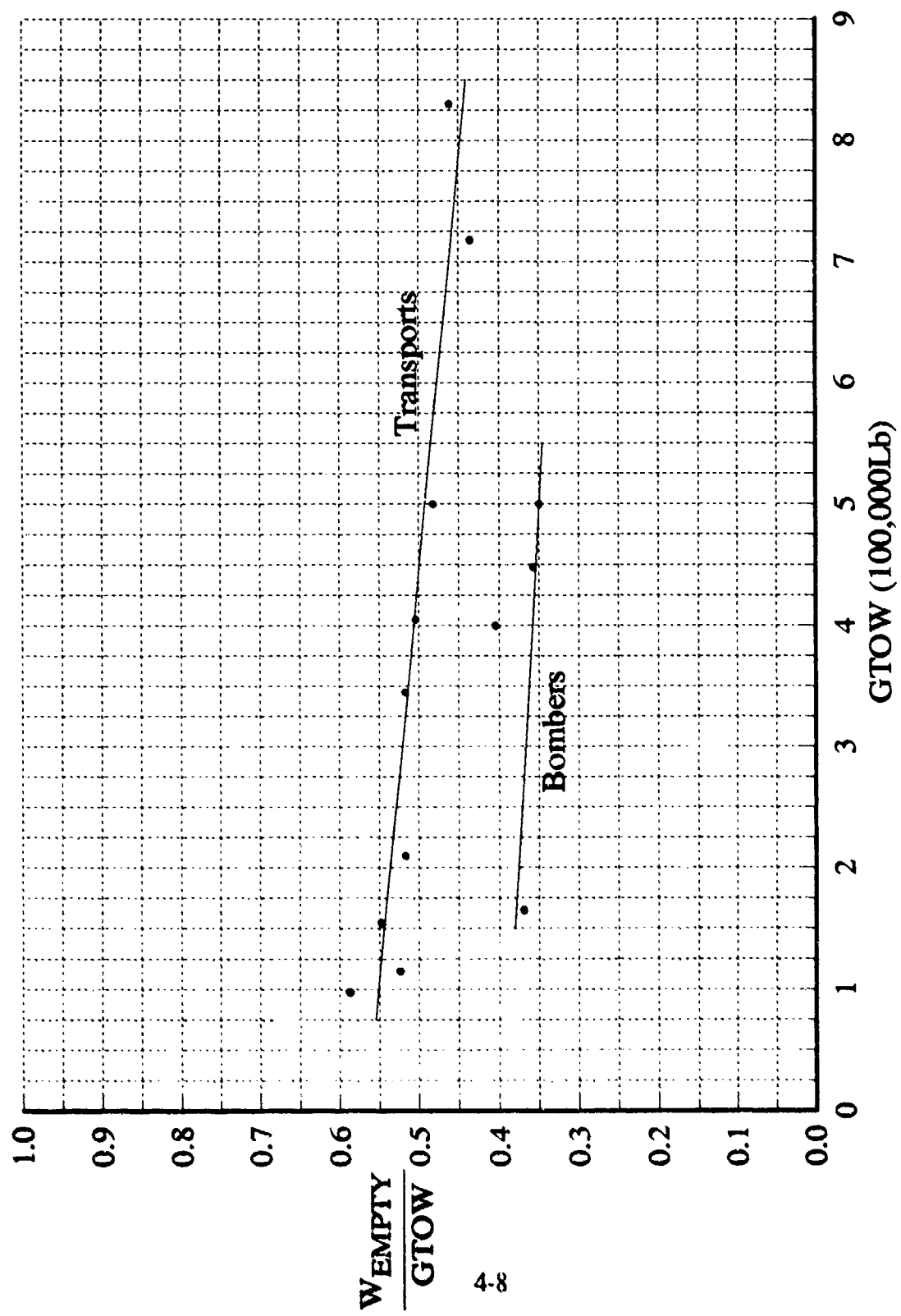


FIGURE 4-5 Empty Weight Fraction For Bombers and Transports

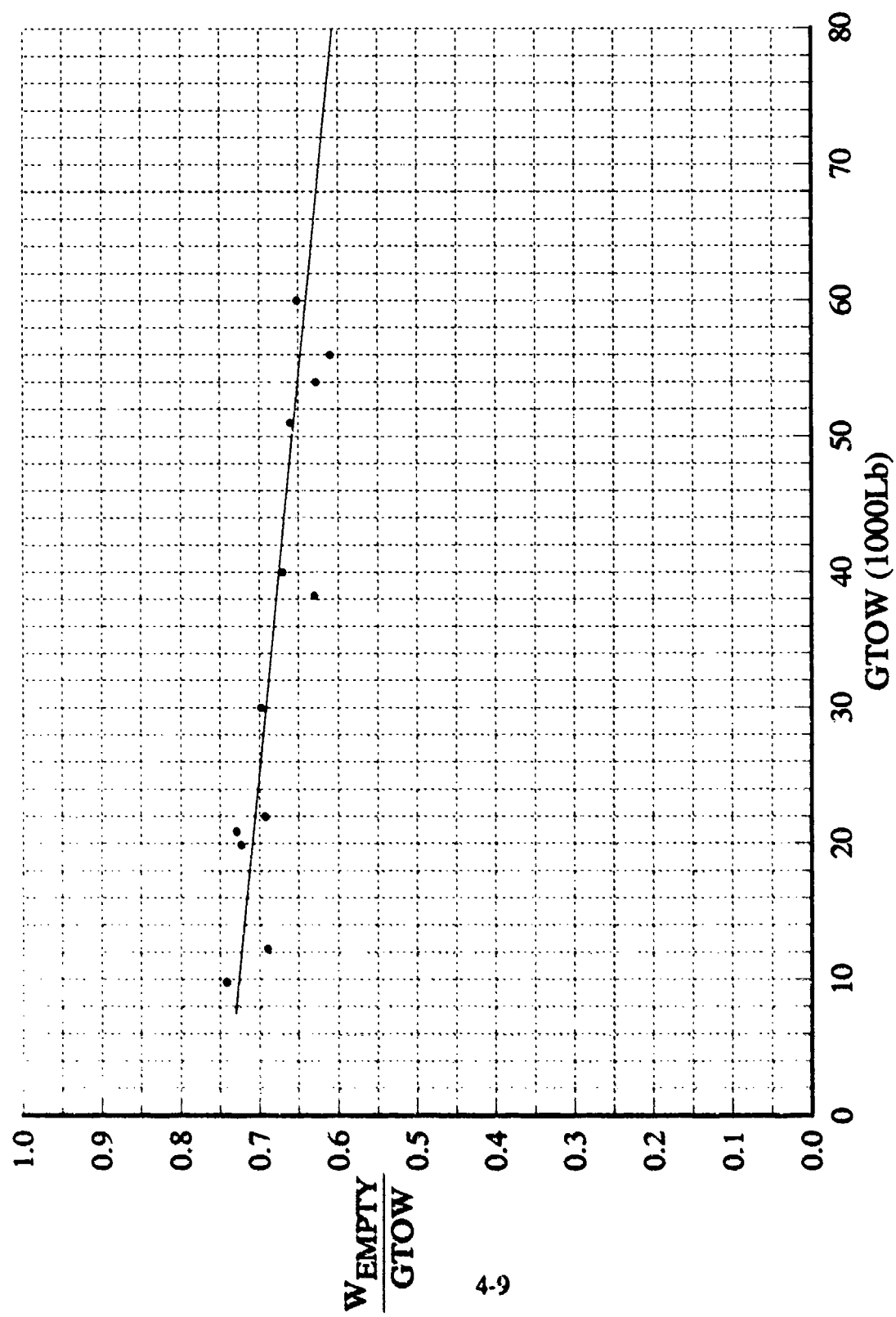


FIGURE 4-6 Empty Weight Fraction For Fighters

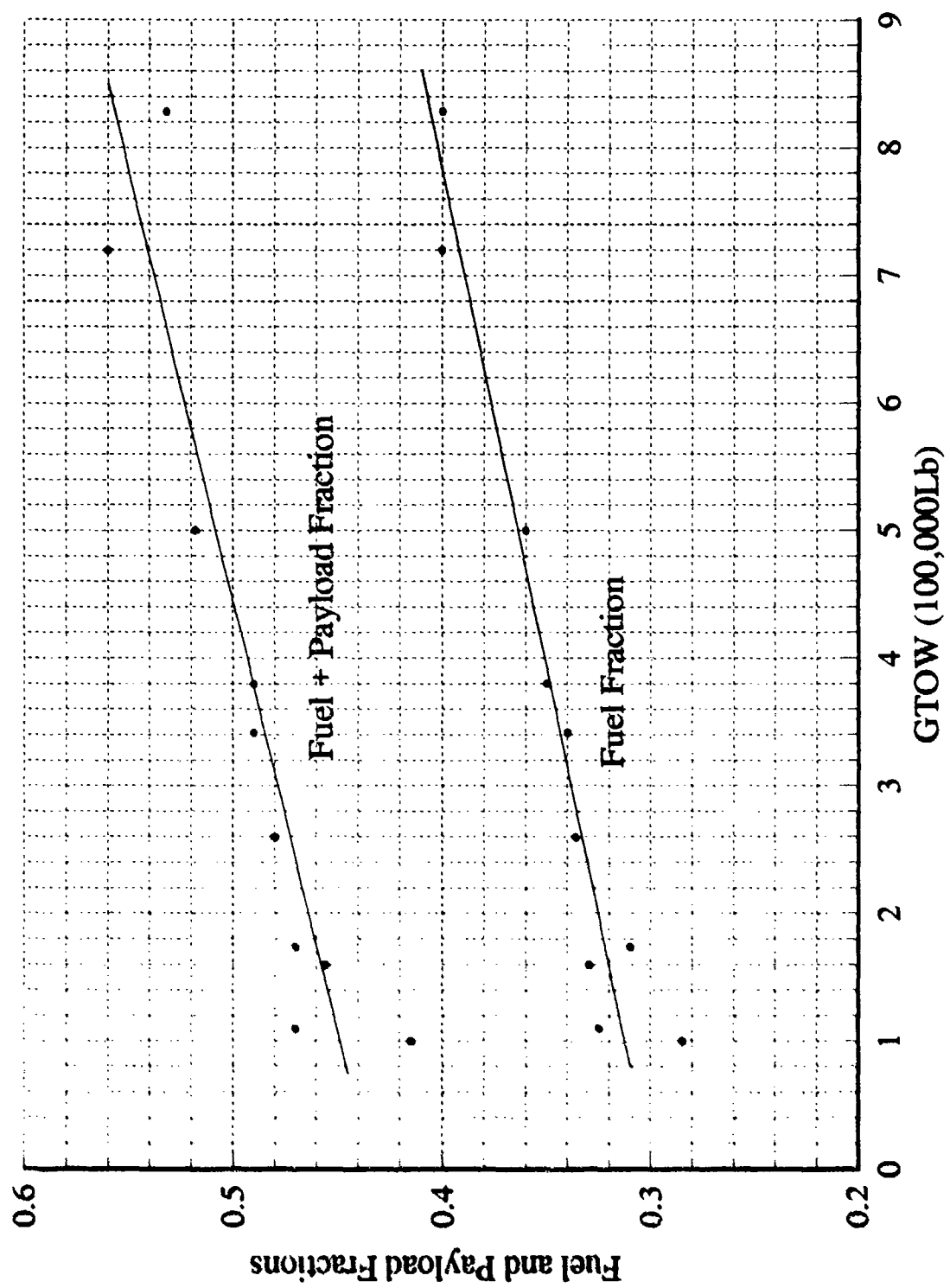


FIGURE 4-7 Fuel And Payload Fraction For Transports

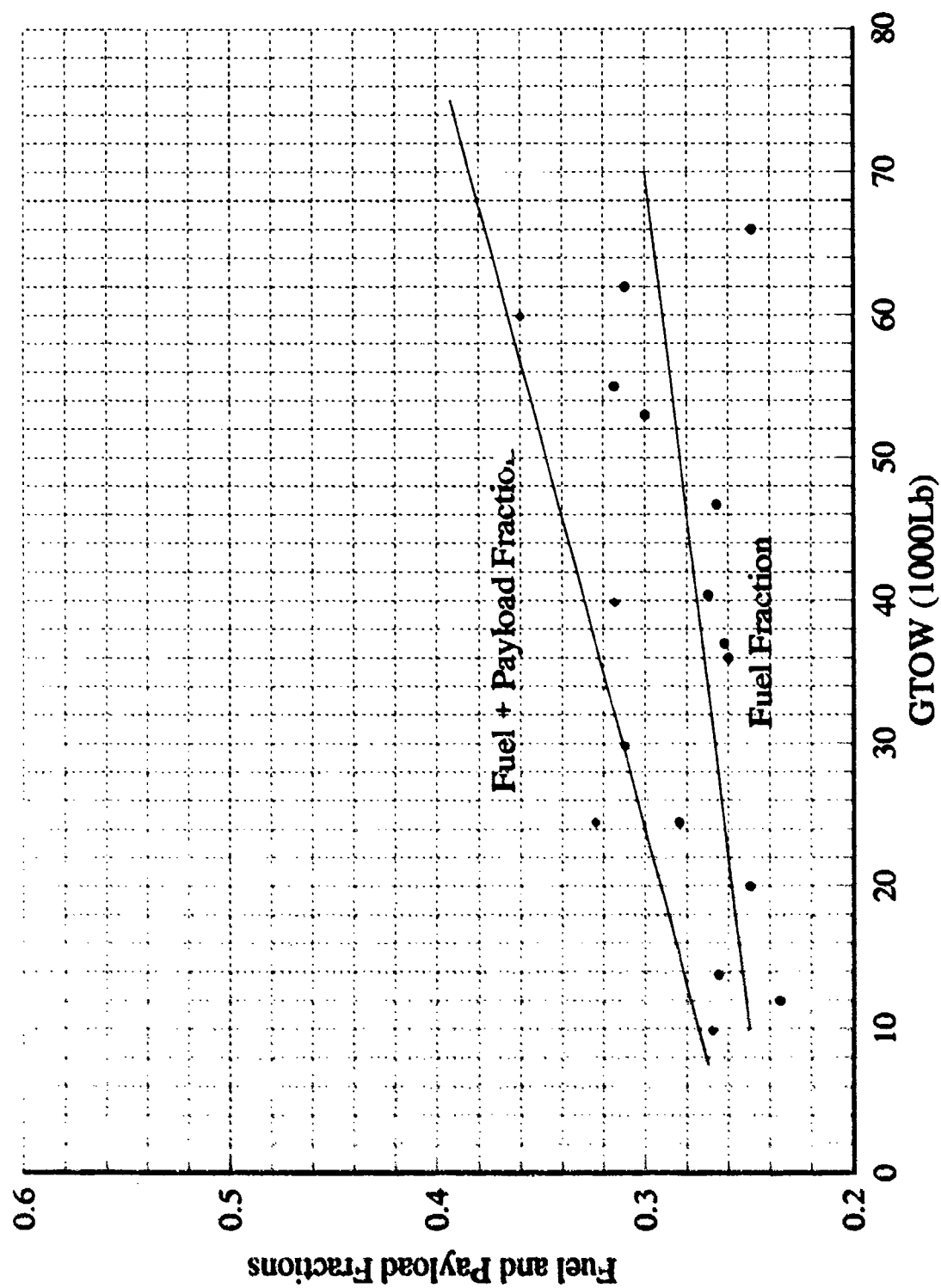


FIGURE 4-8 Fuel And Payload Fraction For Fighters

increases with gross take-off weights up to 60,000 pounds and permits a larger payload to be delivered on targets.

A useful design curve is the wetted area of an aircraft as a function of empty weight. The data for transports and bombers are shown in Figure 4-9. The average weight per square foot of wetted area is 9.25 pounds for cargo planes and 10.4 pounds for bombers. Thus once the wetted area is known, a check can be made on the empty weight or vice versa. Data for fighters are presented in Figure 4-10. There is a little more scatter in the data for fighters because of the more diverse maneuver and landing requirements. The average weight is 12.7 pounds per square foot. This increase in weight is related to the higher load for fighters.

The wetted area and volume of various aircraft were correlated by Caddell in Reference 14. This data, supplemented with additional aircraft by the authors, is presented in Figure 4-11. There is a surprising consistency of the data, and the curve fit equation $A_{WET} = 13.6(V)^{0.688}$ is very useful in sizing the initial configuration. Appendix B contains several volume and wetted area relationships for bodies that are easily defined mathematically, such as Sears-Haack bodies and ellipsoids. The importance of these relationships cannot be over emphasized in the formulation of configurations.

Aircraft density is an interesting parameter to correlate the structural and empty weight of various aircraft. Empty weight was found to correlate the data better than gross take-off weight, since the fuel density (48.6 pounds per cubic foot) is very heavy in comparison to the average dry density of an aircraft, and different amounts of fuel are carried by each aircraft. The dry density parameter is displayed in Figure 4-12 as a variation with empty weight. This information can be used as a check on aircraft volume and provide additional confidence in the

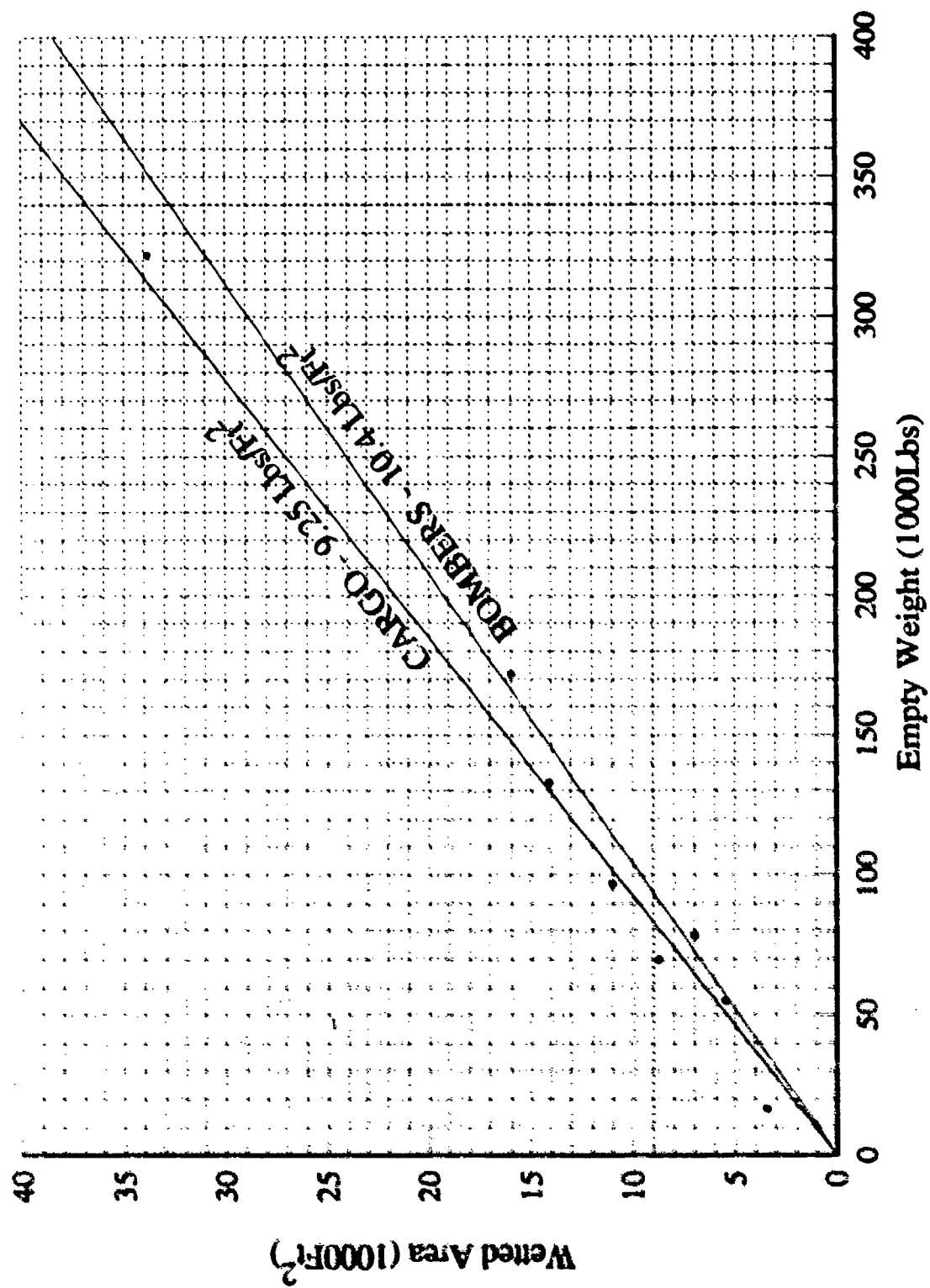


FIGURE 4-9 Wetted Area For Transports And Bombers

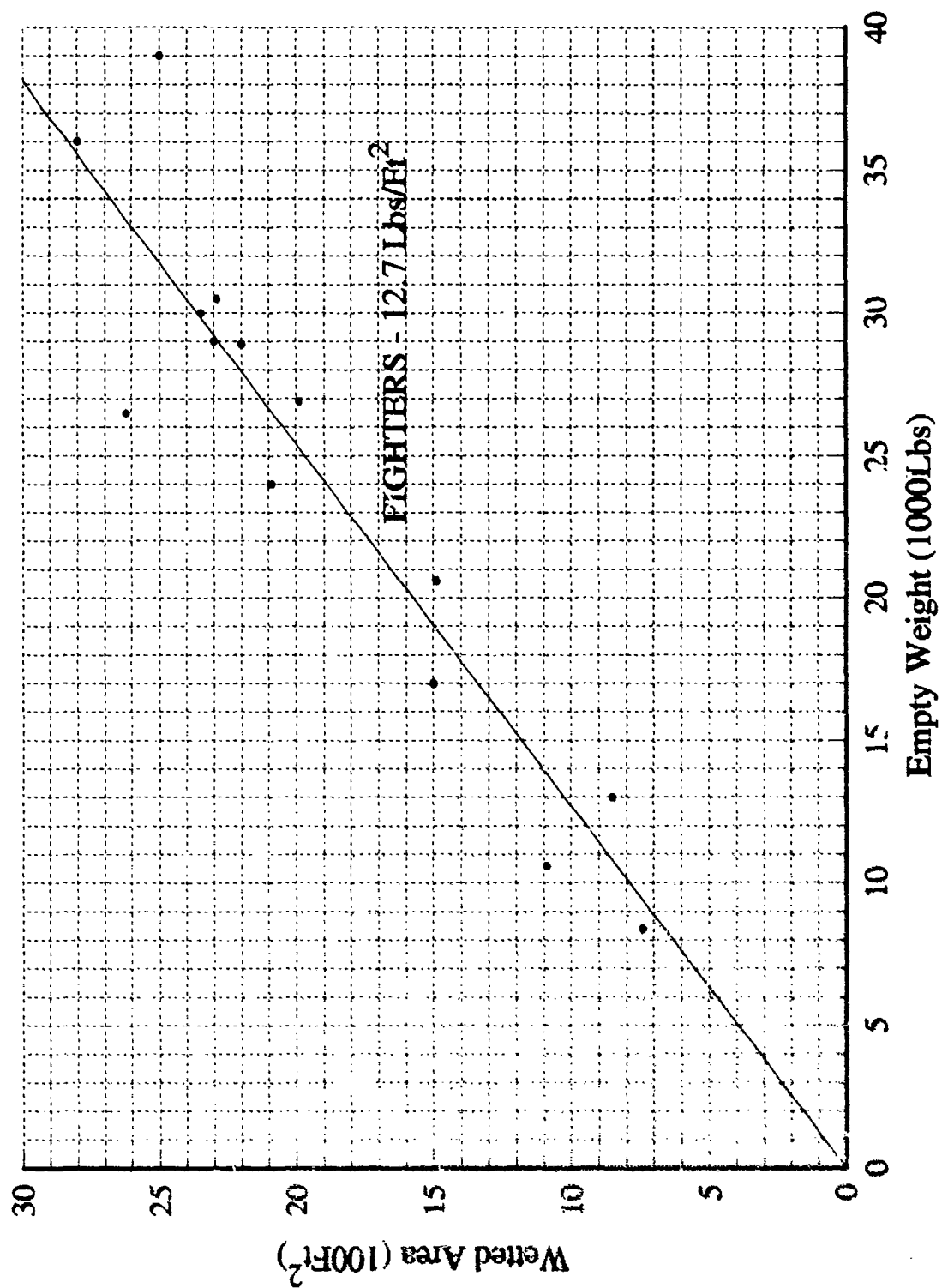


FIGURE 4-10 Wetted Area For Fighters

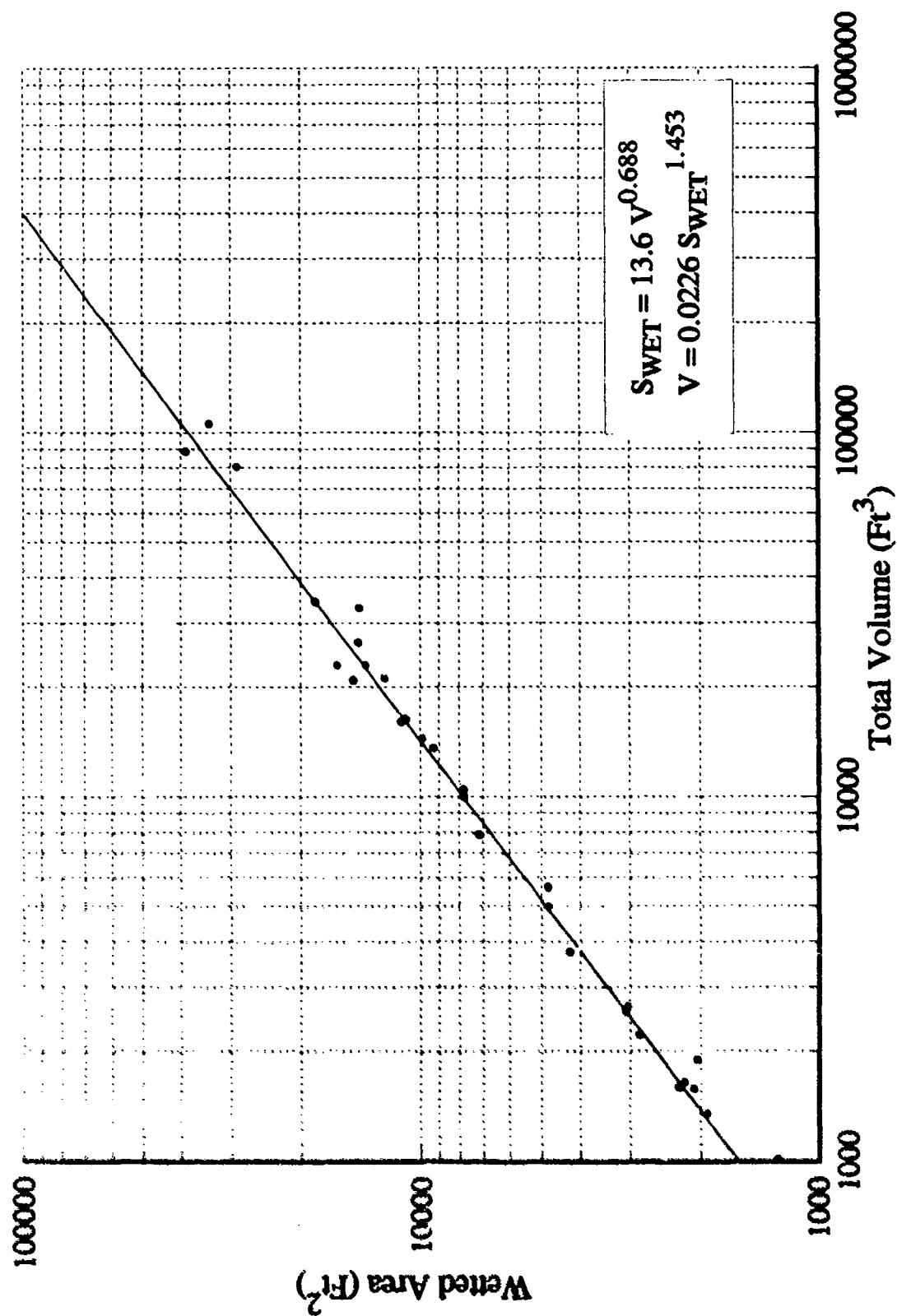


FIGURE 4-11 Aircraft Volume

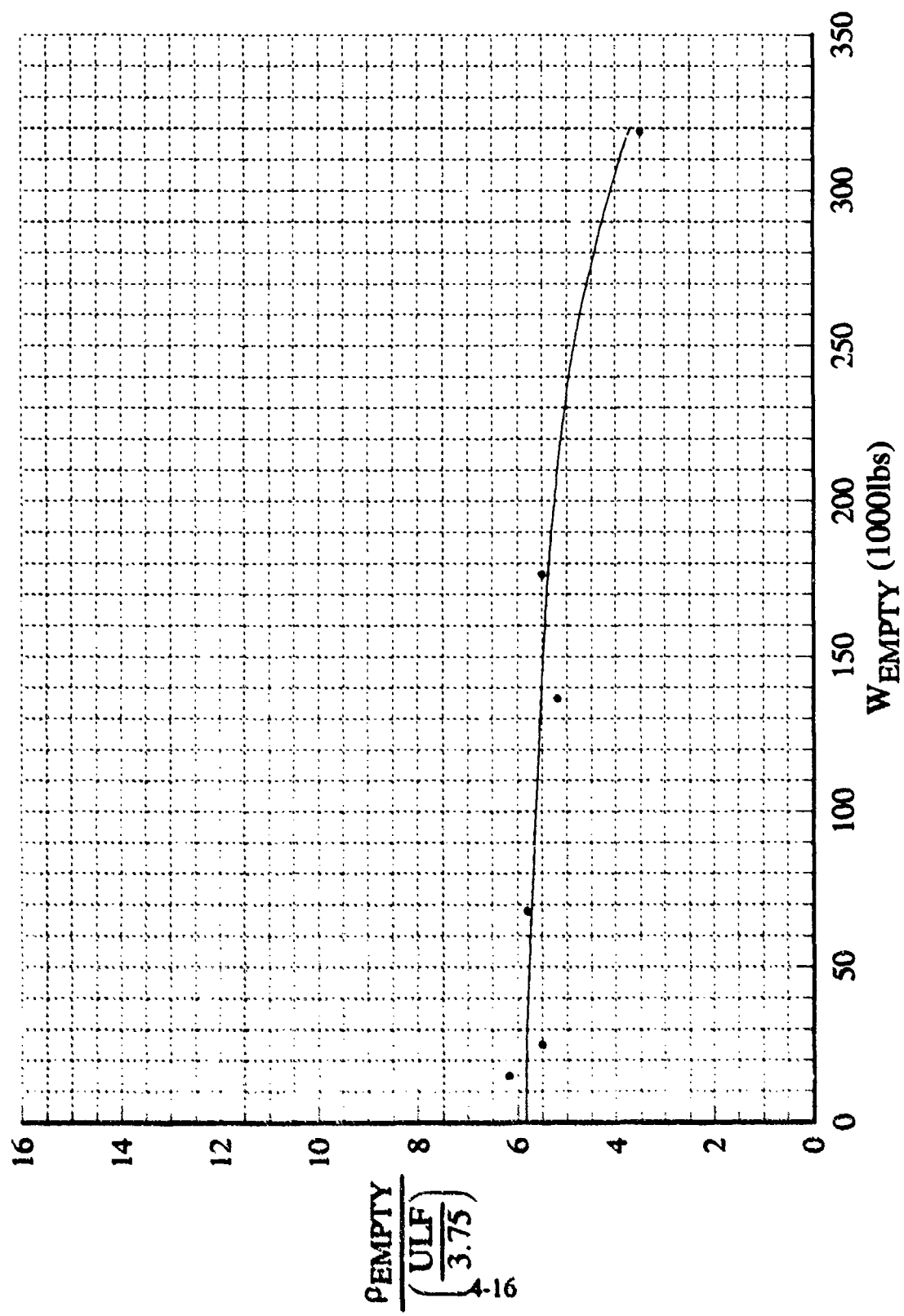


FIGURE 4-12 Aircraft Dry Weight Density Parameter

configuration concept.

The wing area of transport and fighter aircraft can be estimated from wetted area using Figure 4-13. This data has been compiled from a host of aircraft and relates wing area to wetted area. It is informative to observe that fighters range between ratios of 4 and 5 and transports between 5 and 6. Obviously, the above procedure can be reversed. The wetted area may be calculated once the wing area has been defined from other sources. This frequently occurs when estimating the total skin friction drag on a configuration.

The wing geometry and area are extremely important in formulating an aircraft configuration (References 15 - 18). The wing loading parameter, W/S is obtained by dividing the aircraft weight by the wing area. The span loading parameter, W/b^2 is obtained by dividing the aircraft weight by the square of the wing span. These parameters dictate the range and maneuvering efficiency of an airplane. The aspect ratio of a wing relates the wing loading and span loading: $AR = \frac{W/S}{W/b^2} = \frac{b^2}{S}$. A parametric curve illustrating this relationship is presented in Figure 4-14. Various aircraft are displayed on the plot. A close study reveals that fighters have an aspect ratio range of 2.5 to 3.5 and transport aircraft between 7.5 and 8.5. These are values that need to be remembered since they can be used as initial estimates in most aircraft designs.

The wing sweepback angle is shown as a function of wing aspect ratio in Figure 4-15. Most fighters range between 40 to 50 degrees. This is a compromise between low speed cruise, transonic maneuvering and supersonic speed requirements. The design cruise Mach number for several aircraft is illustrated in Figure 4-16. It is instructive to note that as the cruise speed exceeds Mach 1.0, there is a sharp break in the sweepback angle and it gradually increases to a value of 60 degrees at Mach 2.

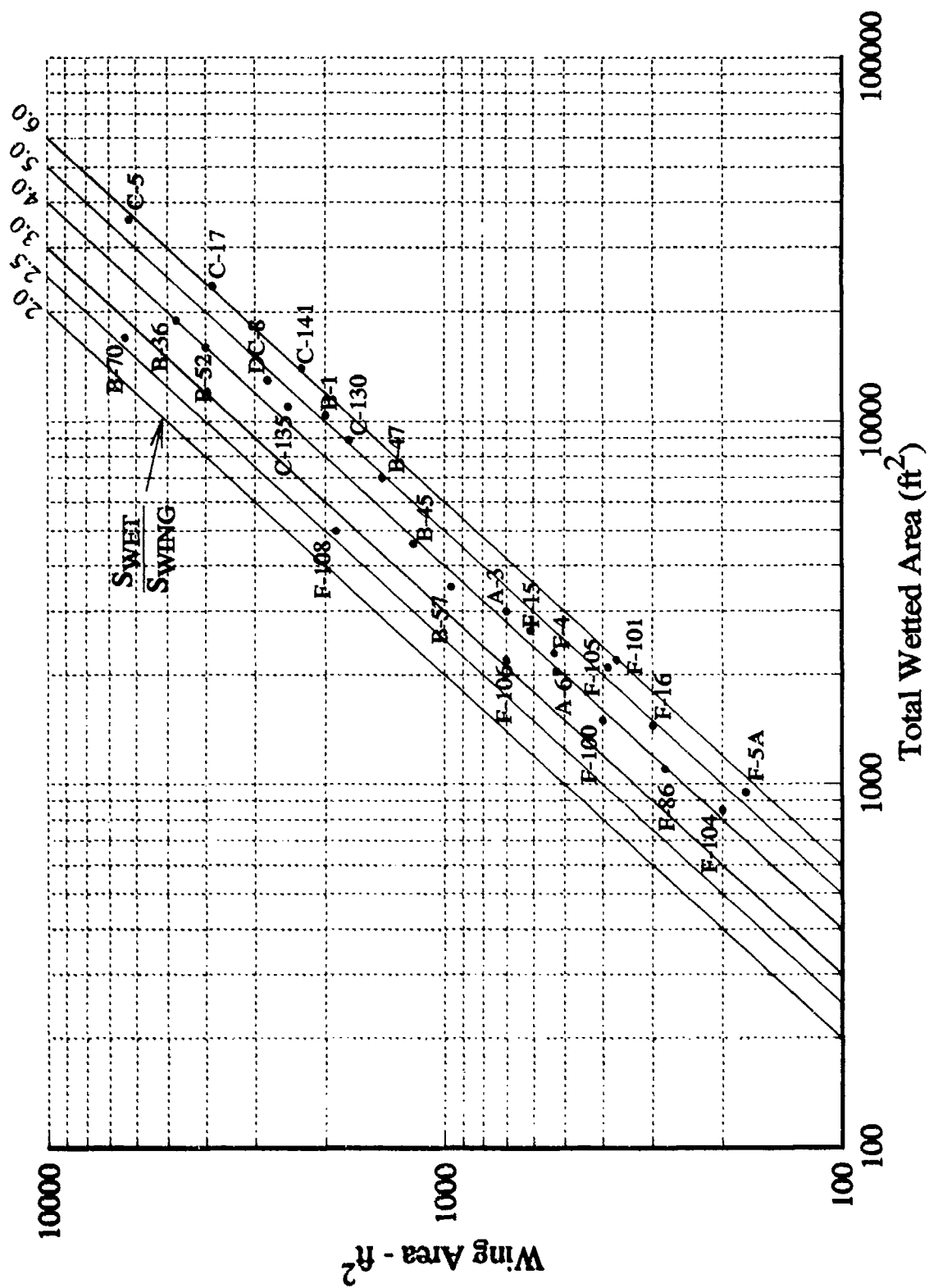


FIGURE 4-13 Wing Area And Wetted Area

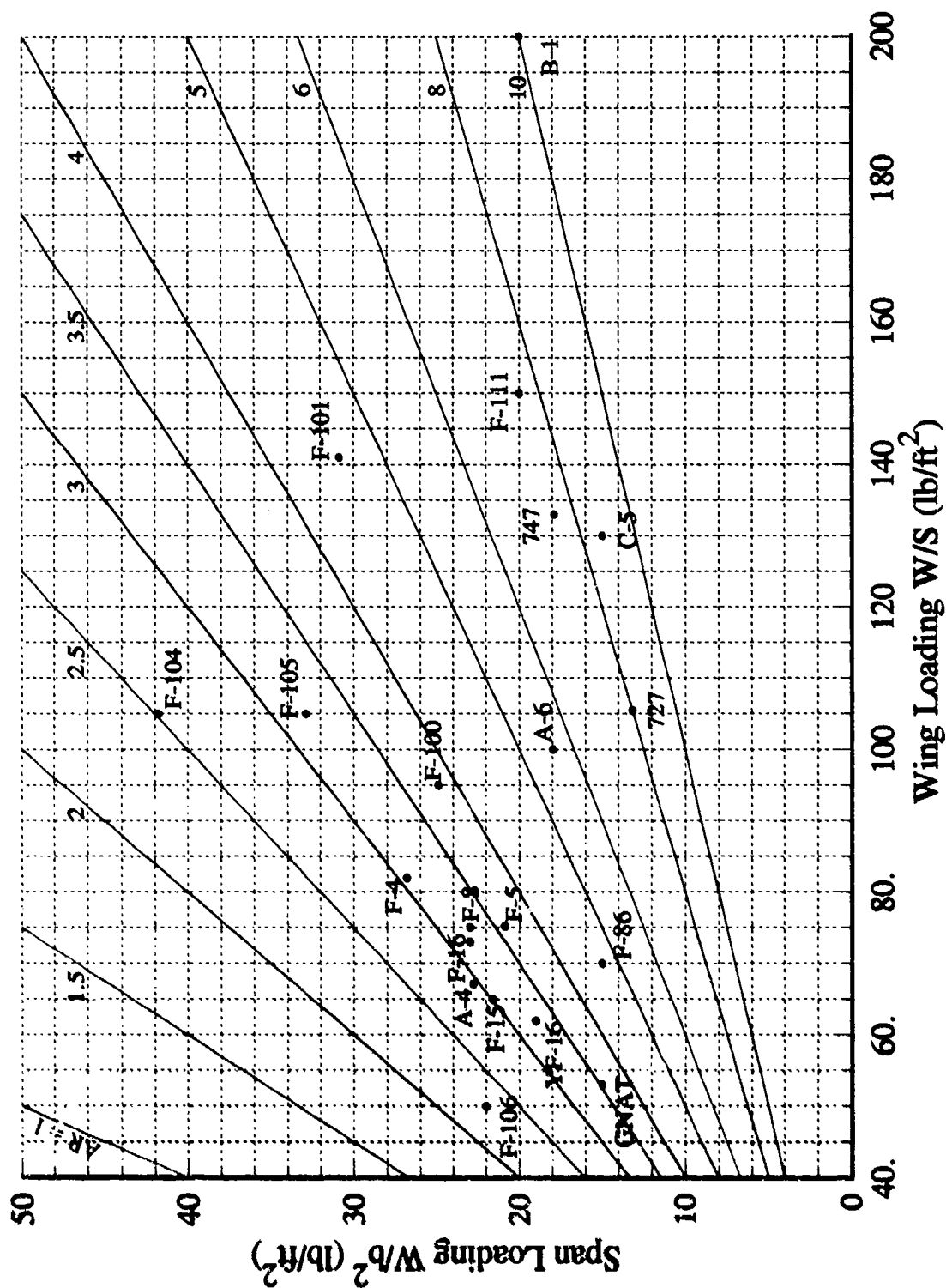


FIGURE 4-14 Span Loading And Wing Loading

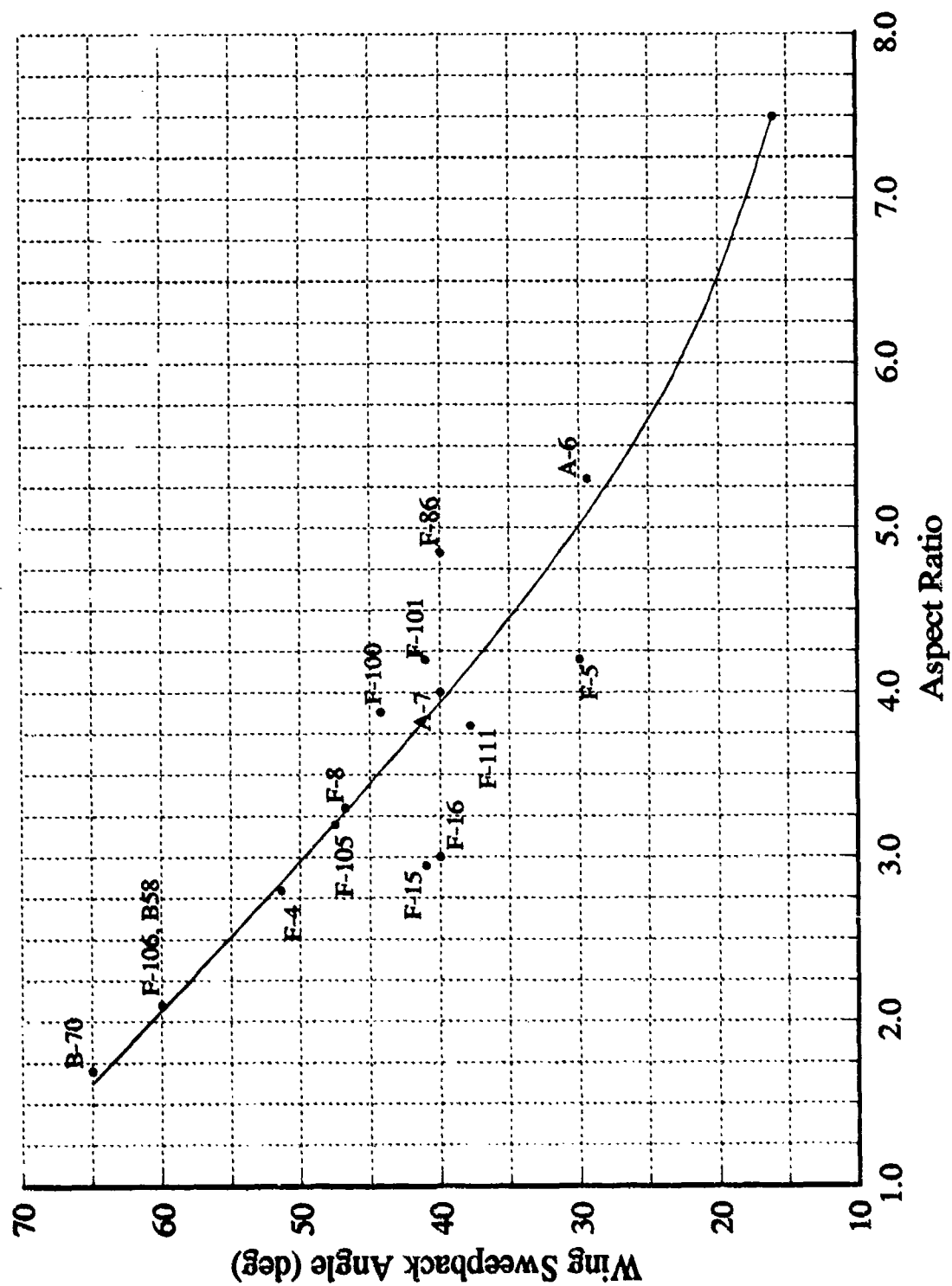


FIGURE 4-15 Fighter Aspect Ratio and Wing Sweepback

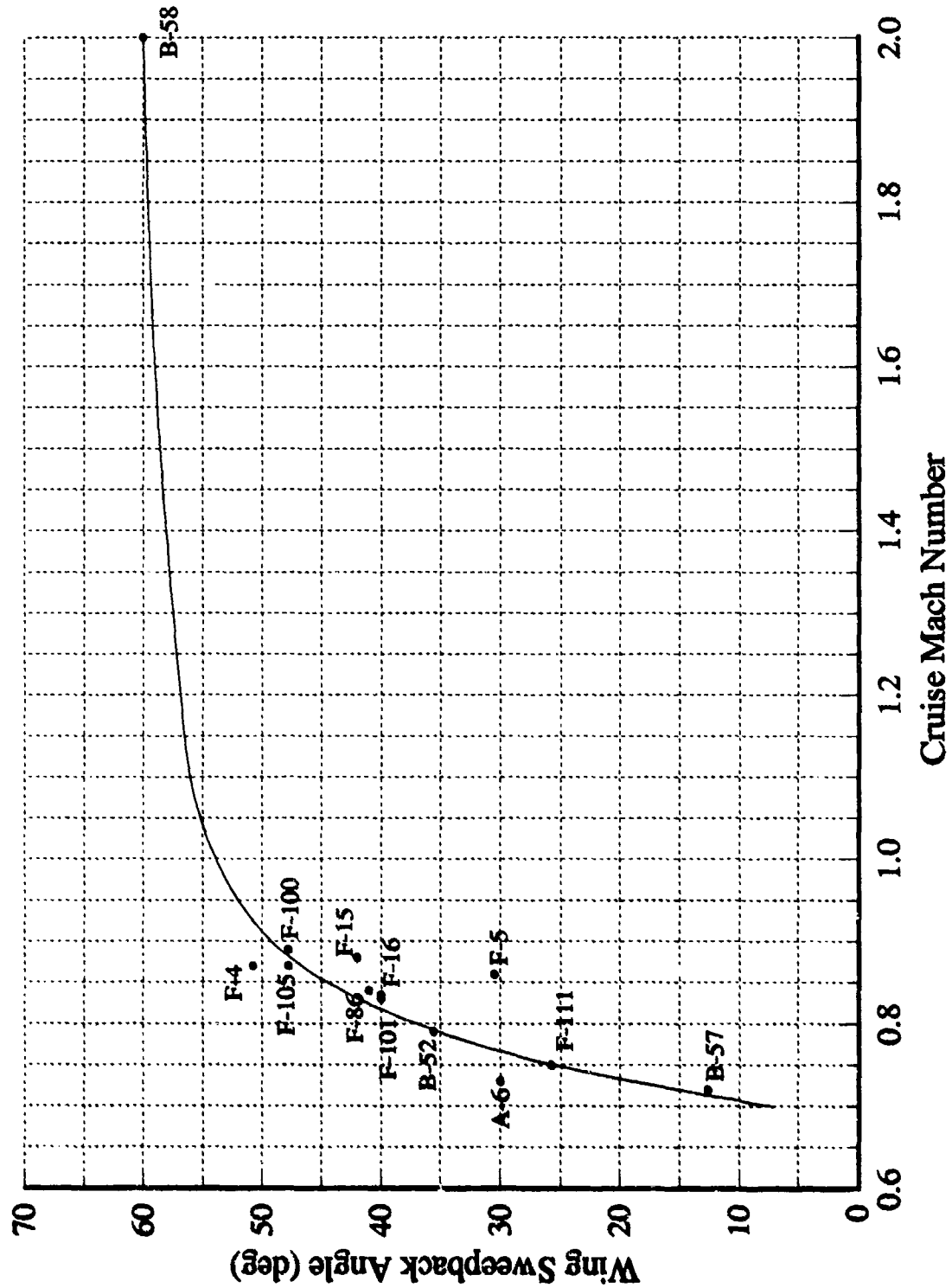


FIGURE 4-16 Wing Sweepback Angle

Another critical wing parameter is the thickness ratio. The higher thickness allows more fuel to be carried internally in the wing but will result in increased wave drag at transonic and supersonic speeds. Thus, the thickness ratio must be tempered if the airplane has a supersonic speed requirement. This is discussed more extensively in the next section of this report. Figure 4-17 shows a range of thickness ratio values for both fighter and cargo airplanes. Fighters tend to be around 5 percent and transports in the range 10 to 12 percent.

A design curve is presented in Figure 4-18 to rapidly configure a wing, based on wing area, wing span, wing root chord and wing taper ratio λ . It may be used for rectangular wings ($\lambda = 1$), delta wings ($\lambda = 0$) and for the more common trapezoidal wings.

The size of the horizontal tail in initial designs is estimated from tail volume coefficients. This coefficient is defined as:

$$C_{HT} = \frac{l_{HT} S_{HT}}{c S_{Wing}}$$

Data from previous aircraft are presented in Figure 4-19. It can be seen the relationship is linear and corresponds to a nominal value of $C_{HT} = 0.267$. Through a 3-view layout of a conceptual configuration a nominal value of the distance from the horizontal tail quarter chord to the wing quarter chord (l_{HT}) may be estimated. This permits the determination of the horizontal tail area. If a drawing is not available, a representative horizontal tail area of 15 to 20 percent of the wing area may be used at this stage of the design cycle. The exact size and location will be determined from longitudinal stability requirements at a later stage in the design.

The size of the vertical tail is estimated in a similar fashion with a vertical tail volume coefficient:

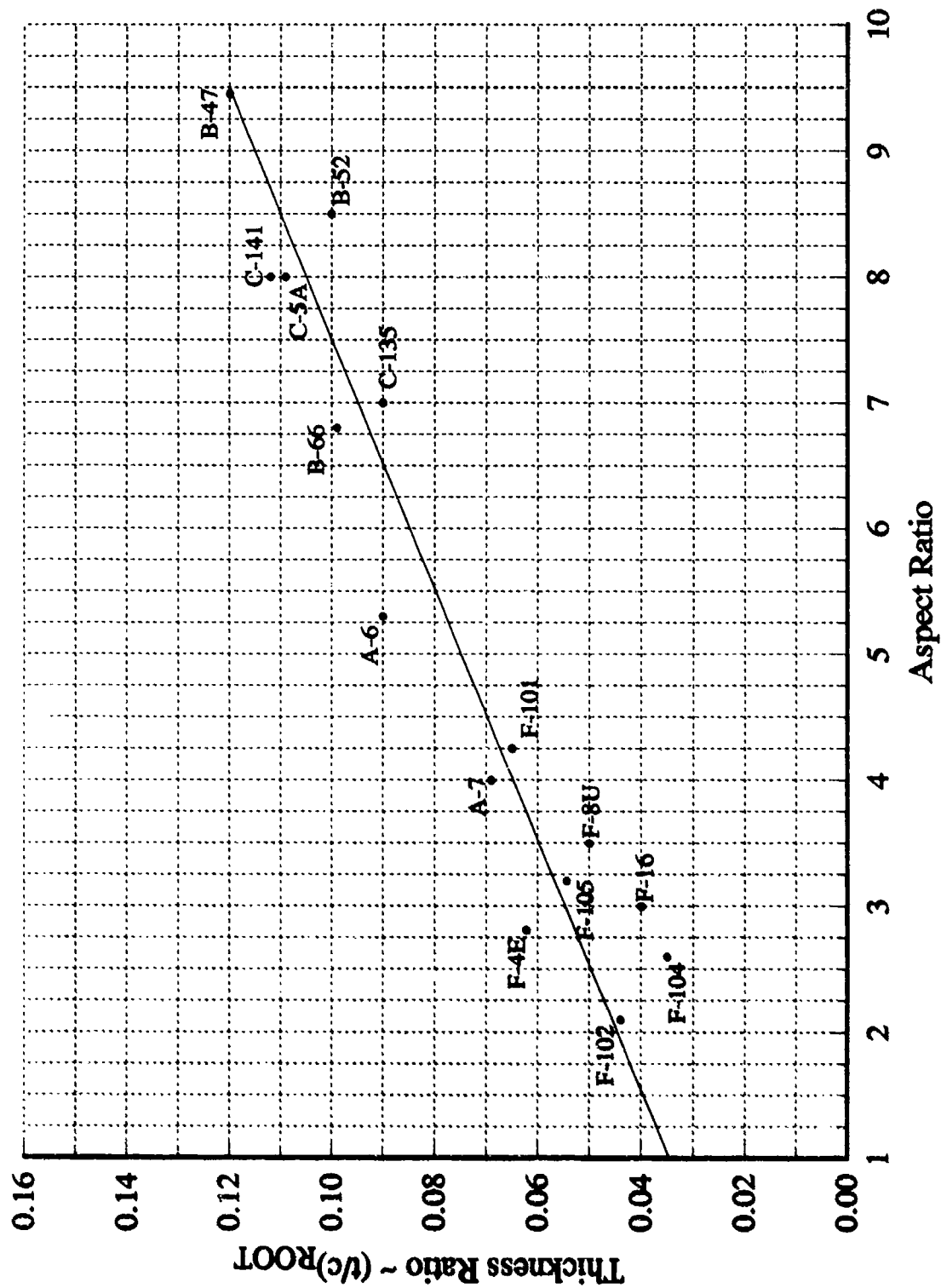


FIGURE 4-17 Aspect Ratio and Wing Thickness Ratio

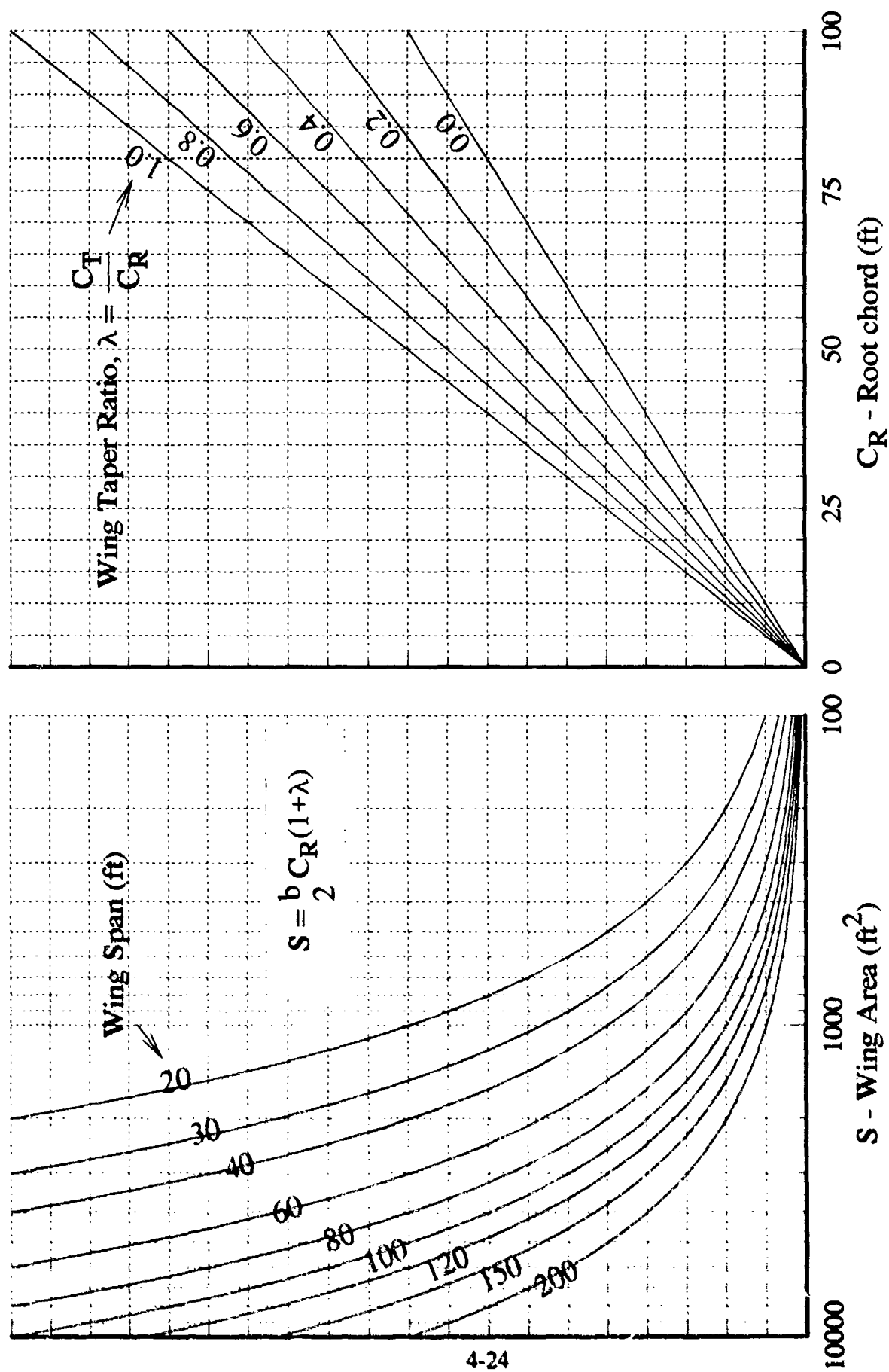


FIGURE 4-18 Wing Characteristics

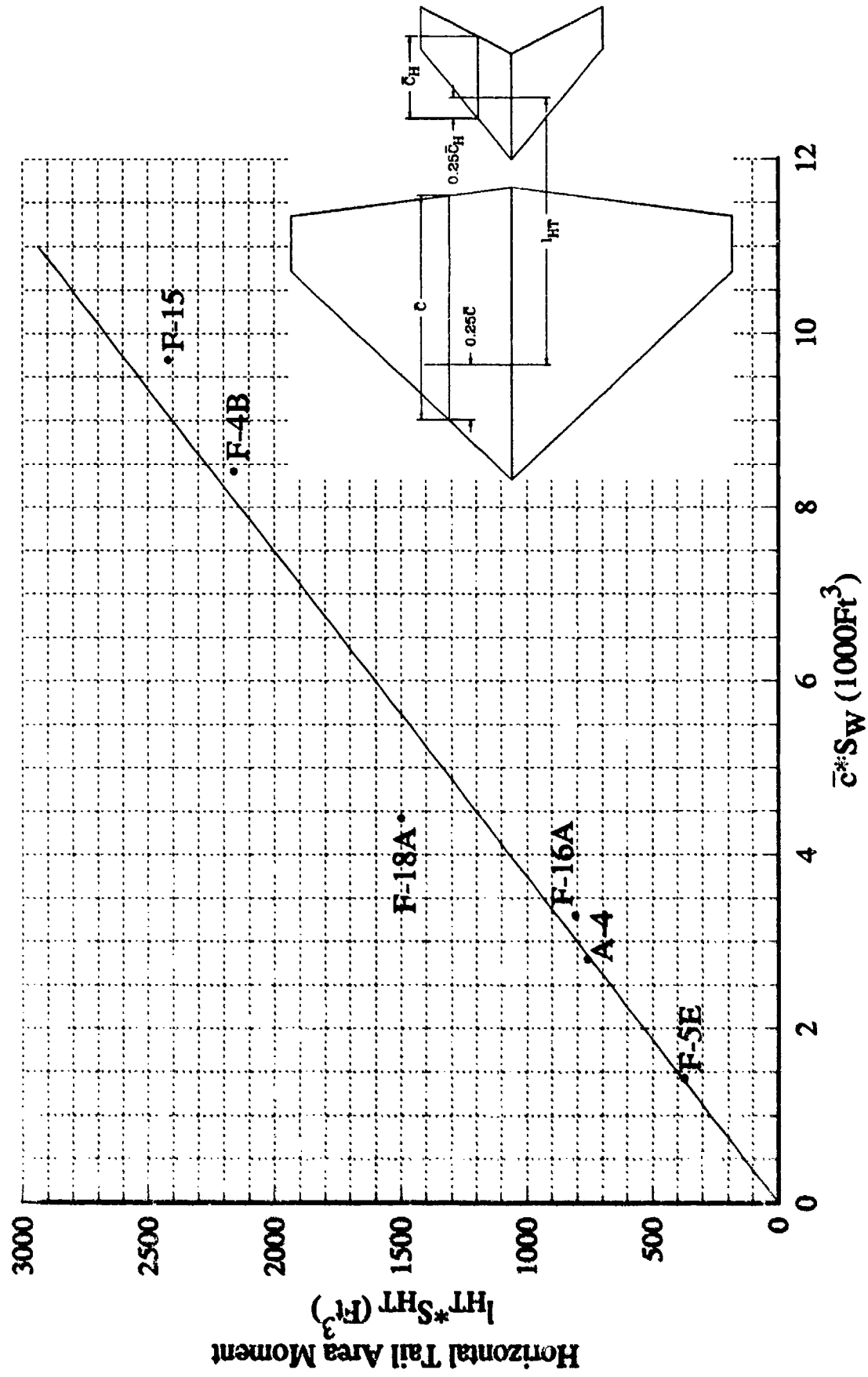


FIGURE 4-19 Horizontal Tail Sizing Guideline

$$C_{VT} = \frac{l_{VT} S_{VT}}{b S_{Wing}}$$

The moment arm l_{VT} is determined from the 3-view drawing. The volume coefficients for various aircraft are shown in Figure 4-20. The nominal vertical tail volume coefficient is 0.077 for these aircraft. If a drawing is not available, a representative vertical tail area of 15 to 20 percent of the wing area may be used at this stage of the design cycle. The exact size and location will be determined from directional stability requirements at a later stage in the design.

The design data contained in this section of the report may be used to formulate initial conceptual aircraft configurations. The initial configuration then requires analyses to predict its aerodynamic characteristics and determine if the airplane can meet its performance characteristics. The configuration could also be used as the input to an automated vehicle synthesis program for more extensive tradeoff analysis and definition.

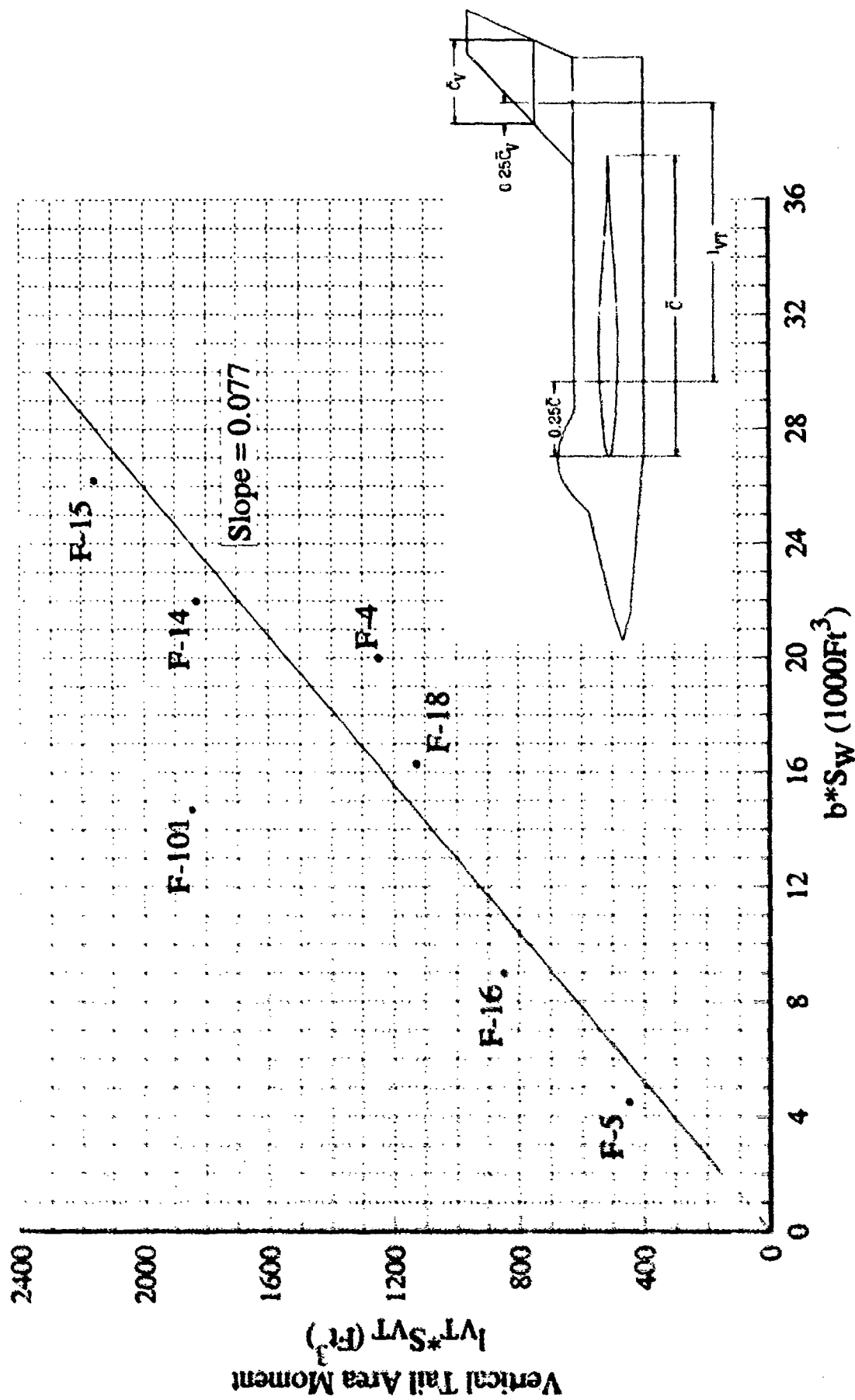


FIGURE 4-20 Vertical Tail Sizing Guideline

5. METHODS AND DATA TO ESTIMATE PRELIMINARY AERODYNAMIC CHARACTERISTICS

There is a growing tendency in the aerospace industry to use sophisticated computational fluid dynamic codes early in the design cycle to predict aircraft flow fields and associated aerodynamic characteristics. This approach is currently very time consuming and needs to be tempered in the early conceptual design phase of a configuration concept. A more simplified approach is to initially use semi-empirical methods (Reference 6) and linear theories to provide rapid and first order estimates of the initial configuration. These results are generally adequate at this stage of configuration development, plus they provide insight into the configuration design drivers. They also can be used for comparison with CFD predictions later in the design cycle. This engineering approach will gradually change to CFD as the codes mature and computers become faster and more economical.

This section of the report provides a convenient compilation of design data and simplified expressions to predict the drag, lift, and lift-to-drag ratio of fighter, bomber and transport aircraft. An extensive discussion of drag is presented because of its critical impact on the range of aircraft and the configuration shape. Of particular interest are design data to estimate drag at Mach 1.2 and the lift-to-drag ratio at various Mach numbers.

A convenient chart of dynamic pressure contours as a function of speed and altitude is presented in Figure 5-1 which can be used in assessing aerodynamic and performance characteristics. Another often needed parameter, shown in Figure 5-2, is Reynolds number per foot as a function of speed and altitude. It is used in estimating skin friction drag of aircraft.

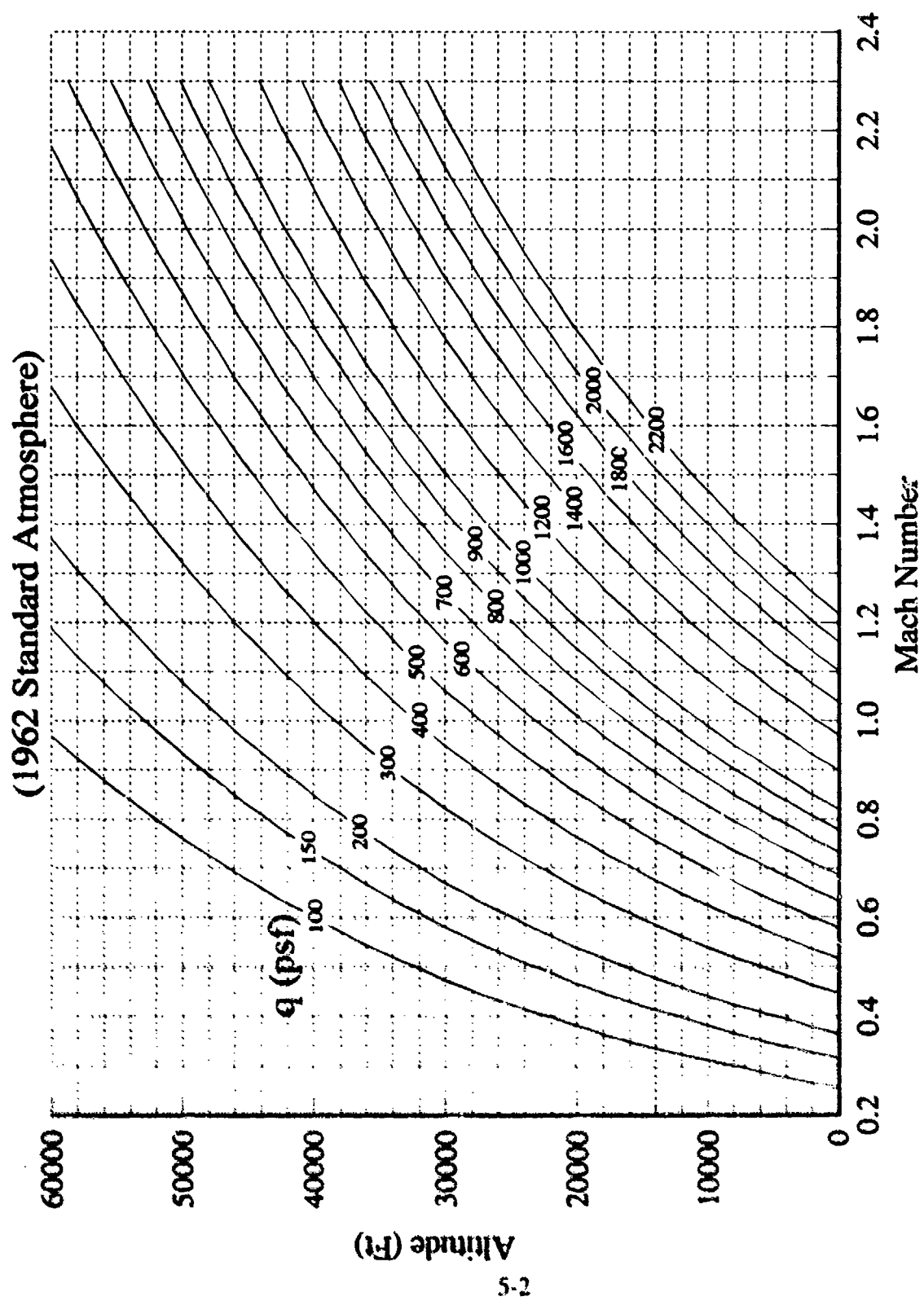


FIGURE 5-1 Dynamic Pressure Contours

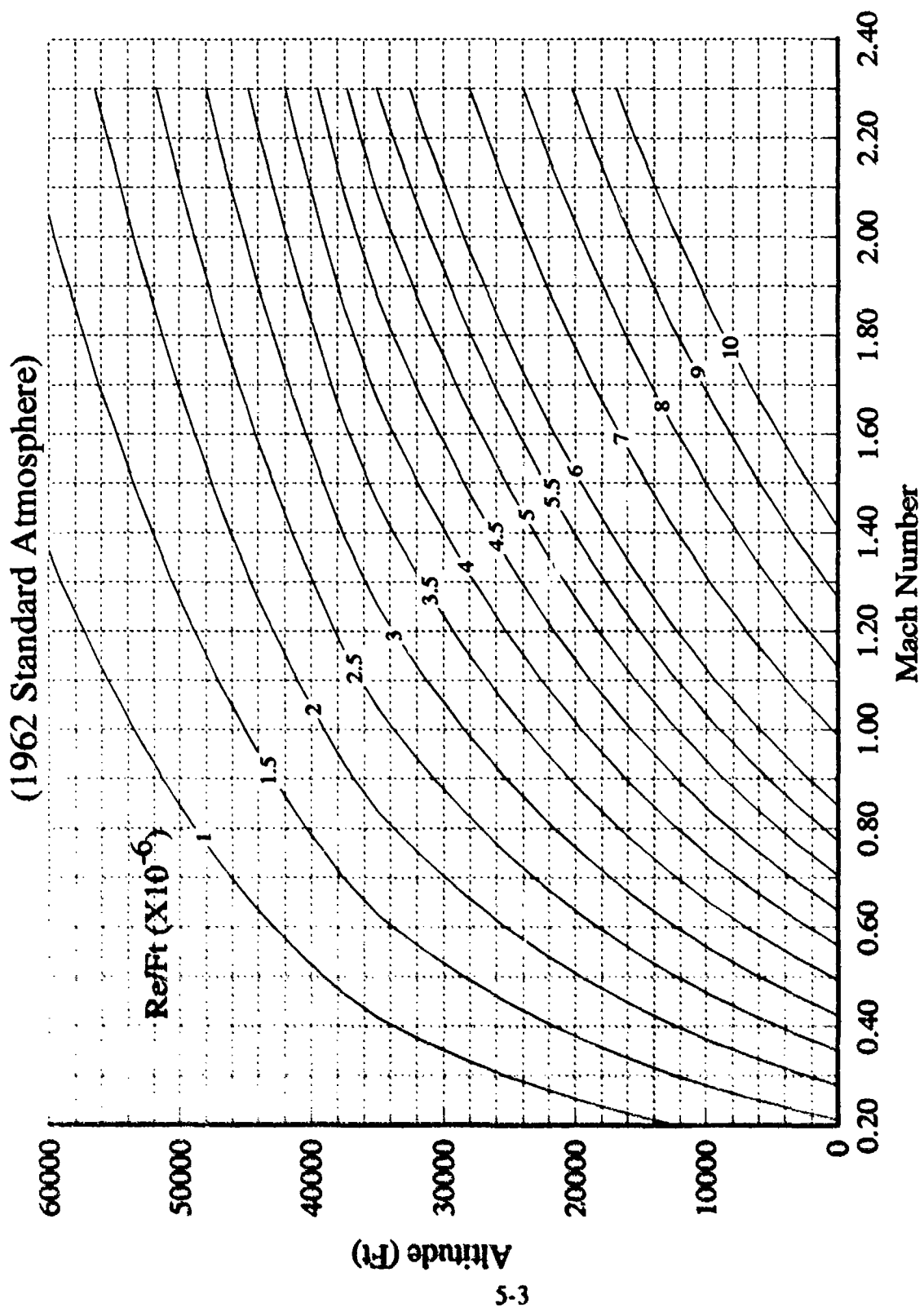


FIGURE 5-2 Reynolds number Contours

AERODYNAMIC DRAG

The aerodynamic drag forces on a body are fundamentally the result of the horizontal components of the normal and tangential forces transmitted from the air to the body (Reference 19). The friction or tangential forces are the result of viscous effects within the boundary layer, and the normal forces are the result of the local surface pressures. To the rear of the body an additional pressure drag results because of separation in the formation of a turbulent wake. The drag resulting from the pressure variation over and behind the body is generally defined as pressure or form drag; that due to the shear forces in the boundary layer is usually called skin-friction drag. For an airplane the summation of the two types is referred to as profile drag, (C_{Dp}) as noted in Figure 5-3. In determining the minimum profile drag, $C_{Dp \text{ Min}}$, several secondary drag forces are normally included: interference, excrescence and roughness. Interference drag is that drag caused by the over-lapping of local pressure or flow fields and would not be found on vehicle components in isolation. Excrescence drag is created by surface irregularities such as gaps, mismatches, small protuberances, and leakage due to pressurization. Roughness drag is drag resulting from surface texture, and is the result of increased disturbances within the turbulent boundary layer.

The total drag of an aircraft can be represented as the sum of minimum profile drag ($C_{Dp \text{ Min}}$), plus the change in profile drag due to angle of attack or lift (ΔC_{Dp}), plus drag due to lift or induced drag (C_{Di}), plus drag due to Mach number such as compressibility or wave drag (C_{DW}), plus drag due to trim (C_{Dtr}). The parts of airplane total drag are illustrated in figure 5-3.

$$C_D = C_{Dp \text{ Min}} + \Delta C_{Dp} + C_{Di} + C_{DW} + C_{Dtr}$$

Drag Prediction / Definition

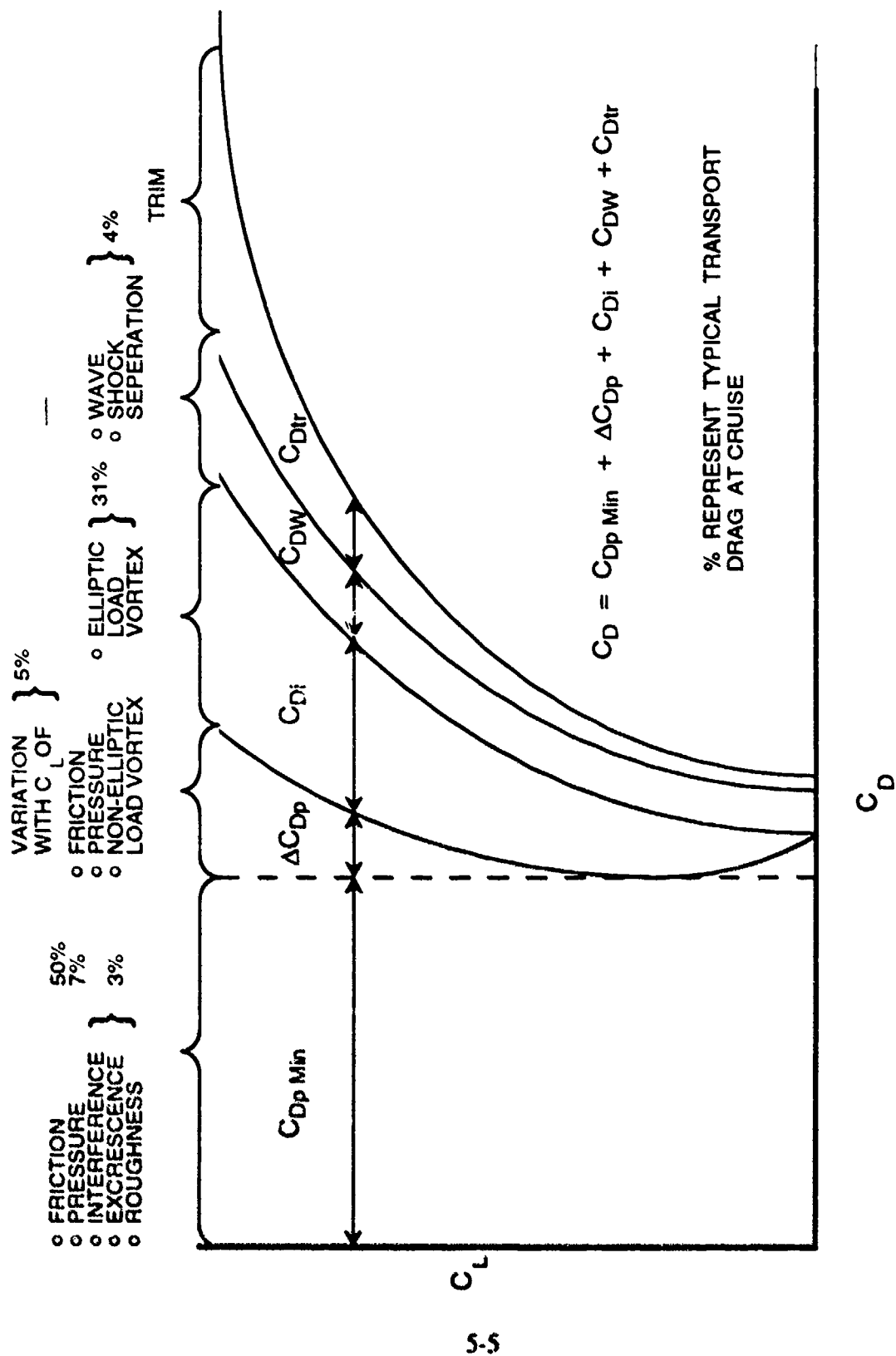


FIGURE 5-3 Drag Prediction / Definition

The estimation of drag can be categorized into four approaches:

- (1) Theoretical estimate requiring solution of the viscous flows around the body.
- (2) Wind tunnel measurement at low RN and extrapolated to full scale using semi-empirical skin friction methods.
- (3) Empirical estimates including semi empirical flat plate skin friction.
- (4) Empirical/statistical methods based on accumulated wind tunnel and flight test data.

Preliminary design of an aircraft configuration will not normally require analysis above approach #3 or #4. The evaluation of $C_{Dp \text{ Min}}$ by approach #3 is briefly discussed here, however approach #4 is the intended level of analysis for this report and data for its use are included.

EMPIRICAL ESTIMATE METHOD

The skin friction portion of minimum profile drag coefficient, $C_{Dp \text{ Min}}$, can be established by determining the friction drag for each component of the airplane through the use of the flat plate skin friction curves shown in Figure 5-4. The summation of these component skin friction coefficient values, as illustrated in Figure 5-5 results in the total friction of the configuration. The skin friction drag coefficient of each component is then multiplied by form factors and interference factors determined from reference 5. Form factors (FF) and interference factors (IF) have been empirically established for various components of the airplane to account for shapes other than flat plates and for general component interference. The resulting skin friction coefficients are then multiplied by the component wetted areas to obtain equivalent parasite area "f". These are summed to obtain total configuration parasite area. The drag coefficient is then determined from the following relationship:

$$C_D = \frac{\sum C_f \cdot FF \cdot IF \cdot S_{WET}}{S_{REF}} = \frac{f}{S_{REF}}$$

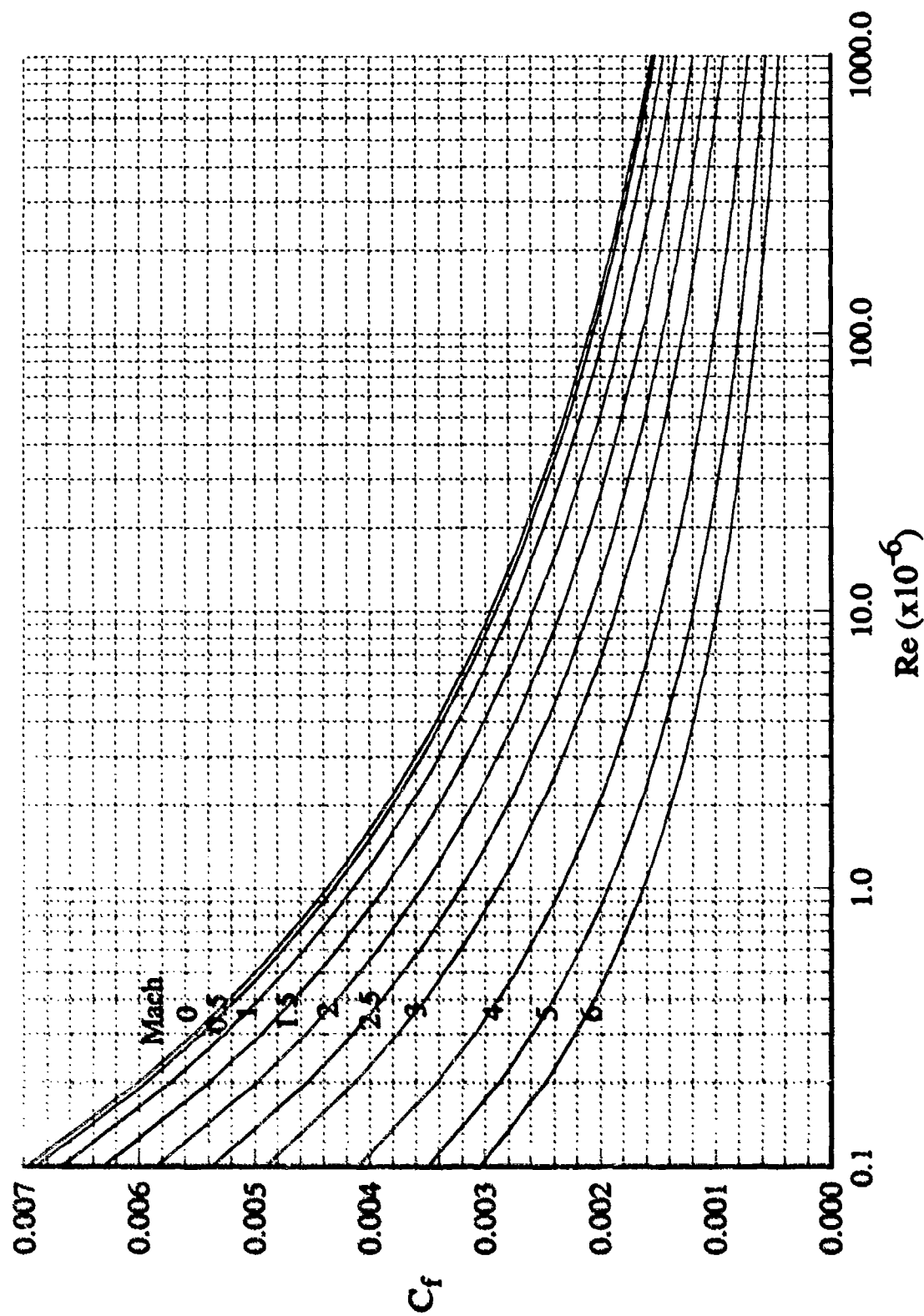
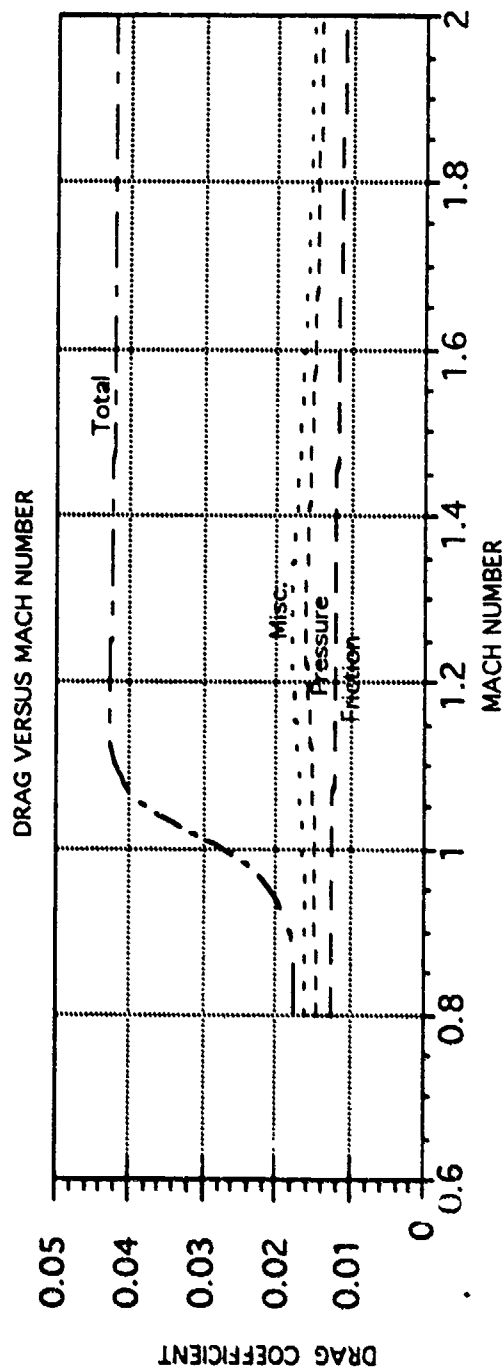


FIGURE 5-4 Turbulent Skin Friction



DRAG BUILD-UP, FIGHTER CLASS Alt. 30000 ft. RN 2.57×10^6 /ft. $S_{ref} = 300 \text{ ft}^2$

Component	A_{wet}	I	RNxl	C_f	FF	IF	$f = A_{wet} \cdot C_f \cdot FF \cdot IF$	$C_D = f / S_{ref}$
Fuselage	532	42	107.9	0.00198	1.1	1.02	1.1819	0.00394
Nacelle	237	33	84.8	0.00203	1.04	1.02	0.5104	0.00170
Canopy	35	12	30.8	0.00238	1.06	1.02	0.0901	0.00030
Wing	345	9	23.1	0.00249	1.06	1.33	1.2111	0.00404
Hor Tail	98	5	12.8	0.00270	1.06	1.33	0.3730	0.00124
Vert Tail	82	6	15.4	0.00252	1.06	1.33	0.2913	0.00097
Dorsal Fin	35	11	28.3	0.00239	1.04	1.02	0.0887	0.00030
Friction								70%
Pressure								7%
Protuberance								4%
Roughness								5%
Leakage								1%
Cooling								3%
(+) 10%								100%
								0.01587
								0.00173
								0.01760

Figure 5-5 Drag Build-up and Mach Number Effects

Reference 5 also describes the empirical estimation of roughness drag which can vary greatly depending on the surface condition, where a "mirror" or polished glass surface is considered aerodynamically smooth and an aircraft painted surface is approximately 0.2 mils (0.0002in). Incorrectly sprayed aircraft paint can have surface roughness of 8 mils (0.008in). The protuberance and excrescence drag can be evaluated after knowing some detail of the configuration by procedures and data shown in "Hoerner", Reference 19 or the percentages shown in Figure 5-5 can be used directly or adjusted as deemed necessary.

The accumulated $C_{Dp \text{ Min}}$ is normally increased by 10% to account for the excrescence drag and any other unaccounted drag items. The base pressure at the aft end of the fuselage and the engine exhaust area may produce additional drag depending on the design of the configuration. If the drag estimated above does not include the form factors (FF) or the interference factors (IF), the accumulated $C_{Dp \text{ Min}}$ should be increased as much as 20%. Detailed information on these drag factors can be obtained in reference 5.

The drag due to lift, or induced drag (C_{Di}), for an elliptical load distribution on the wing is defined as $\frac{C_L^2}{\pi A R e}$ where e is considered 1 (References 19, 20). This is the minimum drag due to lift that can aerodynamically be produced on a planar wing and provides an upper limit to the drag polar shape. The "worst case" drag due to lift is defined by $C_L \tan \alpha$ (Figures 5-6 and 5-7) and represents a wing with no leading edge suction forces which results in a pure normal force on the wing. The wing efficiency factor, e, is used to define wing efficiency if less than that for an elliptical load distribution and is normally defined to also include the increase in profile drag with increased lift. The variation of e with wing aspect ratio for past aircraft is displayed in Figure 5-8 and normally ranges between 75% to 90% up to moderate lift coefficients. It can also be evaluated from the slope of the C_L^2 versus C_D plot ($\pi A R e = \frac{C_L^2}{C_D}$) as shown in Figure 5-7.

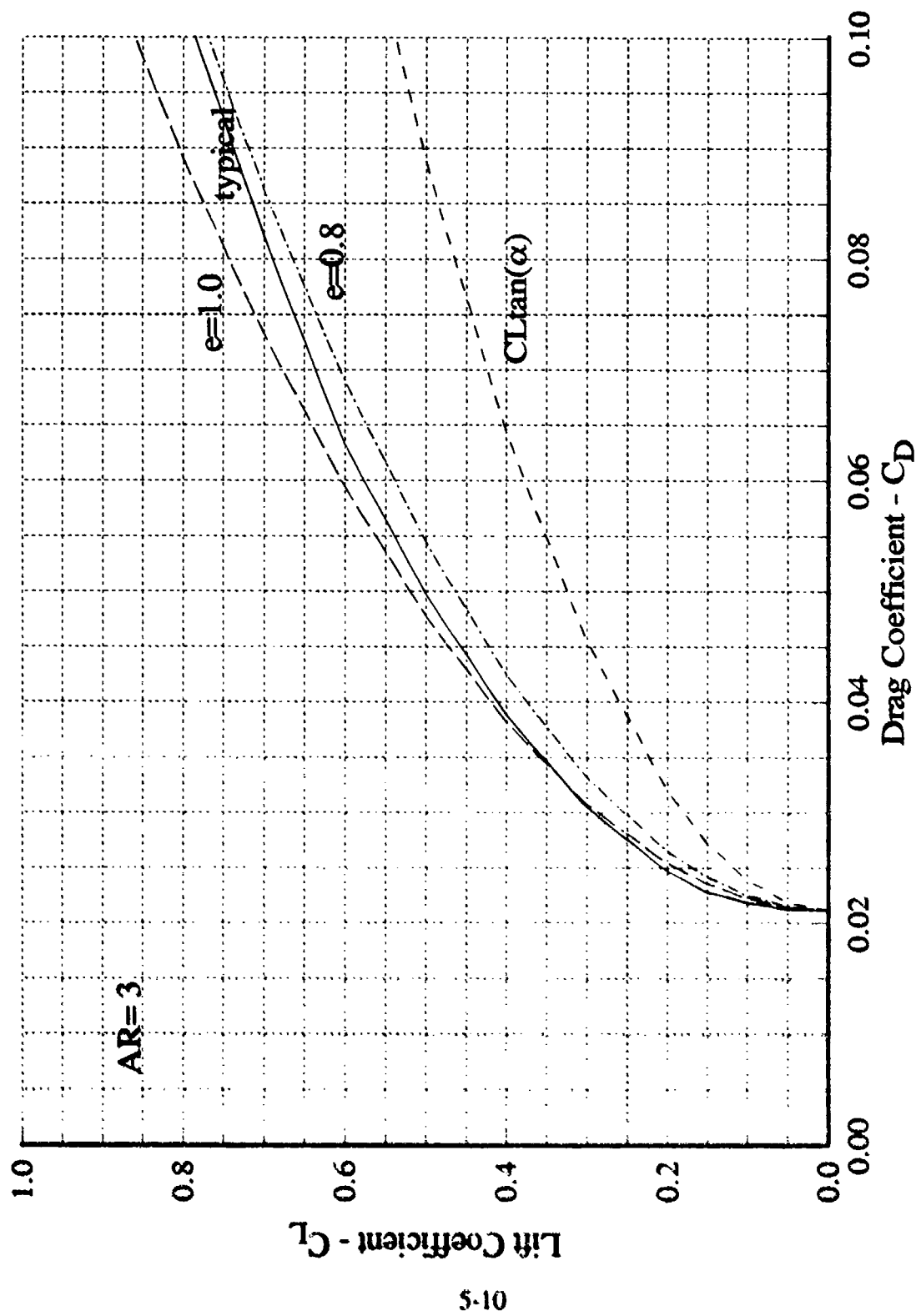


FIGURE 5-6 Fighter Drag Polar - Lift efficiency

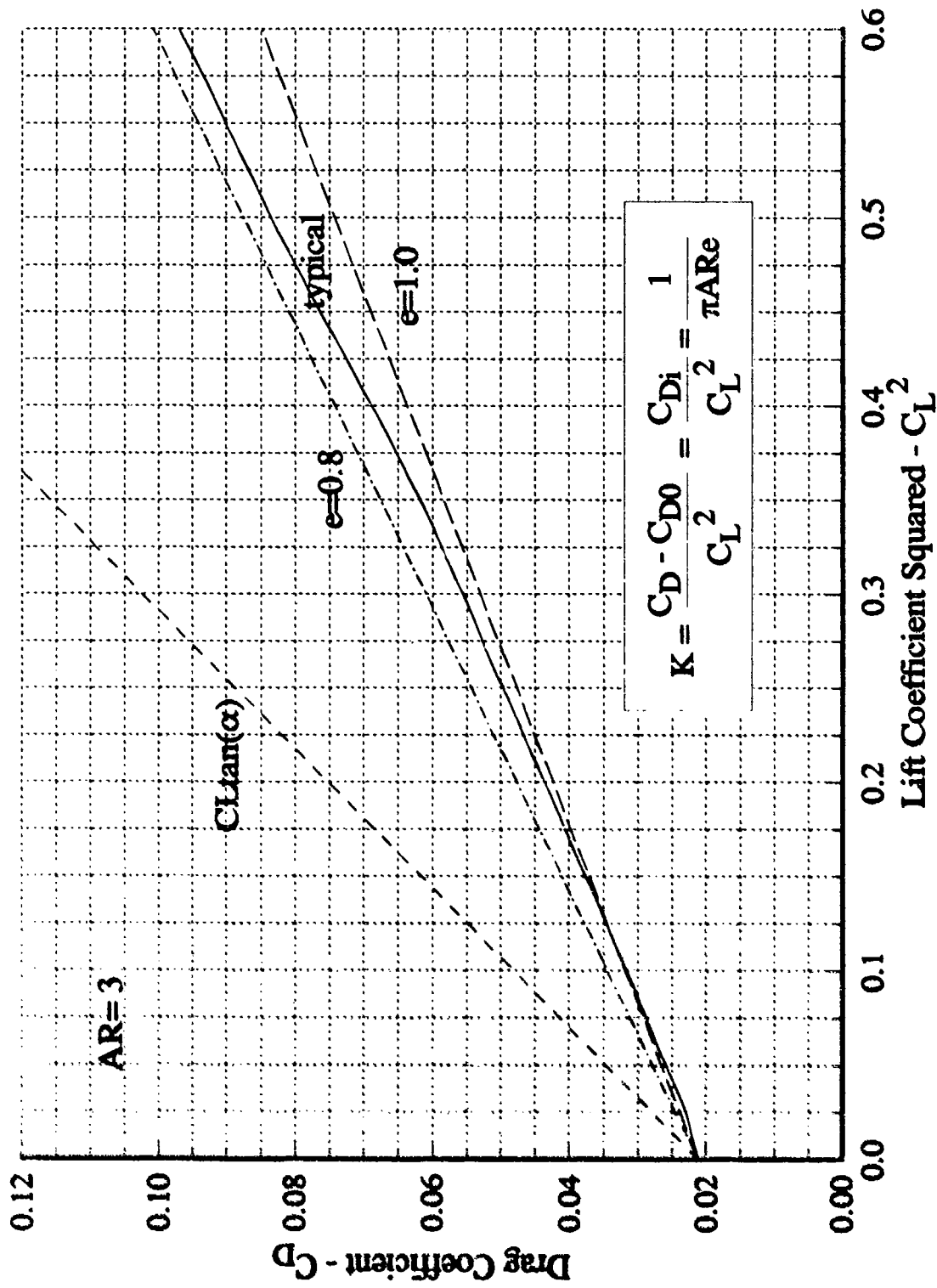


FIGURE 5-7 Drag Due To Lift

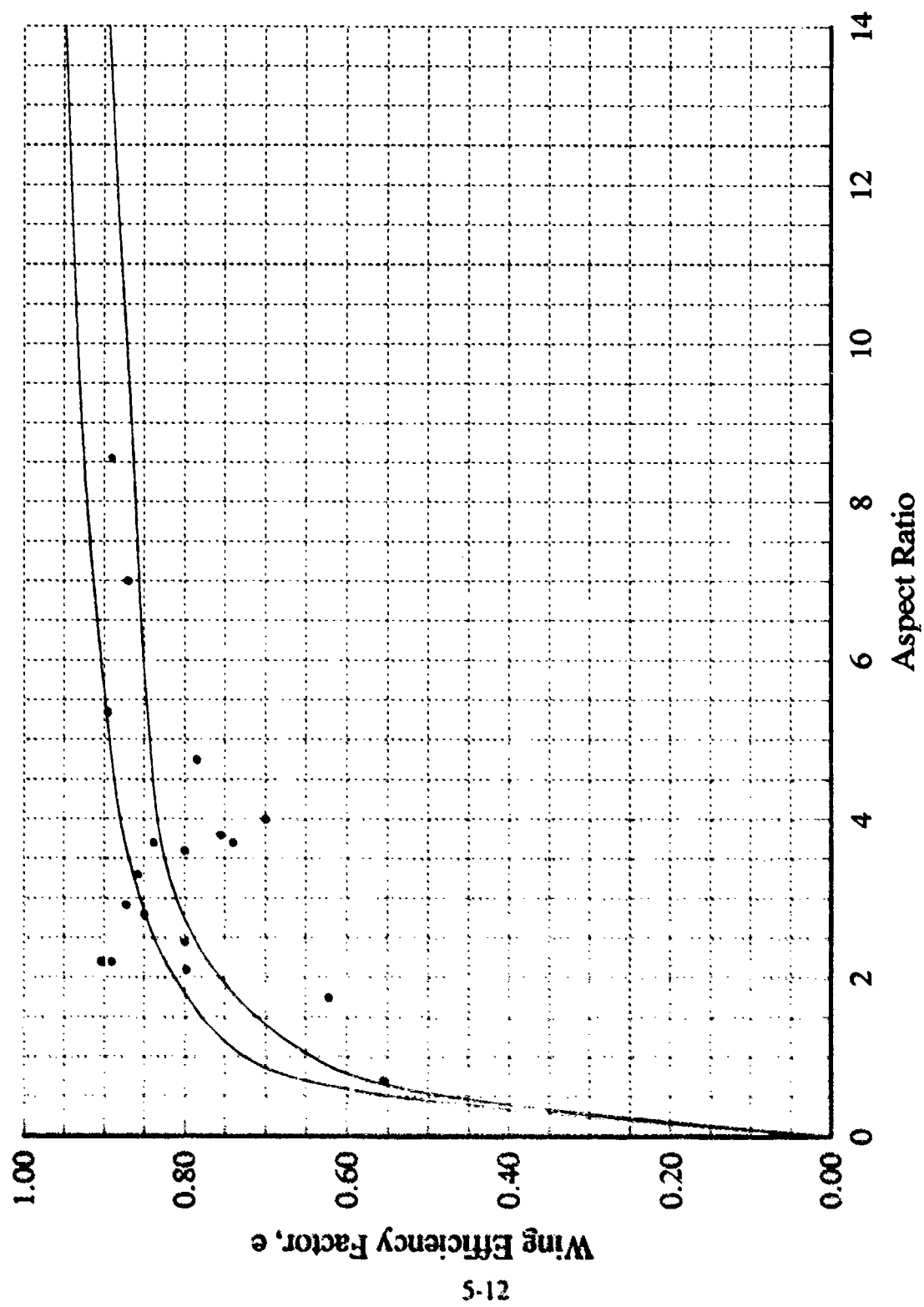


FIGURE 5-8 Wing Efficiency Factor

Mach number effects on drag, the compressibility or wave drag (C_{DW}), varies greatly in the transonic region, however most transport aircraft cruise at speeds just below the critical or drag rise Mach number and experience only a small drag (app. 4%) due to compressibility. For more information on this drag, see the Wave Drag section of this report.

TRIM DRAG

Trim drag includes the lift and drag of the control surface deflections required to provide zero pitching moment on the airplane and is a function of the aircraft pitching moment, longitudinal stability and control surface effectiveness. An aircraft designer will normally arrange the configuration such that the pitching moment is near zero at the cruise C_L , therefore, the trim drag will be near zero at the design cruise condition. The data analysis shown in Figure 5-9 will define trim drag at other lift coefficients or load factors.

EMPIRICAL/STATISTICAL METHOD

This method is compatible with the general analysis of this report and establishes minimum profile drag by comparison to the statistical drag of other similar aircraft. Figure 5-10 is a plot of total wetted area versus equivalent parasite (profile) area (f) and is based on the product: $f = C_{f_e} \cdot S_{wet} = C_{D0} \cdot S_{Ref}$. Lines of constant equivalent skin friction coefficient (C_{f_e}) are shown along with the value of several existing types of aircraft. Knowing the wetted area of a preliminary design and assuming a C_{f_e} value based on similar existing aircraft, a $C_{Dp Min}$ can readily be established. This method normally accounts for all the drag items in $C_{Dp Min}$: pressure, interference, excrescence, and roughness drag. The estimation of drag due to lift (C_{DL}) described in approach #3 is straight-forward and is appropriate for this approach also. Mach number effect on drag (C_{DW}) is small for subsonic aircraft and can be considered 0 for this

TRIM LIFT and DRAG PROCEDURE

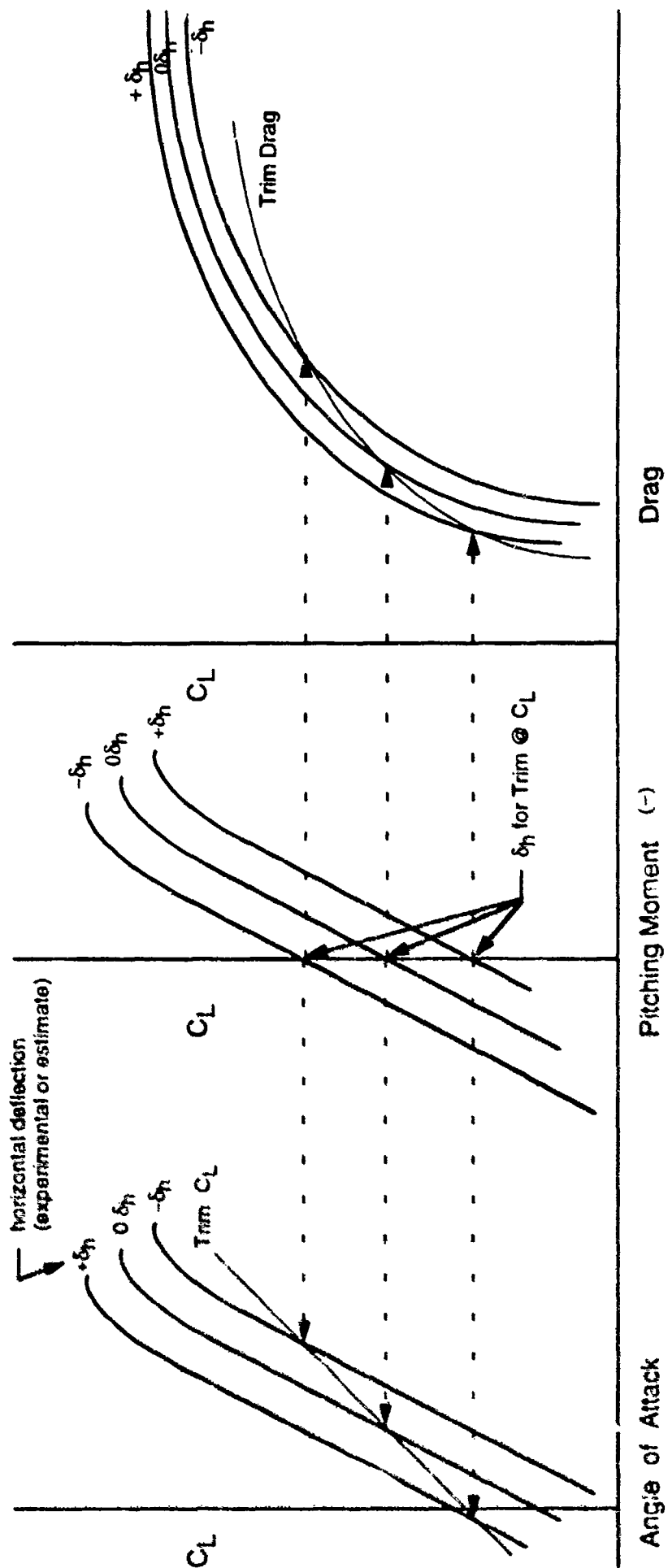


FIGURE 5-9 TRIM LIFT AND DRAG ESTIMATE PROCEDURE

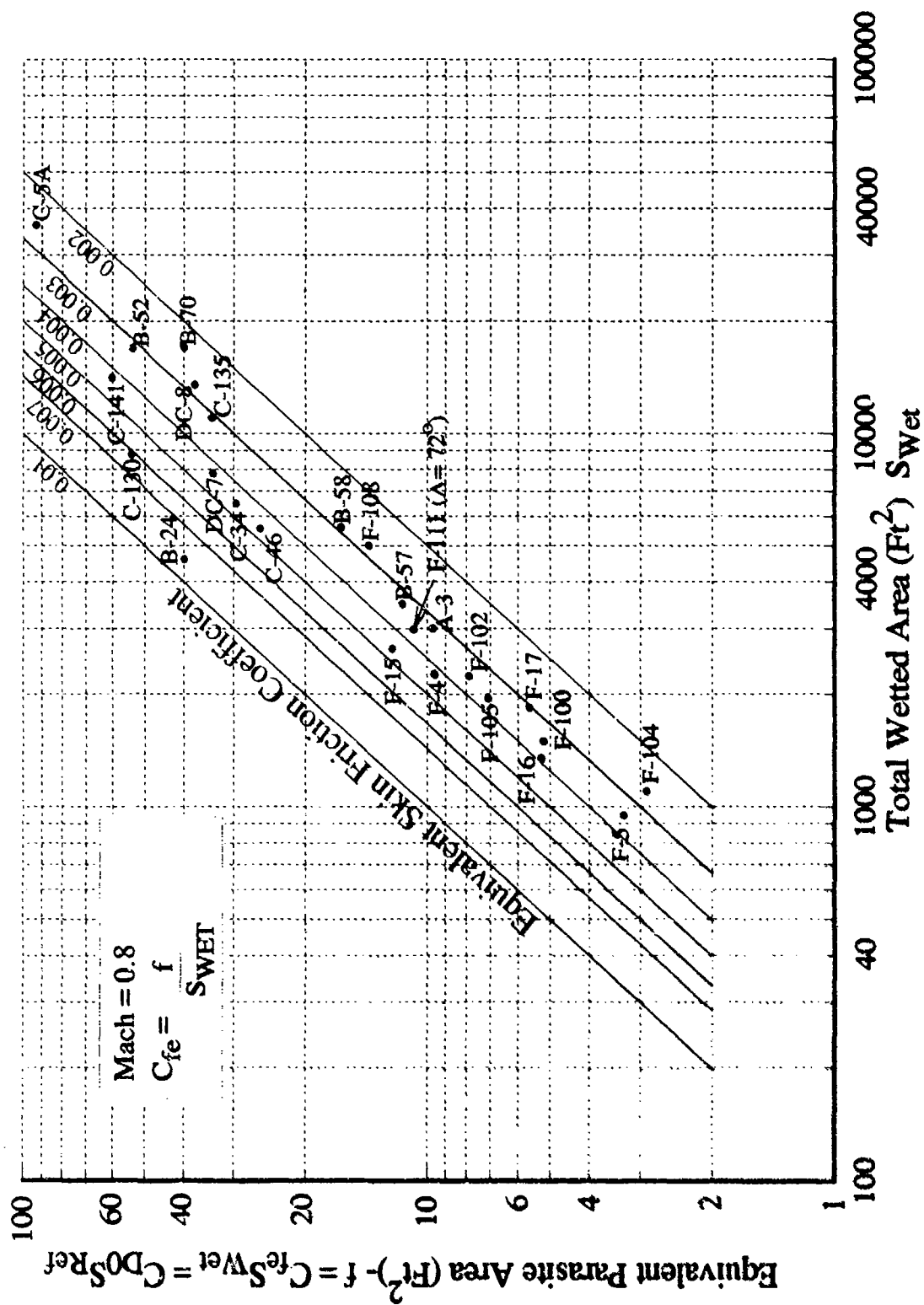
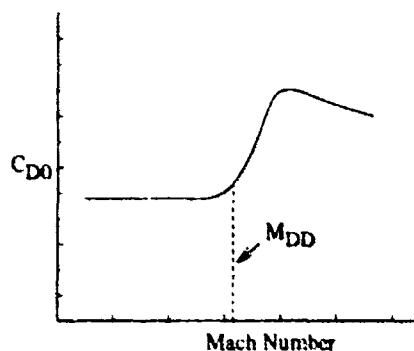


FIGURE 5-10 Aerodynamic Cleanness of Aircraft

approach. The effect of trim on drag (C_{Dtr}) is also considered 0 for this approach at the cruise condition.

WAVE DRAG

Wave Drag is the drag of an aircraft associated with the appearance of shock waves as aircraft components of finite thickness approach supersonic velocities. As a typical aircraft reaches transonic flight velocities ($M \geq 0.8$) the flow velocities about components exceed the speed of sound creating local supersonic velocities. The free stream Mach number at which wave drag initially appears is called the drag divergence mach number, M_{DD} , as shown in the sketch below.



SKETCH A

The wave drag variation depicted in sketch A can be associated with the Mach dependence of wing wave drag and the changing characteristics of the flow field associated with increasing Mach number ("supersonic area rule"). Simple methods for estimating wave drag make use of supersonic linear theory (References 21 through 23). Estimates of aircraft wave drag can be made by breaking the configuration into components such as wings and bodies. This approach is generally used in the early conceptual design phase.

The wave drag of bodies of revolution have been defined by Sears & Haack, who defined three classes of optimum bodies as presented in Figure 5-11. These classes are:

- (1) given volume and length
- (2) given length and diameter
- (3) given diameter and volume.

The class (1) Sears-Haack body is the most frequently used because of its higher volume relative to its wave drag. The wave drag for this class of body is given by the relationship:

$$C_{D \text{ WAVE}} = \frac{9}{8} \pi^2 \left[\frac{1}{\left(\frac{L}{d} \right)^2} \right] \quad (5-1)$$

The drag coefficient equation is based on the maximum cross-sectional area of the bodies and indicate that for Sears-Haack bodies wave drag is solely a function of fineness ratio, L/d . Fineness ratio represents the dominate parameter in determining the wave drag of supersonic aircraft. Note the slenderness (high fineness ratio) of such aircraft as the SR-71, XB-70, Concord, F-104, or any of the proposed U.S. supersonic transports (SST) as examples of the fineness ratio principle.

The estimation of wave drag for wings is more "complicated" than bodies of revolution due to the many more aerodynamic parameters involved. Aspect ratio, Mach number, thickness, airfoil profile, leading edge sweep, taper ratio, and maximum thickness locations are each important in determining wing wave drag. Detailed charts (References 24 - 26) present analytical wave drag predictions for a host of wing shapes. The wave drag of uncambered and untwisted trapezoidal wings can be estimated by

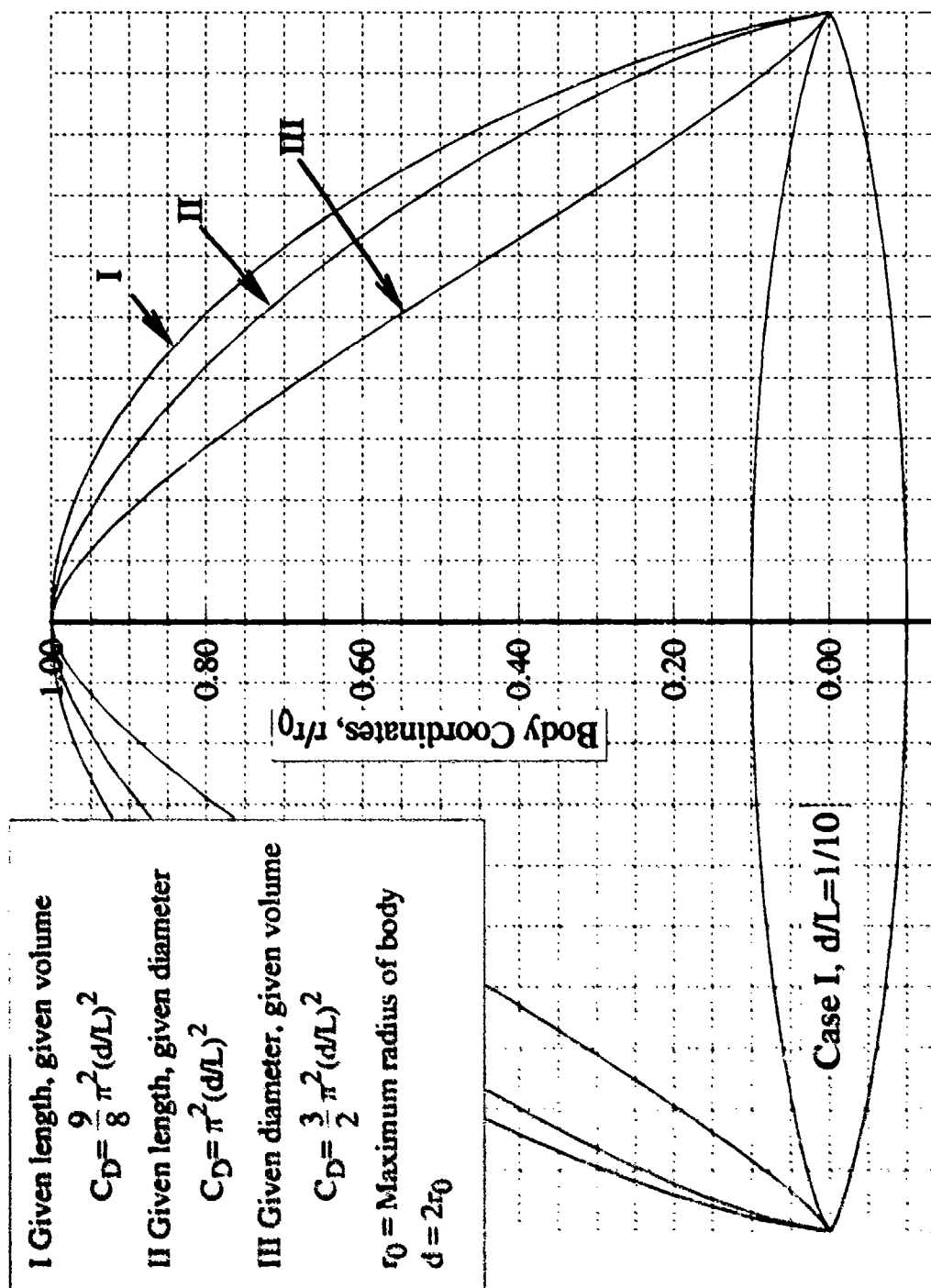


FIGURE 5-11 Minimum Wave Drag Bodies of Revolution

$$C_{D \text{ WAVE}} = \frac{K}{\beta} \left(\frac{t}{c} \right)^2 \quad \text{For a supersonic wing leading edge (5-2)}$$

$$C_{D \text{ WAVE}} = K \tan \epsilon \left(\frac{t}{c} \right)^2 \quad \text{For a subsonic wing leading edge (5-3)}$$

with

$$\epsilon = 90^\circ - \Lambda_{LE}$$

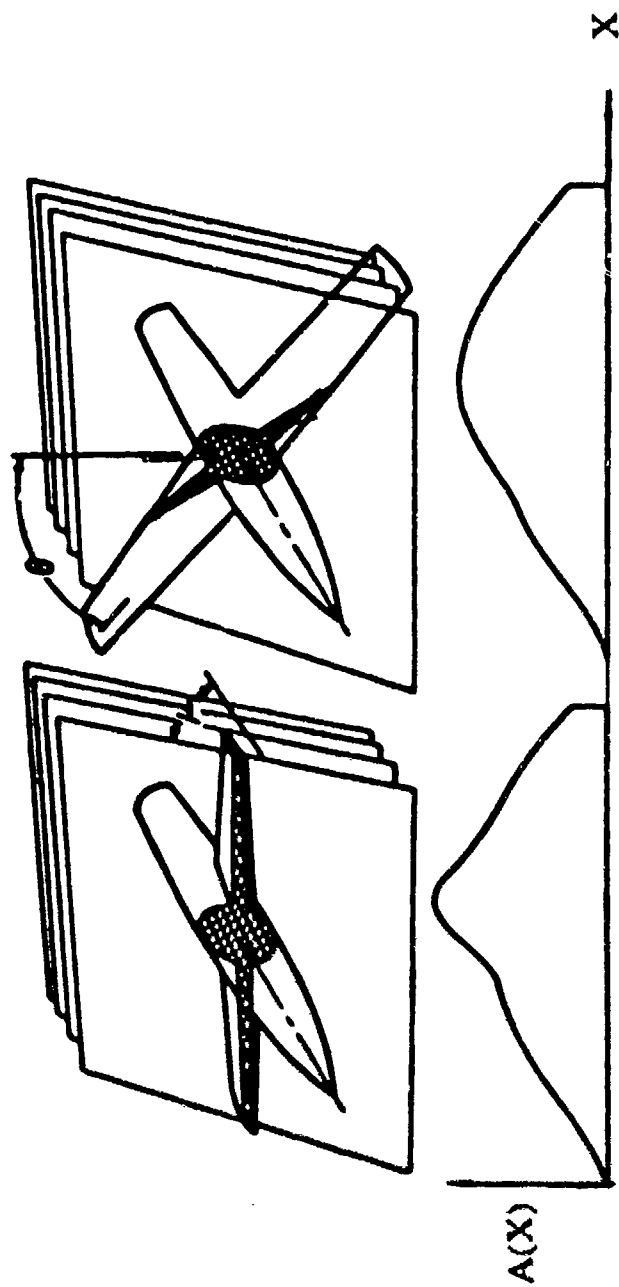
$K = 16/3$ for biconvex airfoils

$K = 4$ for double wedge airfoils

The above expressions are for rough estimates only and do not capture many of the finer details that determine wing wave drag. Leading edge bluntness, aspect ratio, camber and location of maximum thickness are all important parameters which can significantly effect wing wave drag. A complete description of wing wave drag, including subsonic and supersonic leading edges is contained in Appendix C.

The wave drag of complete configurations can be estimated more accurately using the transonic and supersonic area-rule concept. The area-rule concept assumes the wave drag of an aircraft is essentially the same as the wave drag of an equivalent body of revolution having the same cross-sectional area distribution as the aircraft. Numerous computer programs exist to calculate and optimize the wave drag of aircraft (References 4 and 27). The Harris far field wave drag program, by far the most popular, is used throughout government and industry. Far field wave drag programs are straight forward. Cutting planes inclined at the Mach angle are passed through the vehicle as shown in figure 5-12. A plot of cross-sectional area versus length results and the wave drag integral involving slopes of this plot is evaluated. At other than $M = 1.0$ this area plot will be a function of aircraft roll angle so an integrated average is established.

Supersonic Area-Rule Concept



$$D(\theta) = -\frac{\rho V^2}{4\pi} \int_0^{\theta} \int_0^{\theta} A''(X_1) A''(X_2) \log|X_1 - X_2| dX_1 dX_2$$

$$D = \frac{1}{2\pi} \int_0^{2\pi} D(\theta) d\theta$$

FIGURE 5-12 Supersonic Area Rule Concept

Reference 27 is the classical reference for this procedure which allows rapid assessment of wave drag increments associated with configuration changes. This more detailed approach is generally incorporated in computerized vehicle synthesis programs.

The transonic wave drag at Mach 1.2 for a Sears-Haack body and several fighter aircraft is shown in Figure 5-13 . This semi-empirical approach may be used to estimate the drag rise for supersonic aircraft during the formulation of a configuration. It is apparent the Sears-Haack optimum bodies have considerably less wave drag than complete aircraft and in early conceptual studies should only be used to predict the lower bound for wave drag. A more detailed correlation of wave drag at Mach 1.2 for complete configurations is displayed in figure 5-14. This correlation contains experimental data for numerous aircraft as a function of configuration fineness ratio, wing sweep and wing thickness ratio. This parameter provides excellent correlation and may be used with confidence in the initial stages of design to predict the transonic wave drag. Most fighters are designed to have a maximum speed near Mach 2. Thus the drag at this Mach number needs to be evaluated early in the design cycle.

Supersonic drag at Mach 2 (Figure 5-15) has been correlated as a function of wetted area and equivalent parasite area. These are the same parameters used to correlate the subsonic drag. Thus a rapid estimate of the supersonic drag can be made by assuming a C_{fe} value based on similar aircraft. The zero lift drag for several aircraft is shown in Figure 5-16 to illustrate representative numerical values and the trend with Mach number. It is important to remember values from past aircraft since they are a good guide for any new configuration.

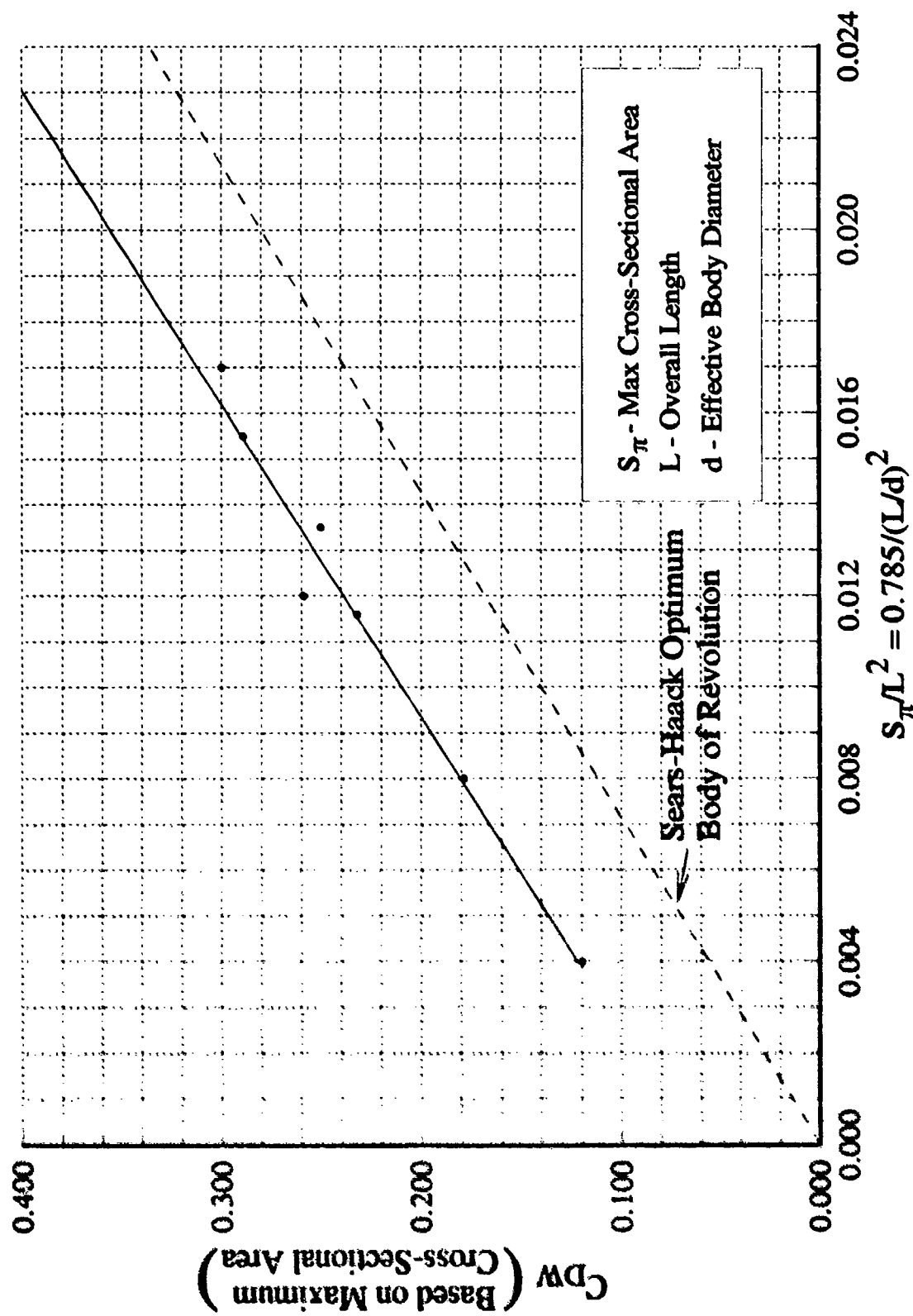


FIGURE 5-13 Transonic Drag Rise at $M=1.2$

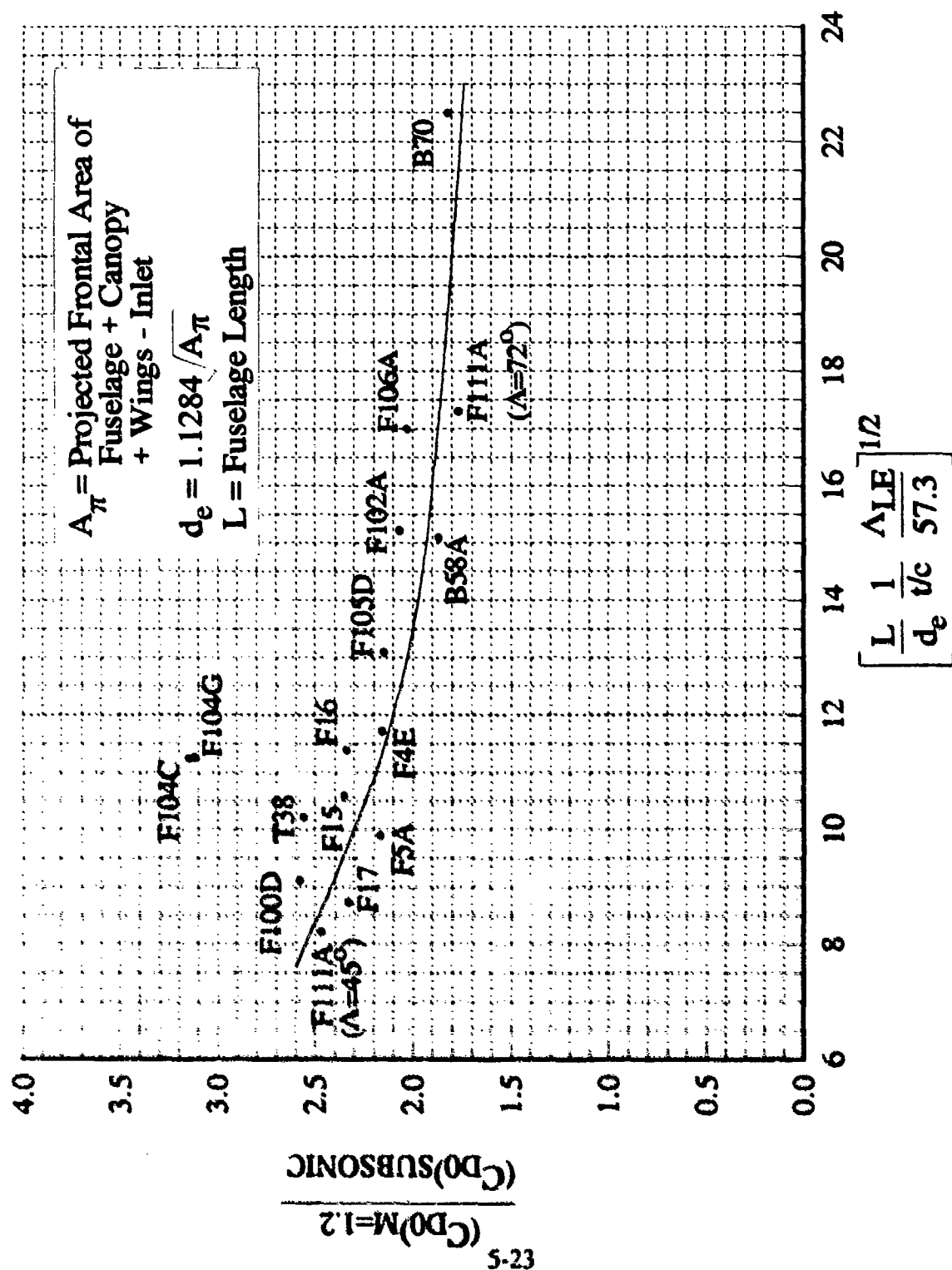


FIGURE 5-14 Transonic Drag Rise Correlation

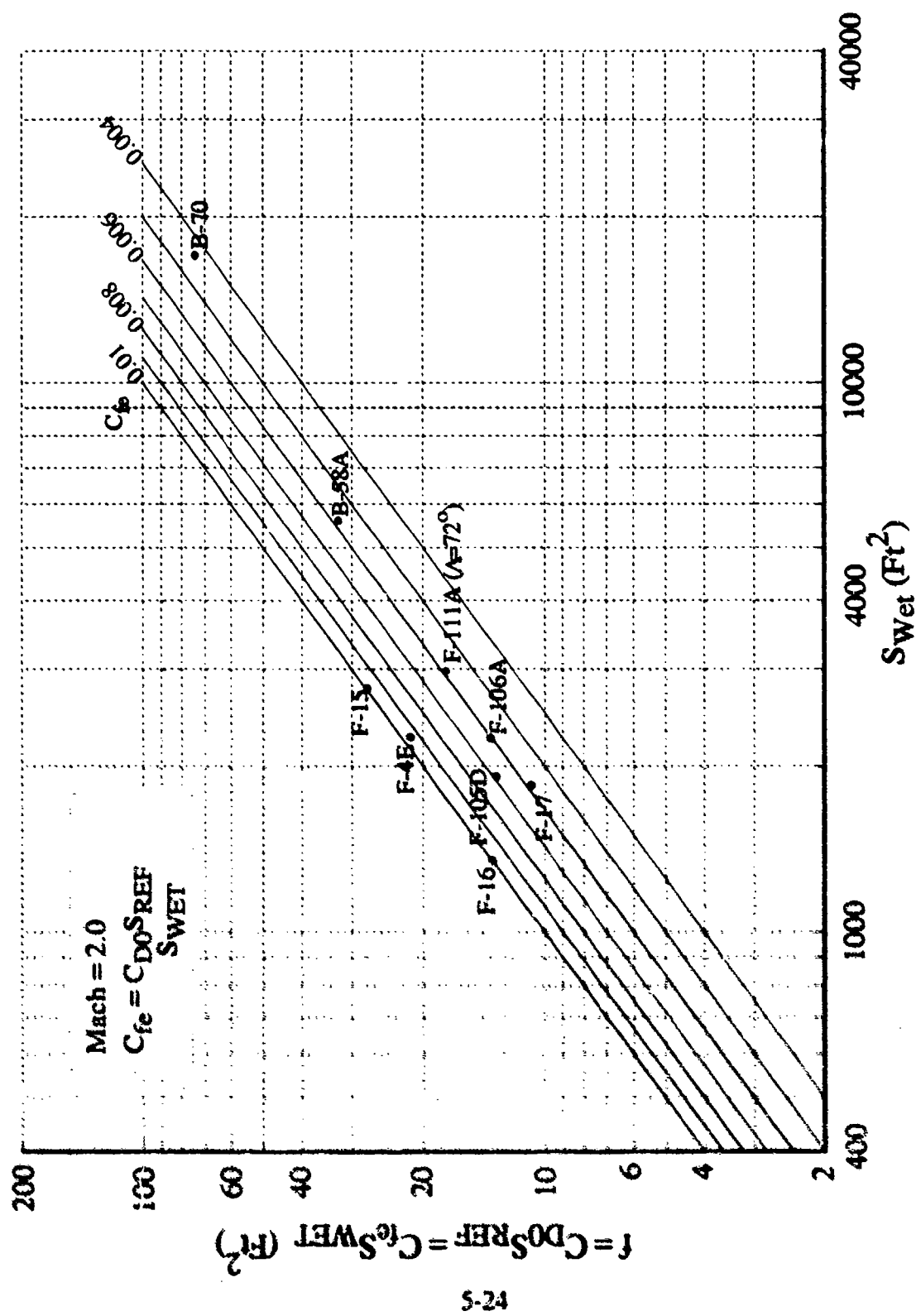


FIGURE 5-15 Parasite Drag Area Correlation at Mach 2

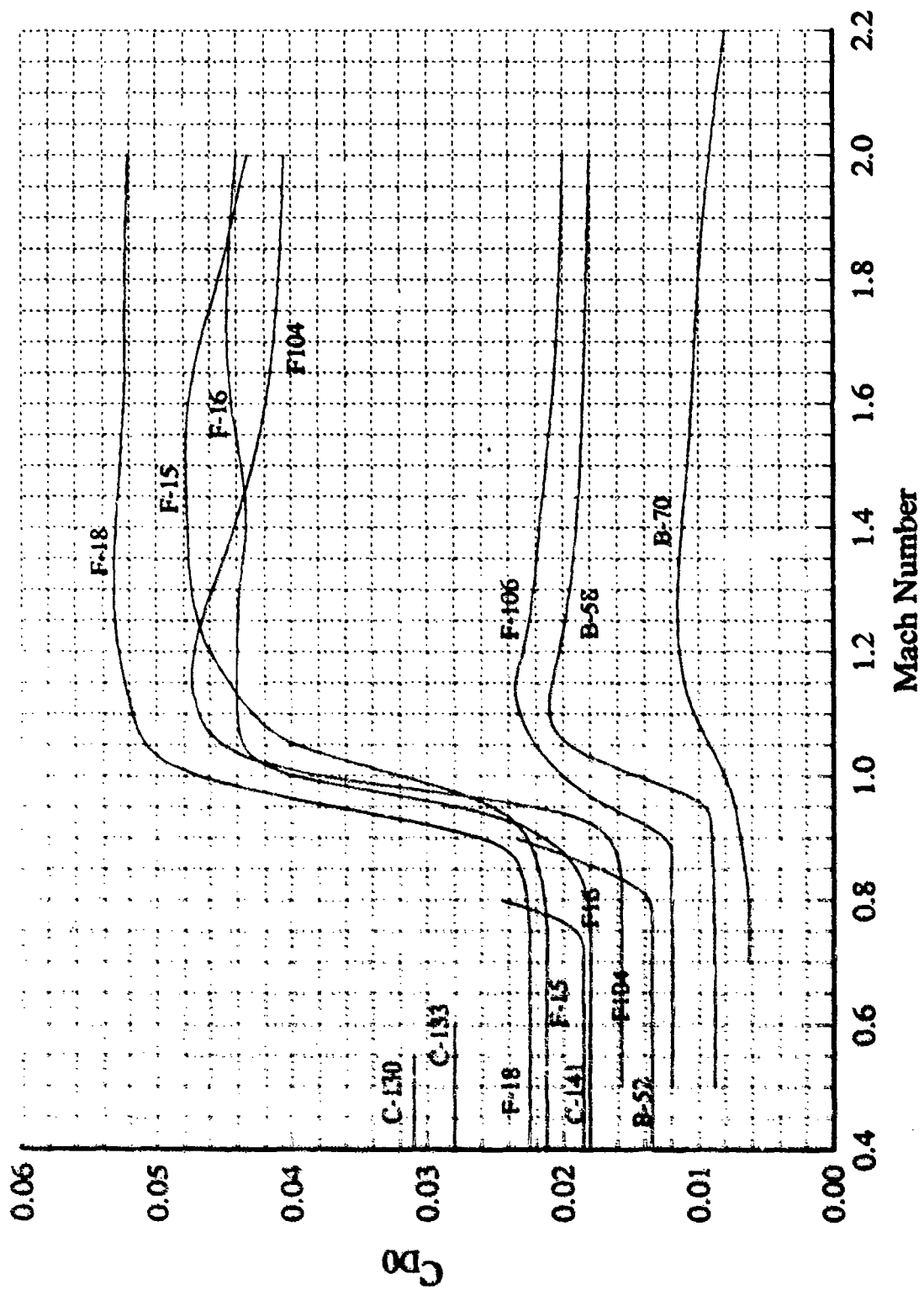


FIGURE 5-16 Variation of C_D With Mach Number

LIFT

The lift on an aircraft is primarily produced by the wing at subsonic speeds and only minorly affected by the fuselage. It is highly dependent on wing aspect ratio and sweepback as illustrated in Figure 5-17. The expression

$$C_{L\alpha} = \frac{\pi AR (2 \cos \Lambda_{1/4c})}{AR + 2 \cos \Lambda_{1/4c}}$$

is independent of Mach number, and can be used for rapid estimates of the lift curve slope at subsonic speed. In general, transports have high aspect ratios and small sweepback angles because of long range requirements. Fighters have relatively low aspect ratios and moderate sweepback angles because of speed and maneuverability requirements. These are the considerations the designer faces in the formulation of configurations. The effects of Mach number on the subsonic lift curve slope can be determined from the following relationship (Reference 6):

$$C_{L\alpha} = \frac{2\pi AR}{2 + \sqrt{4 - AR^2 \beta^2 \left(1 - \frac{\tan^2 \Lambda_{1/4c}}{\beta^2}\right)}} \quad (5-4)$$

$$\text{where: } \beta = \sqrt{1 - M^2}$$

The impact of Mach number on the supersonic lift curve slope is displayed in Figure 5-18. There is a rapid decrease in lift up to Mach 2.5 and then a more gradual decline. The prediction of lift is very forgiving on an aircraft and relatively straight forward. The more complex CFD codes can quite accurately predict the lift coefficient, however, simplified expressions provide reasonable values and are very useful early in the design cycle.

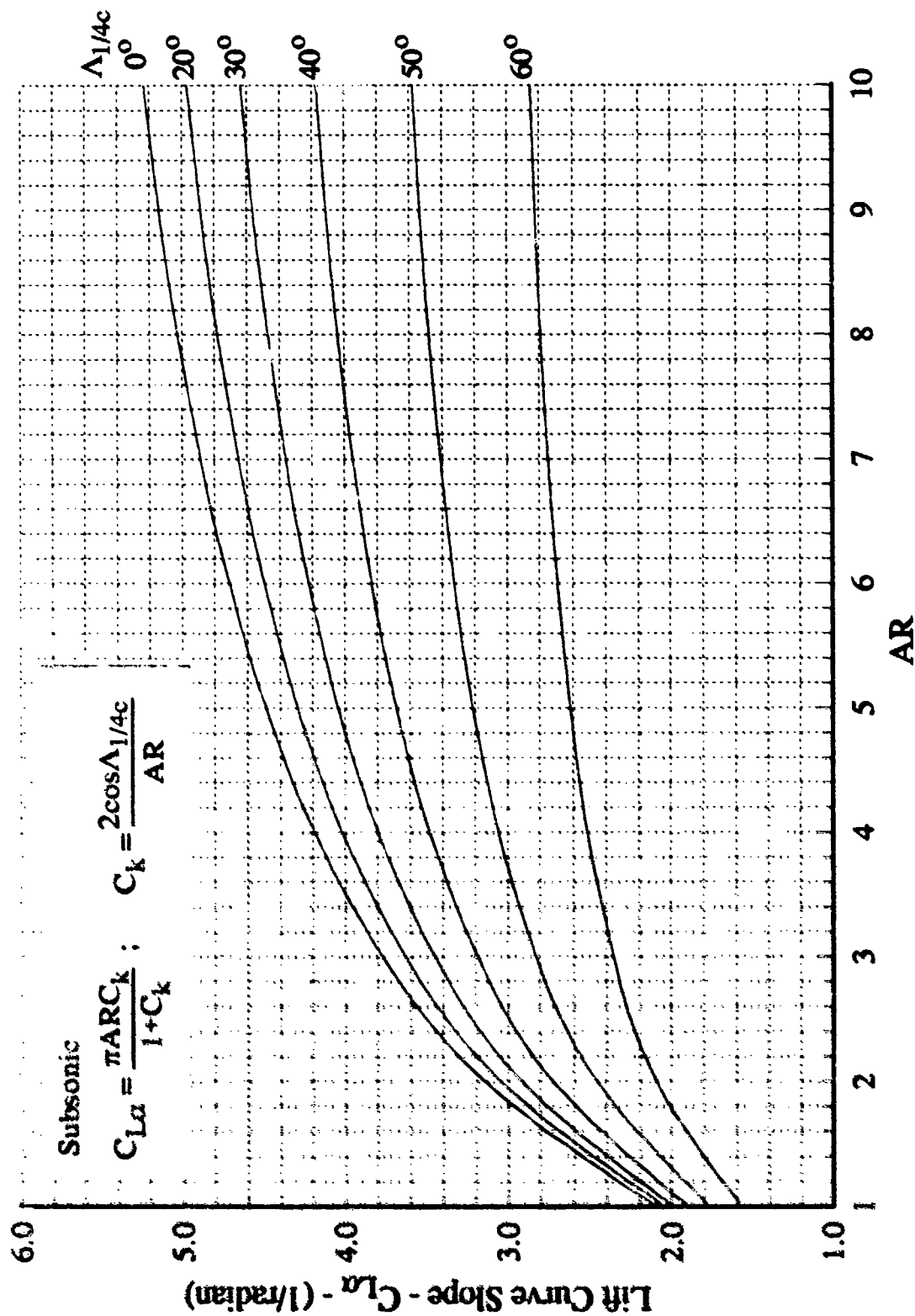


FIGURE 5-17 Subsonic Lift Curve Slope

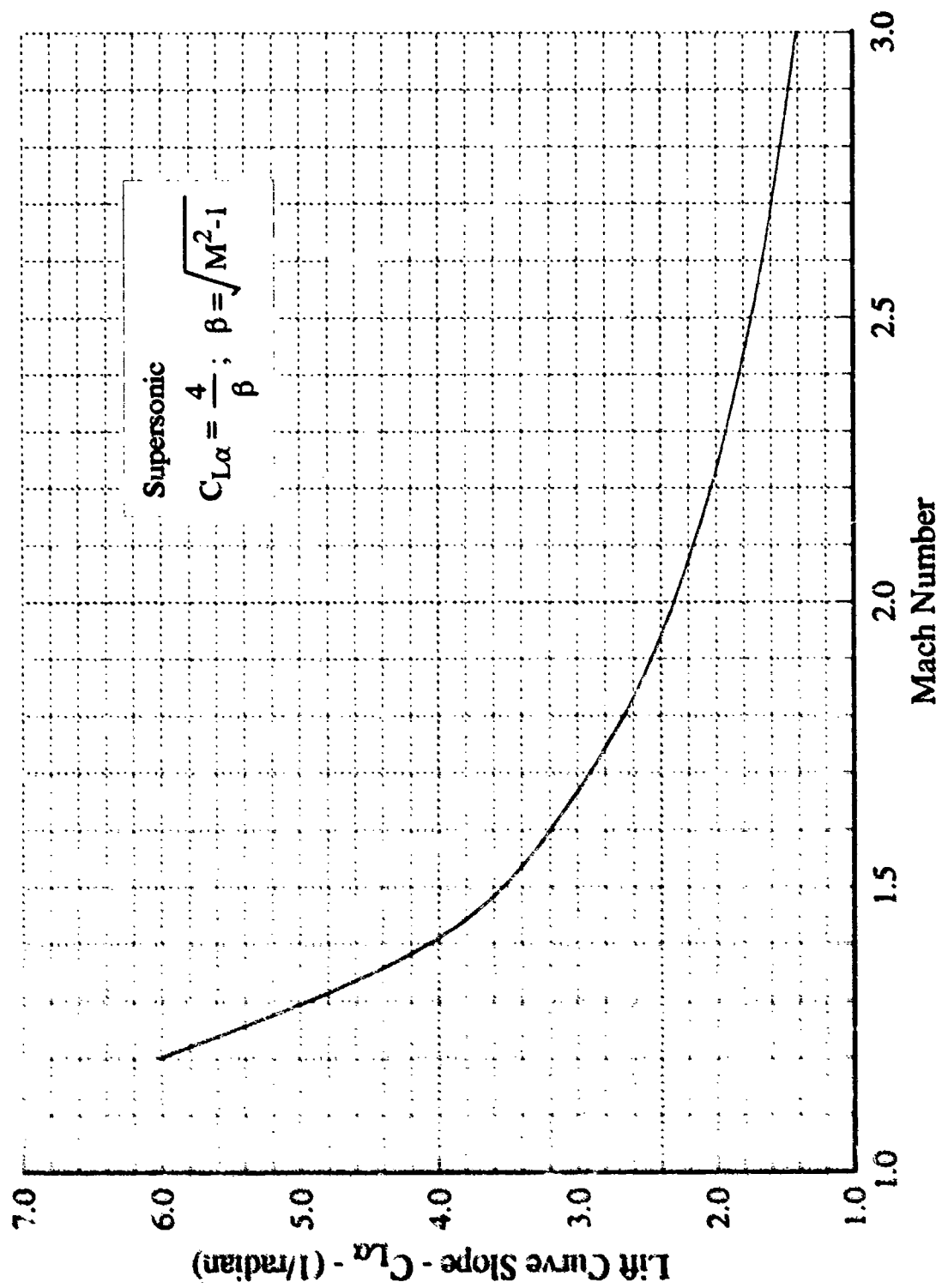


FIGURE 5-18 Supersonic Lift Curve Slope

Lift-To-Drag Ratio

The early determination of maximum lift-to-drag ratio, $(L/D)_{MAX}$ at subsonic speeds is extremely important to the designer in trying to achieve range requirements. The maximum L/D may be predicted from a relatively simple relationship.

Since:
$$C_D = C_{D0} + KC_L^2 = C_{D0} + \frac{1}{\pi A Re} C_L^2$$

$$\frac{L}{D} = \frac{C_L}{C_D} = \frac{C_L}{C_{D0} + KC_L^2}$$

$$\left(\frac{L}{D}\right)_{MAX} \text{ when } \frac{d\left(\frac{L}{D}\right)}{dC_L} = 0 = \frac{-2KC_L^2}{[C_{D0} + KC_L^2]^2} + \frac{1}{[C_{D0} + KC_L^2]}$$

$$C_L \left(\frac{L}{D}\right)_{MAX} = \sqrt{\frac{C_{D0}}{K}}$$

$$\left(\frac{L}{D}\right)_{MAX} = \frac{1}{2\sqrt{KC_{D0}}} = \frac{1}{2\sqrt{\frac{C_{D0}}{\pi A Re}}} \quad (5-5)$$

This expression is used in Figure 5-19 which displays $(L/D)_{MAX}$ as a function of C_{D0} and aspect ratio.

Since
$$\frac{b^2}{S_{Ref}} = AR$$

and
$$C_{D0} S_{Ref} = C_{fe} S_{wet} \rightarrow C_{D0} = \frac{C_{fe} S_{wet}}{S_{Ref}}$$

Substituting in equation (5-5) results in another useful expression for predicting $(L/D)_{MAX}$

$$\left(\frac{L}{D}\right)_{MAX} = \frac{b}{2} \sqrt{\frac{\pi e}{C_{fe} S_{wet}}} \quad (5-6)$$

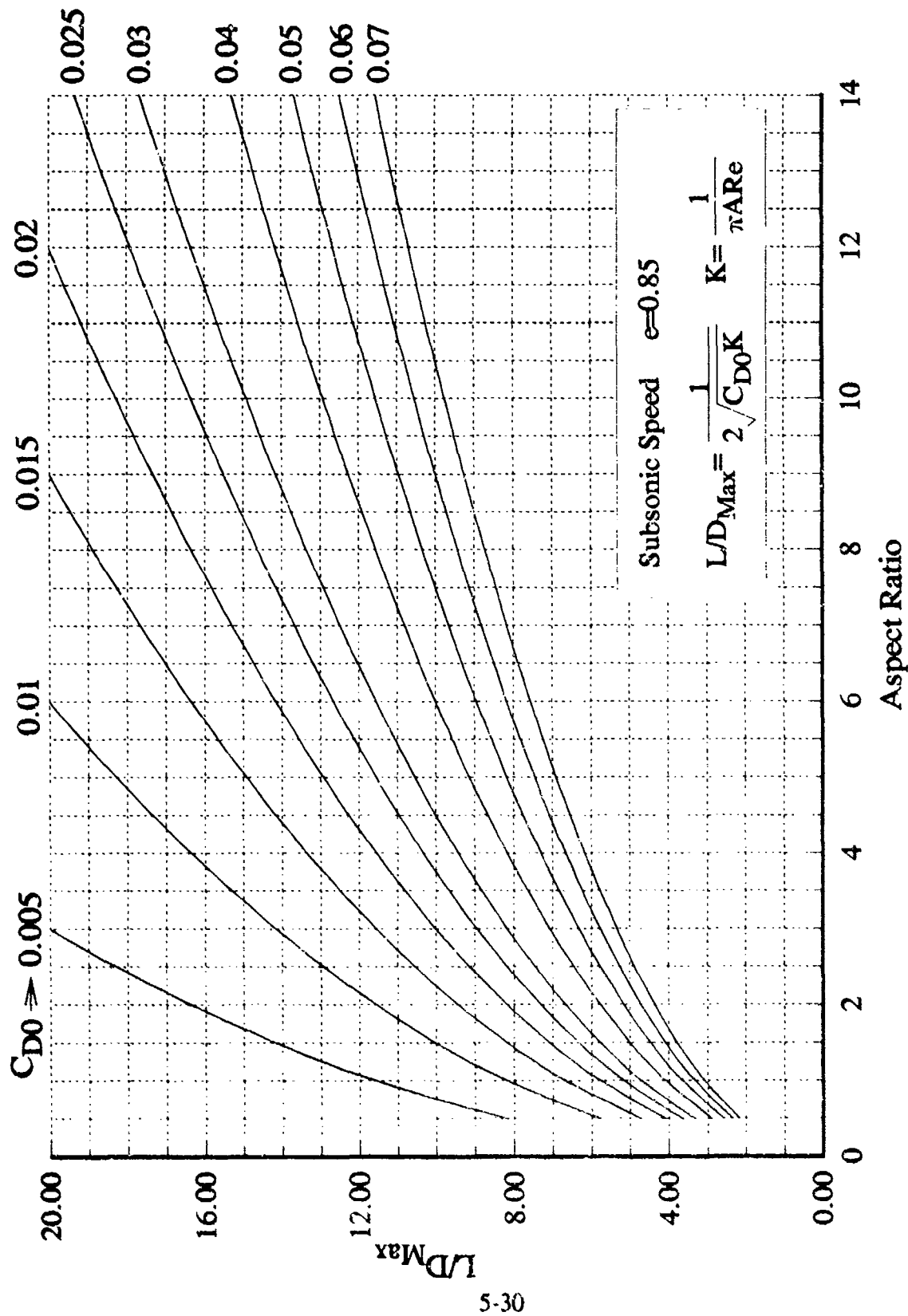


FIGURE 5-19 Maximum Lift-To-Drag Ratio

A useful design curve is presented in Figure 5-20 which can be used to estimate $(L/D)_{Max}$ based on span and wetted area. A wide variety of aircraft are listed and fall into a narrow band. Thus it can be used with a high degree of confidence. In Figure 5-21 $(L/D)_{Max}$ is shown as a function of wing aspect ratio. There is a sharp increase in maximum L/D with aspect ratio up to 3 where it begins to bend and increase only gradually at higher values. It should be noted most fighter aircraft are between aspect ratios of 2 to 3.5.

It is well known that maximum L/D decreases rapidly as an aircraft approaches sonic speed (Mach 1) due to the rapid increase in wave drag. Representative aircraft are displayed in Figure 5-22 to illustrate actual values and trends with Mach number. Typical subsonic $(L/D)_{Max}$ values are 11 to 12 and only around 4 at Mach 2. Figure 5-23 illustrates another approach to emphasize the trend of maximum L/D with Mach number. It may be noted from observing the B-70 value that an aircraft can be designed for relatively high aerodynamic efficiency at supersonic speed. This requires the aircraft to have very high fineness ratios and slender, highly swept back wings. The penalty for these design features are an increase in structural weight and reduction in payload. These are the trade-offs and challenges that constantly face the designer in the early stages of a configuration development.

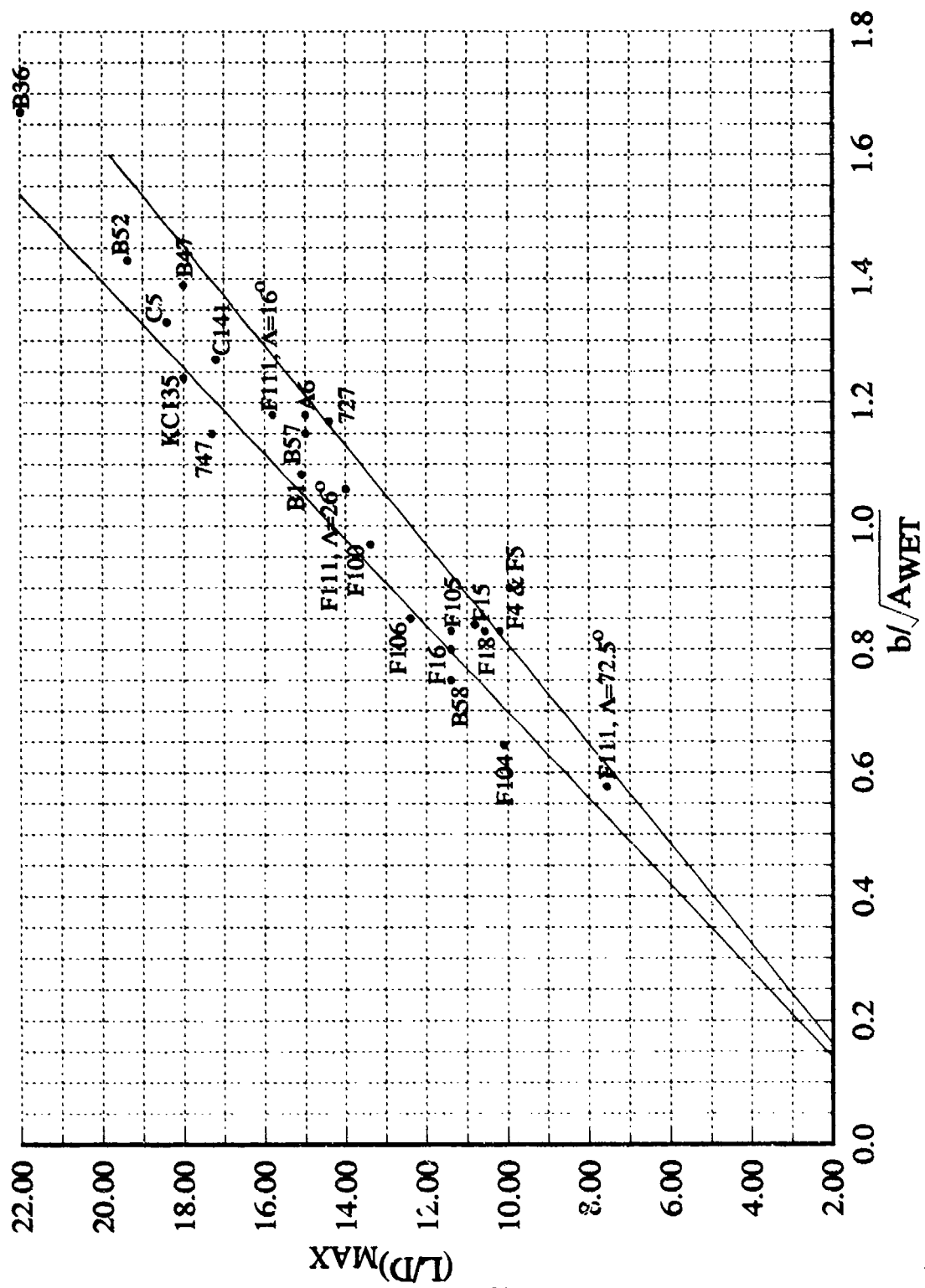


FIGURE 5-20 Subsonic Maximum L/D Correlation

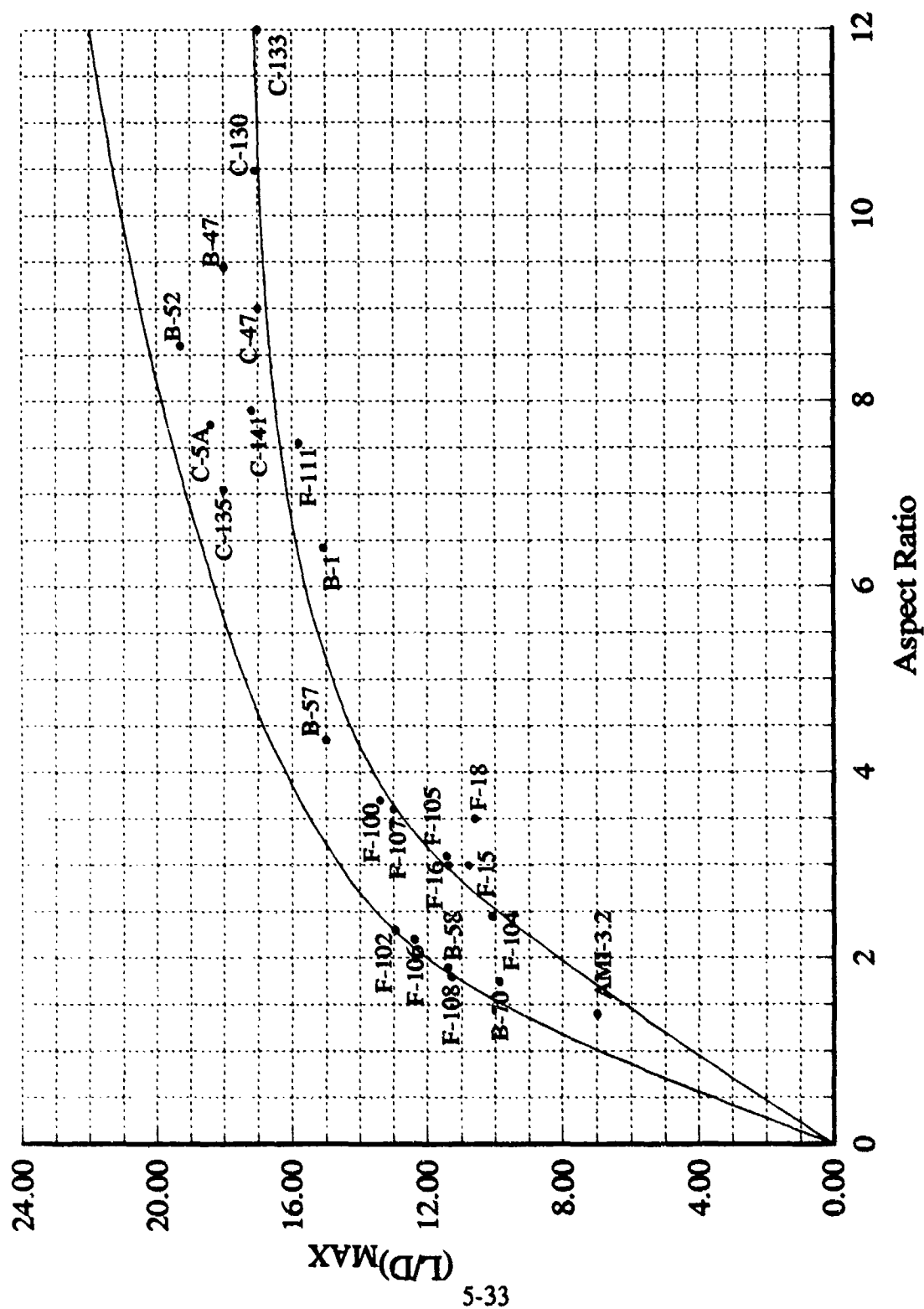


FIGURE 5-21 Subsonic Maximum L/D Variation With Aspect Ratio

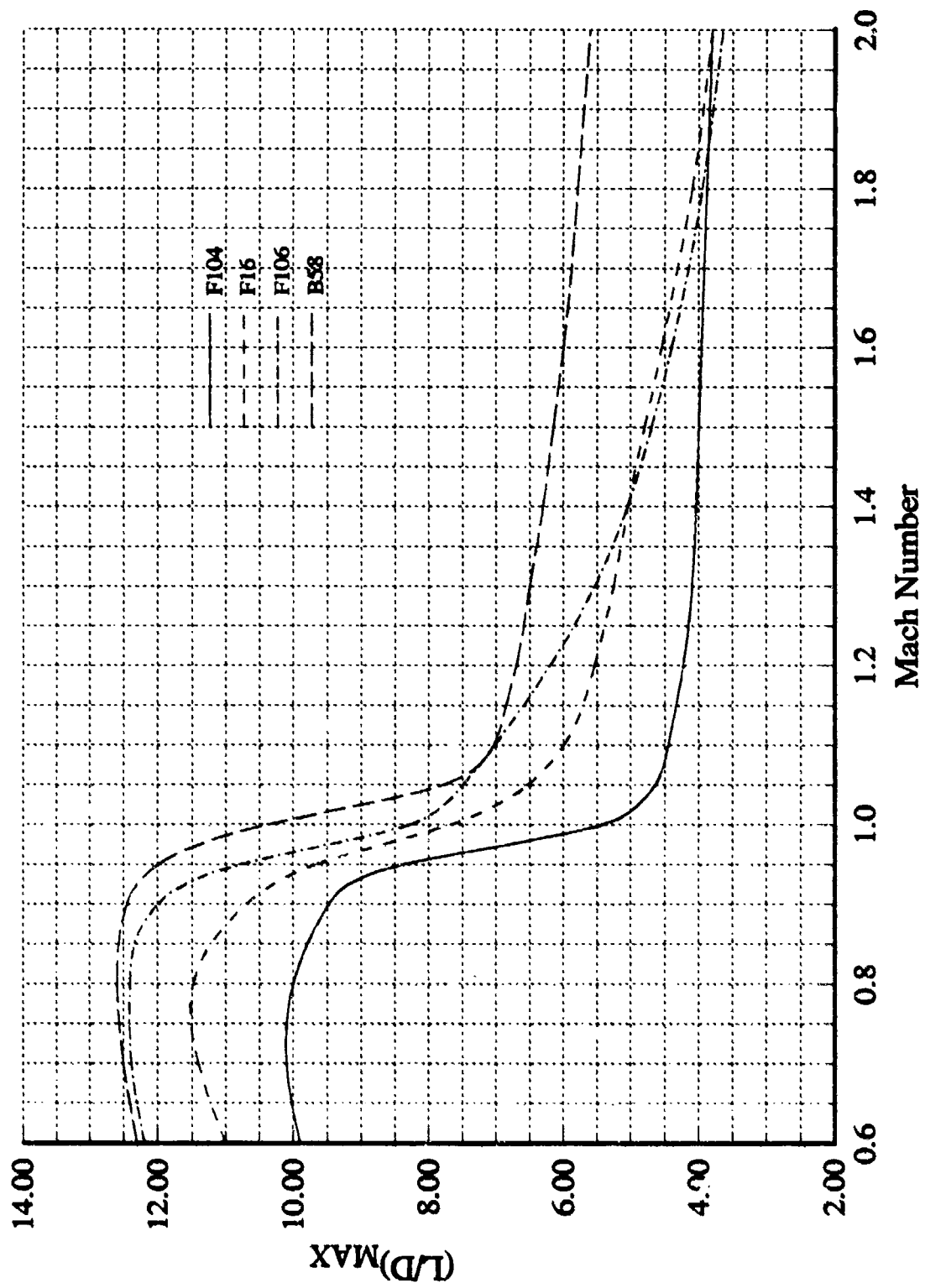


FIGURE 5-22 Variation of Maximum L/D With Mach Number

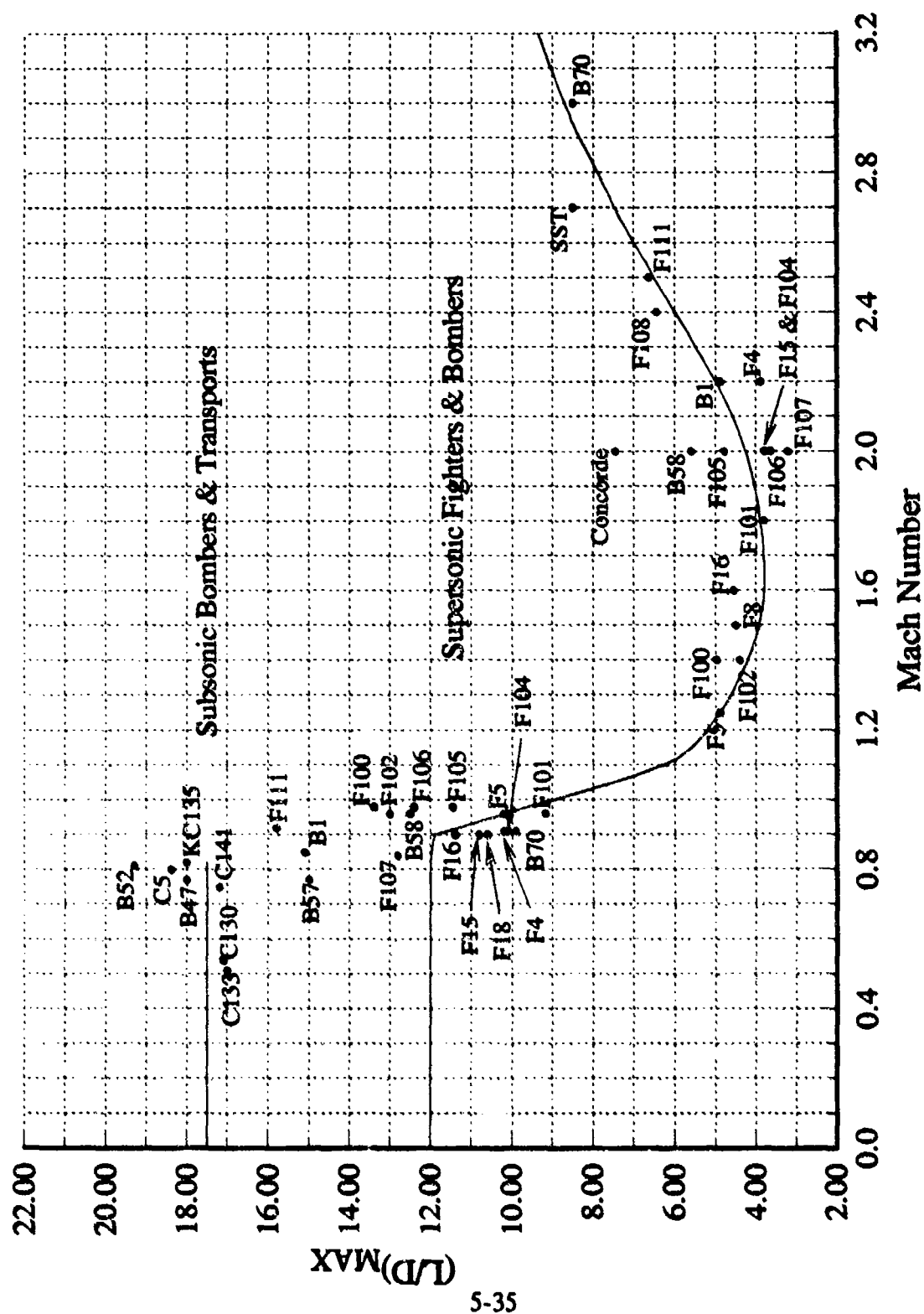


FIGURE 5-23 Maximum L/D at Subsonic Cruise and Maximum Speed

6. INFLUENCE OF AERODYNAMIC AND CONFIGURATION PARAMETERS ON PERFORMANCE

The initial design of a configuration is strongly dependent on the performance requirements. These requirements dictate the general appearance of a configuration, wing loading, thrust-to-weight, wing sweepback, fuselage fineness ratio and almost every other major feature of an aircraft. Thus it is important to have an awareness of how each mission performance segment influences the selection of key vehicle parameters. A typical fighter mission consists of take-off, acceleration to speed and altitude, cruise, combat, cruise, and land.

TAKE-OFF

Take-off performance is dependent primarily on the weight of the aircraft, the lift generated by the aircraft wing and the takeoff power available from the engine. The maximum lift coefficient (Reference 28) is a function of wing planform (AR , Λ , λ), wing thickness and camber, as well as the type of high lift devices employed (slot or drooped leading edge flaps, plain hinge or fowler trailing edge flaps) and the percentage of the wing area that these devices encompass. In the early preliminary design phase, most of these details are not known. However, $C_{L \text{ Max}}$ can be estimated based on data from existing aircraft of a similar configuration. Figure 6-1 shows the $C_{L \text{ Max}}$ that is available for several fighter and transport aircraft. With the estimate of $C_{L \text{ Max}}$, the stall velocity (ignoring thrust effects) can be determined as a function of the wing loading (W/S) as shown in Figure 6-2. If the stall velocity is a requirement, this curve can be used to determine the W/S and thus the wing area (S) required to meet the stall speed. The takeoff velocity is normally based on using only 75% of $C_{L \text{ Max}}$ and is shown in Figure 6-3. The take-off distance is shown in Figure 6-4 as a function of thrust loading, wing loading, and $C_{L \text{ TO}}$. This curve is based on data from many aircraft and is presented in terms of the most important

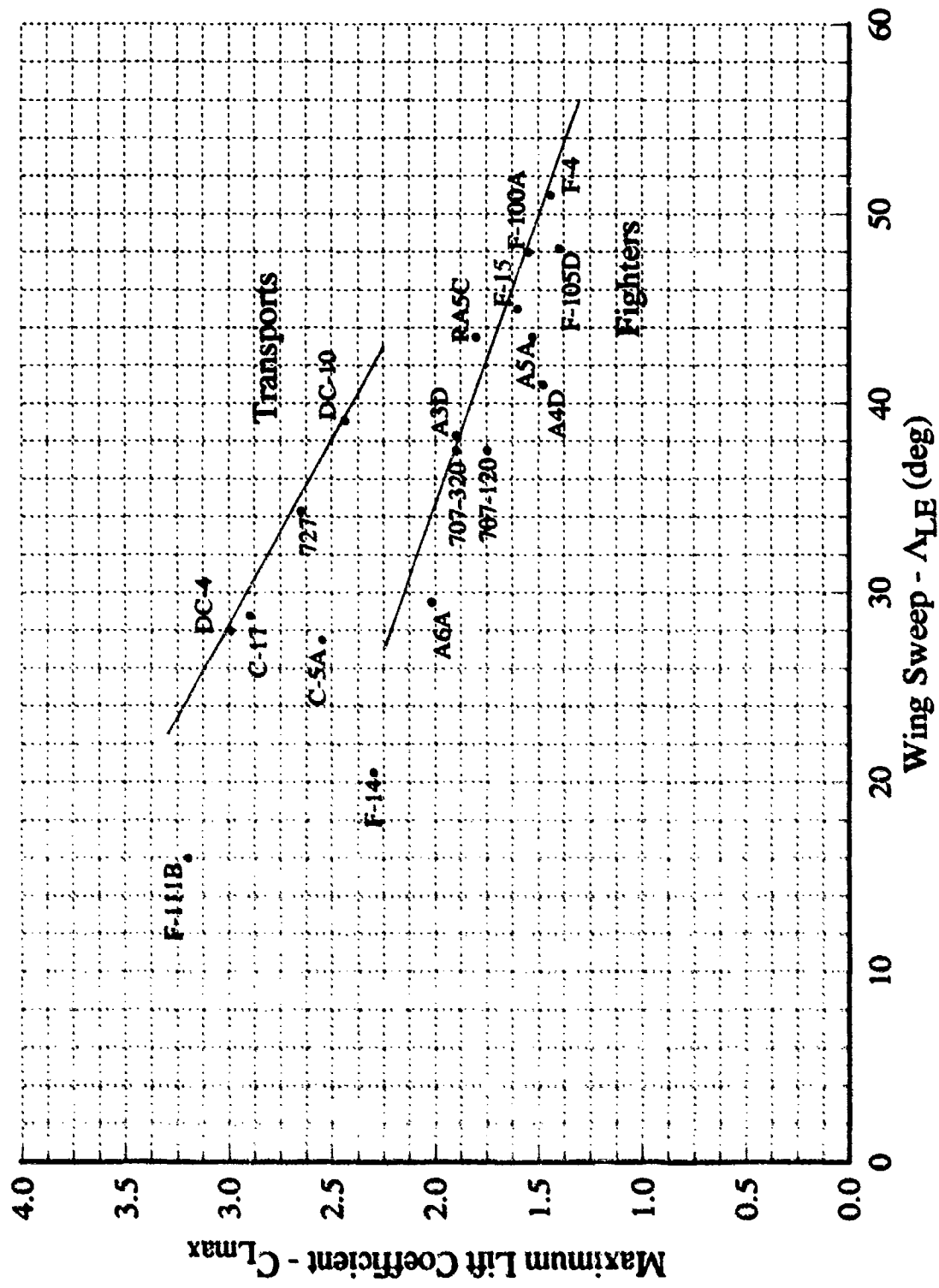


FIGURE 6-1 Flaps Down C_{Lmax}

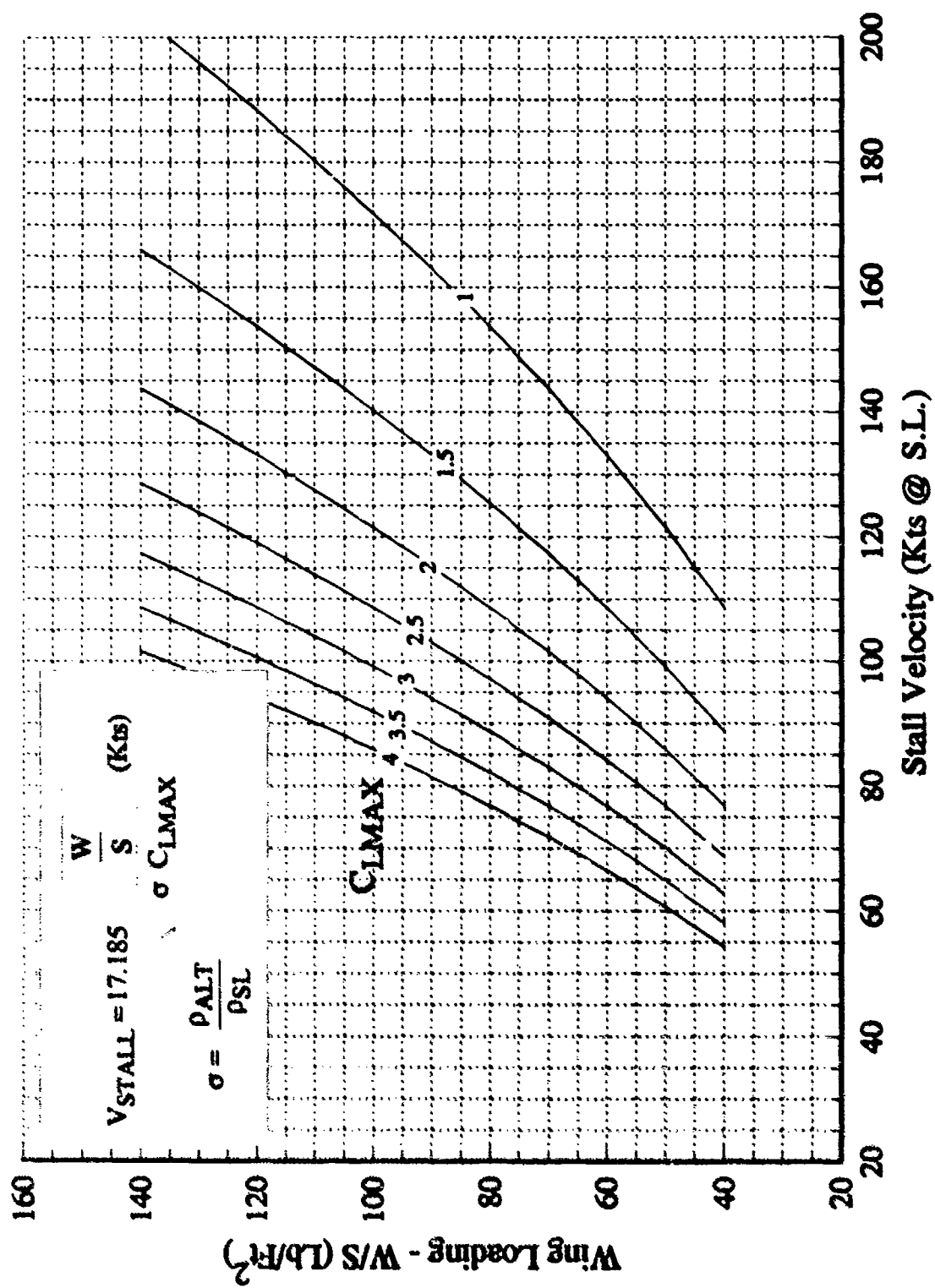


FIGURE 6-2 Stall Velocity Versus Wing Loading

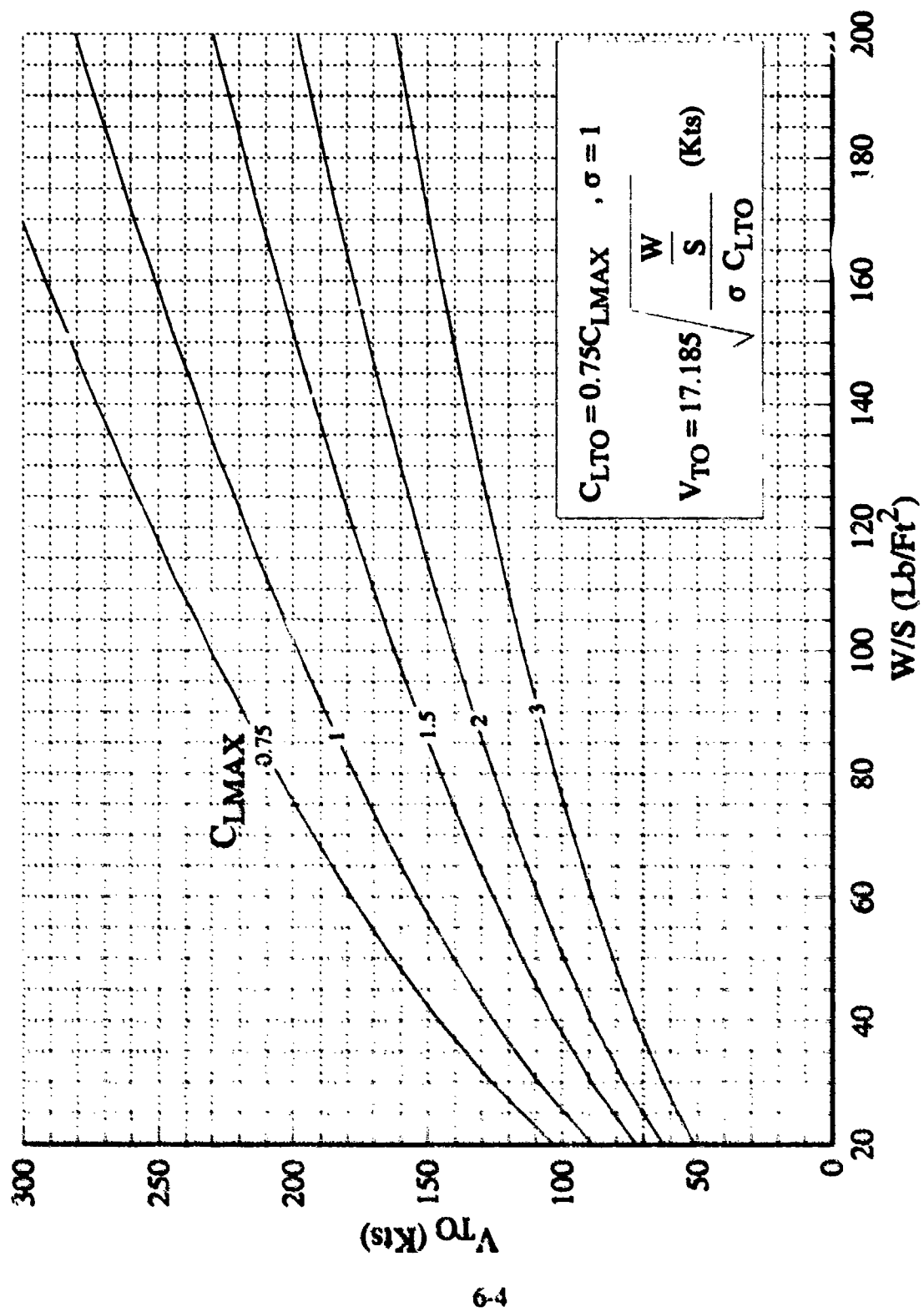


FIGURE 6-3 Take-Off Velocity

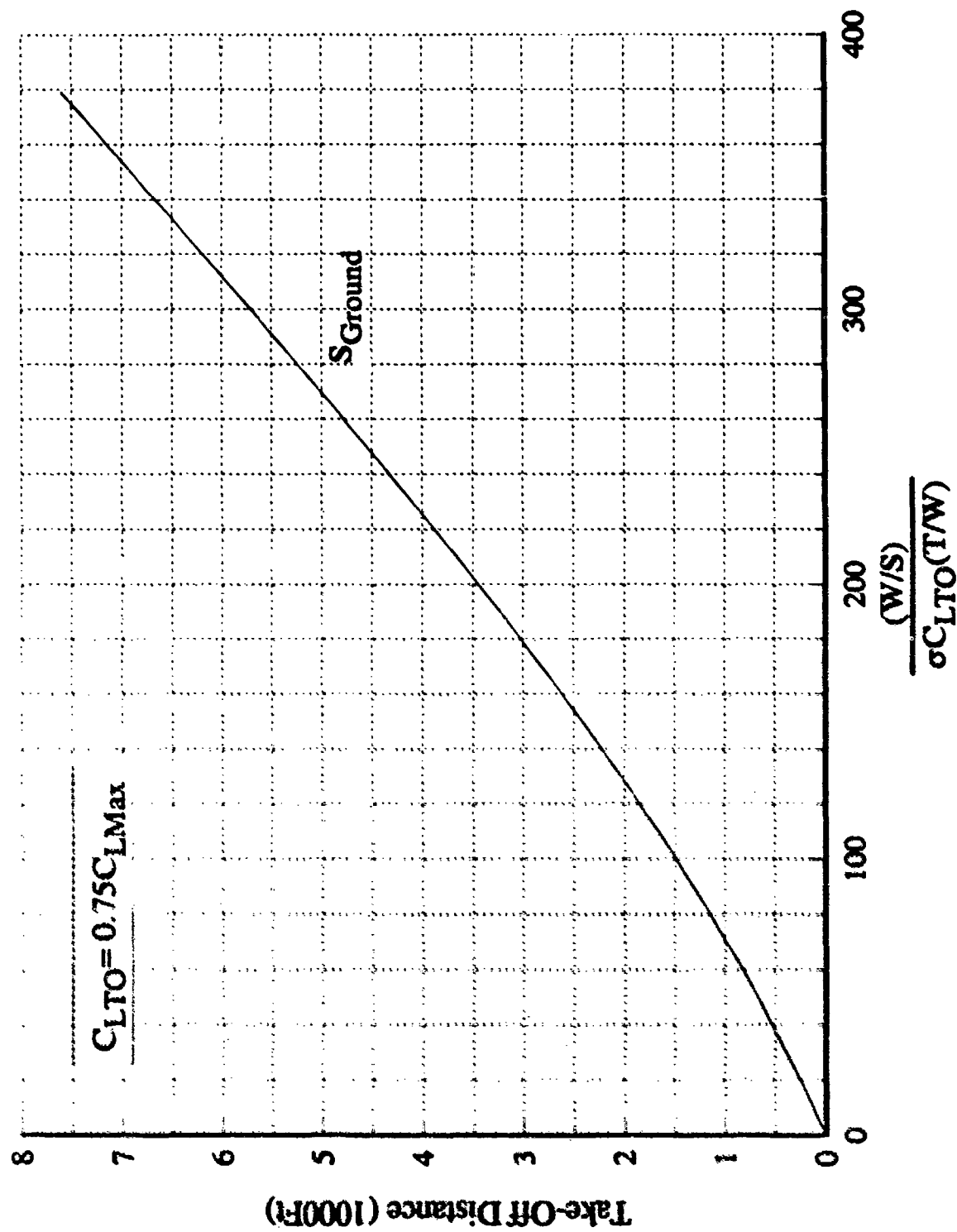


FIGURE 6-4 Take-Off Distance

airplane and engine parameters.

RANGE AND SPECIFIC RANGE

The range of an aircraft is a critical performance parameter and it strongly influences the wing design. The primary aerodynamic parameter which drives the configuration is maximum lift-to-drag ratio, $(L/D)_{Max}$. The lift coefficient for $(L/D)_{Max}$ is called the optimum C_L and is

given by:
$$C_{L Opt} = \sqrt{\frac{C_{D0}}{K}} \quad (6-1)$$

and the required C_L for one g level cruise flight is:

$$C_{L Req} = \frac{W}{qS} \quad (6-2)$$

then for $C_{L Req} = C_{L Opt}$
$$\frac{W}{S} = q \sqrt{\frac{C_{D0}}{K}} \quad (6-3)$$

Therefore, at maximum L/D, airplanes fly at an altitude and velocity to satisfy equation (6-2).

Hence for a fixed velocity and wing loading, the cruise altitude is defined for maximum L/D.

Historical data is presented in Figure 6-5 to evaluate cruise altitude based on take-off wing loading. The data indicates cruise altitude decreases as wing loading increases, but begins to level off at wing loadings above 160psf. The cruise range of an aircraft can be estimated quite accurately by the Breguet range equation given below:

$$R = 2.3 \left(\frac{V}{SFC} \right) \left(\frac{L}{D} \right) \log_{10} \left[\frac{W_i}{W_f} \right] \quad (6-4)$$

with R in nautical miles

V in knots

SFC in lbs of fuel per hour per pound of thrust

L/D lift to drag ratio

W_i/W_f initial cruise weight/final cruise weight

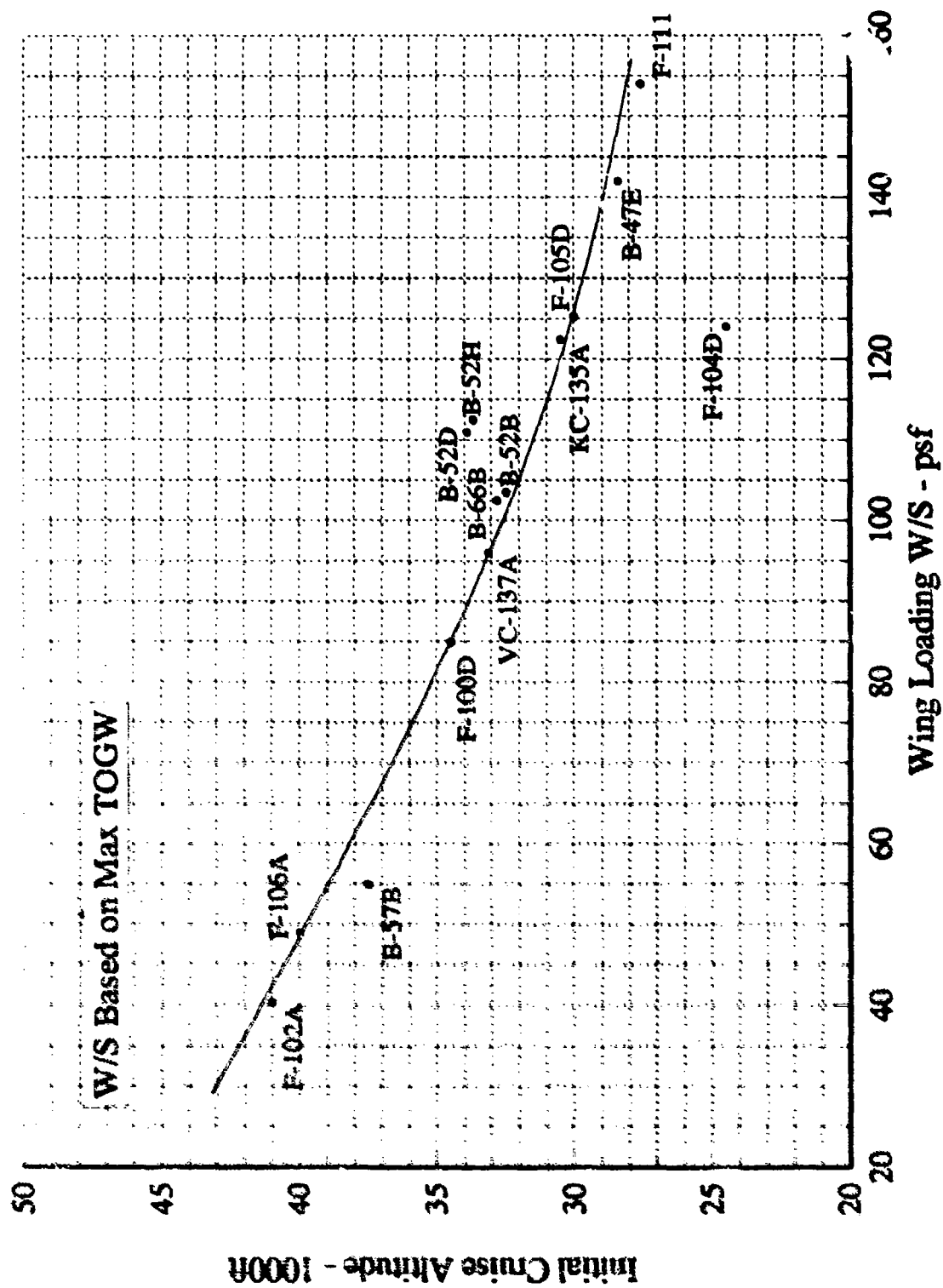


FIGURE 6-5 Cruise Altitude

Assumptions used in developing this equation include cruising at constant (L/D) (not constant altitude), constant velocity and constant SFC. Thus an increase in L/D, a reduction in SFC, and an increase in fuel fraction will lead to increased range.

The impact of lift-to-drag ratio on cruise range for transports is shown in Figure 6-6. Since fuel fraction for transports (Figure 4-7) varies between 35 and 45 percent of the gross take-off weight, and typical cruise fuel loads account for 45 to 55 percent of the total fuel load, a representative range of values for cruise fuel weight to gross take-off weight is 0.15 to 0.25. Hence, a transport with an $L/D = 16$, an initial cruise weight to final cruise weight ratio of 1.25 would have a nominal range of 3800 nautical miles. A similar chart for fighters is presented in Figure 6-7. Since the nominal fuel fraction for fighters is 27 percent of gross take-off weight and typical internal cruise fuel loads are about 30 to 40 percent of the total fuel load, a nominal range of values for initial cruise fuel weight to gross take-off weight is 0.075 to 0.125. Therefore, a fighter with an $L/D = 10$, an initial cruise weight to final cruise weight ratio of 1.10, would have a nominal range of 500 nautical miles.

The impact of supersonic speed on fighter range is readily apparent in Figure 6-8. Assuming an $L/D = 4$, at an altitude of 40,000ft, $SFC = 2.0$ and an initial to final cruise weight ratio of 1.10, the fighter range is only 225 nautical miles. This is over a 55 percent reduction in range capability. This is optimistic since large quantities of fuel will be consumed during acceleration from Mach 0.9 to 2.0. The acceleration fuel will decrease the fuel available for cruise flight. Thus there is a significant penalty for supersonic speeds. This large penalty may be reduced through the use of very high fuselage fineness ratios, increased wing sweepback angles and small wing thickness ratios.

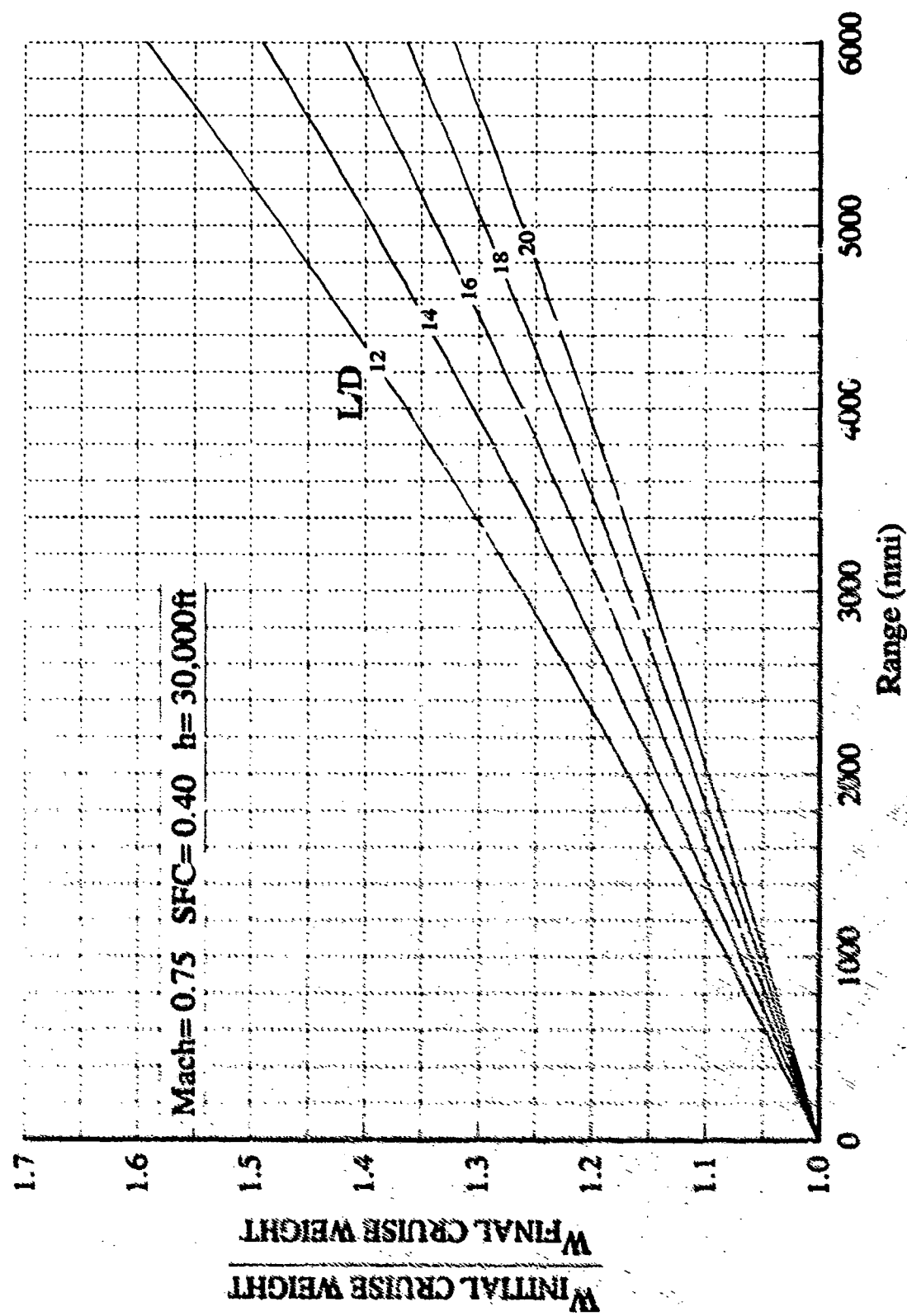


FIGURE 6-6 Impact Of Cruise Fuel On Transport Range

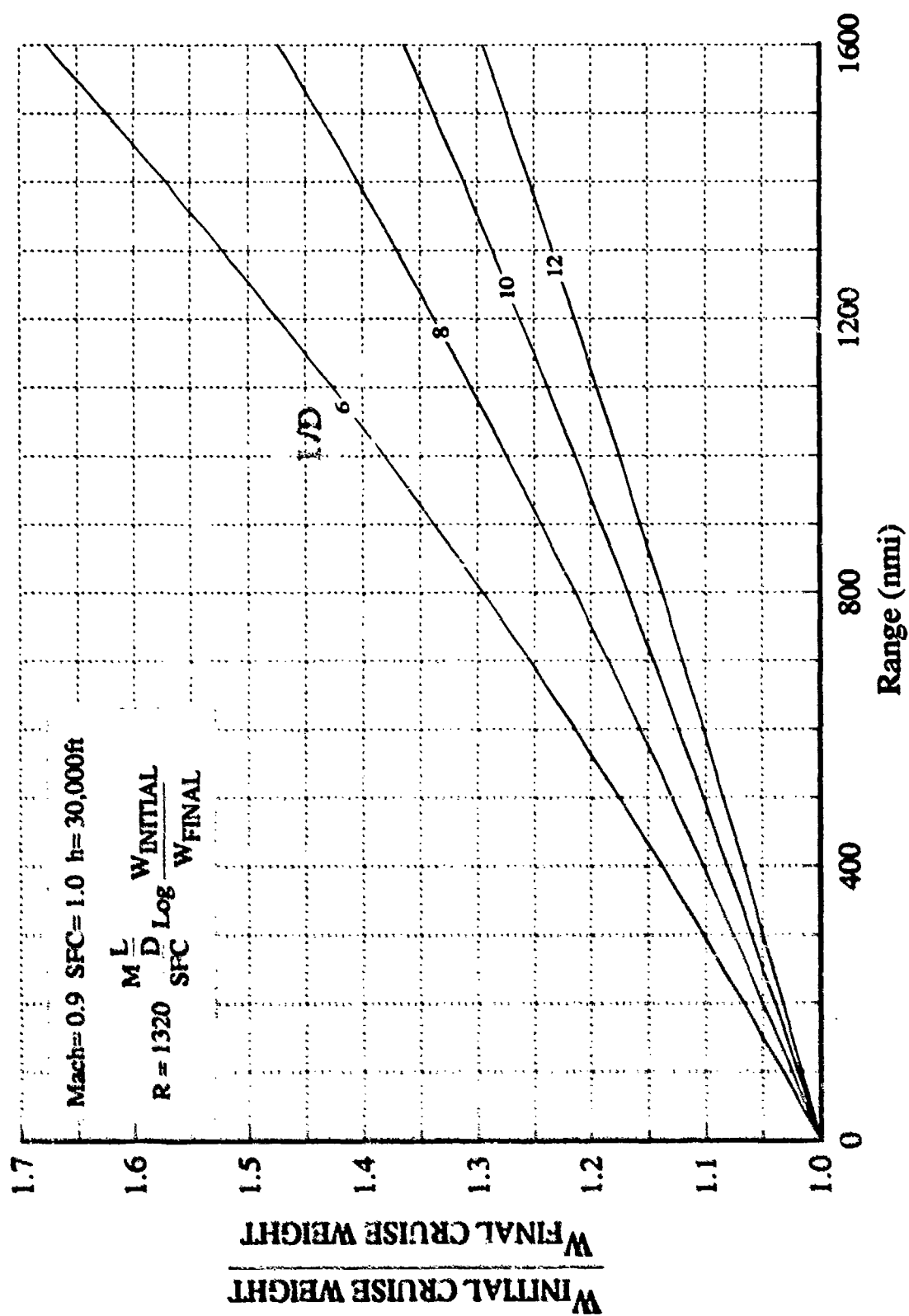


FIGURE 6-7 Impact Of Cruise Fuel On Fighter Range

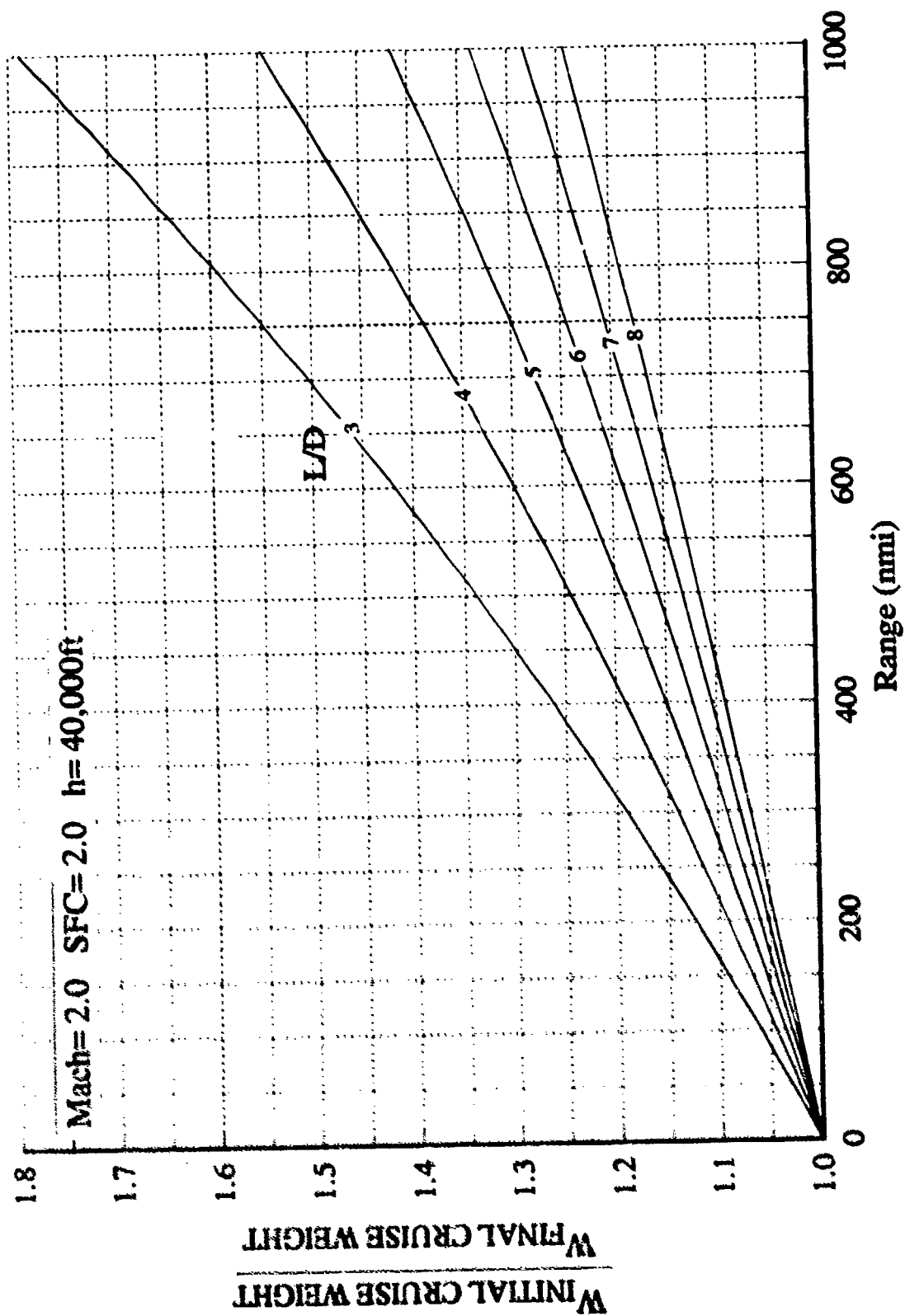


FIGURE 6-8 Impact Of Supersonic Speed On Fighters

Much attention in the 1970's and 80's was given to investigating the technologies which maximize the range parameter $\frac{M(L/D)}{SFC}$ (References 29-32). A class of vehicles called "supercruisers" were envisioned where L/D at higher Mach numbers was maximized while keeping engine throttle setting below afterburner for low SFC. This was a severe challenge to the aerodynamicist in trying to maximize supersonic L/D and maintain acceptable transonic maneuvering characteristics. The design options for increasing high speed L/D impact the available fuel fraction, while the thrust required at non-afterburner engine power settings defines engine size, which in turn impacts vehicle size, shape, weight, fuel fraction and L/D. These are the conflicts which must be resolved early in the design cycle.

In order to permit rapid estimates involving aircraft range the following approach can be used. If a cruise range segment is divided by the fuel consumed for the distance traveled a parameter called specific range is formed, with units of nautical miles per pound of fuel. This is an average value of how far a particular aircraft can travel on one pound of fuel. The instantaneous specific range is found by dividing the flight velocity by the fuel flow

$$SR = \frac{V}{FF} \quad (6-5)$$

where: V - nautical miles per hour
 FF - lbs of fuel per hour
 SR - nautical miles per lb of fuel

Equation (6-5) may be expressed as

$$SR = \frac{V}{FF} = \frac{V}{SFC \times T}$$

and for $T=D$; $L=W$; and $D = \frac{W}{L/D}$

$$SR = \frac{V \left(\frac{L}{D} \right)}{SFC \times W} \quad (6-7)$$

For a modern aircraft at Mach 0.9 and 30,000 feet:

$$\begin{aligned} L/D &= 10, \\ SFC &= 1.0 \text{ lbs/hr/lb} \\ V &= 516 \text{ knots} \\ W_1 &= 25,000 \text{ lbs} \end{aligned}$$

$$\begin{aligned} \text{then } SR &= \frac{(516)(10)}{1.0(25,000)} \\ &= 0.206 \frac{nmi}{lb} \end{aligned}$$

Another often used parameter is the range parameter which is composed of parameters from the Breguet range equation.

$$RF = \frac{V \left(\frac{L}{D} \right)}{SFC}$$

It is often used to compare aircraft capability based on aerodynamics and propulsion efficiencies. A rapid approximation for the fuel required for a cruise mission segment can be made by dividing the range required by the specific range.

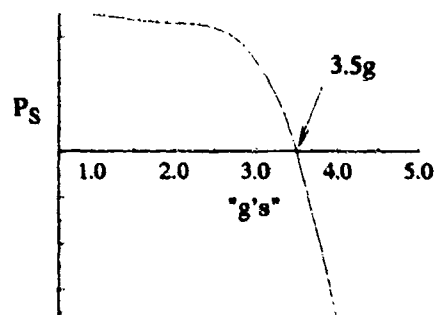
SPECIFIC EXCESS POWER/MANEUVERING

Specific excess power is defined as

$$P_s = V \left[\frac{T - D}{W} \right] \quad (6-8)$$

and is expressed in the units of feet per second. Simple aircraft force equilibrium shows that P_s is the rate of climb an aircraft can achieve under the approximations of shallow climb angles and non-accelerated flight (References 33 to 35). However as currently used, P_s is better

characterized as the excess power available to an aircraft for maneuvering or climbing. This interpretation is based on the fact that P_S is calculated at flight conditions other than 1 "g". For example, at a specific altitude, velocity, and weight all terms in the P_S equation are fixed except drag.



SKETCH A

Sketch A indicates the maximum value of P_S at 1 "g", the $P_S = 0$ point of about 3.5 "g's" and negative P_S beyond 3.5 "g's"

Aircraft performance specifications are often expressed partially in terms of P_S . A matrix of values are used with different levels of P_S required at various combinations of altitude, velocity, thrust level, maneuver level, and weight. A sample matrix is shown below.

MACH	ALTITUDE	"g's"	THRUST	P_S (ft/sec)
0.8	10K	1g	Max A/B	1000
0.8	10K	7g	Max A/B	-100
0.9	30K	1g	Max A/B	400
0.9	30K	1g	Mil Power	100
0.9	30K	5g	Max A/B	..
1.2	45K	1g	Mil Power	0

Aircraft designers will vary design parameters such as T/W, W/S, AR and fineness ratio in

an attempt to meet these performance requirements (as well as others). Often meeting one particular requirement such as the 5g, M=0.9, h=30,000 ft. point in the example above will ensure that the other requirements are also met.

Contour plots of P_S against altitude and Mach number are often generated to show the global performance capability of an aircraft. A typical example is shown in Figure 6-9. The $P_S = 0$ lines indicate on a "1g" chart the flight envelope capability of the vehicle. On charts for conditions above 1 "g" (Figure 6-10) the $P_S = 0$ line indicates for each Mach number the maximum altitude at which the aircraft can sustain the "g" level of the figure.

Another valuable use of the P_S performance parameter is in comparing one aircraft against another. This is typically done in evaluating various aircraft design solutions and in evaluating the performance advantages and disadvantages of threat aircraft. An advantage of 100 feet per second is generally accepted as significant when comparing aircraft performance.

SUSTAINED MANEUVERING

Another classic performance parameter utilized is maximum sustained "g" capability. As indicated in the previous discussion P_S and maximum "g" capability are closely related. When P_S is equal to zero an aircraft is at its maximum sustained "g" level with thrust equal to drag at the maneuver level. This "g" level can be determined as follow:

$$\text{When } P_S = 0; \quad \frac{T}{W} = \frac{D}{W}$$

$$\text{Let} \quad D = qS \left[C_{D0} + \frac{C_L^2}{\pi A R e} \right]$$

$$\text{and} \quad C_L = \frac{nW}{qS} \quad (n = \text{"g" level})$$

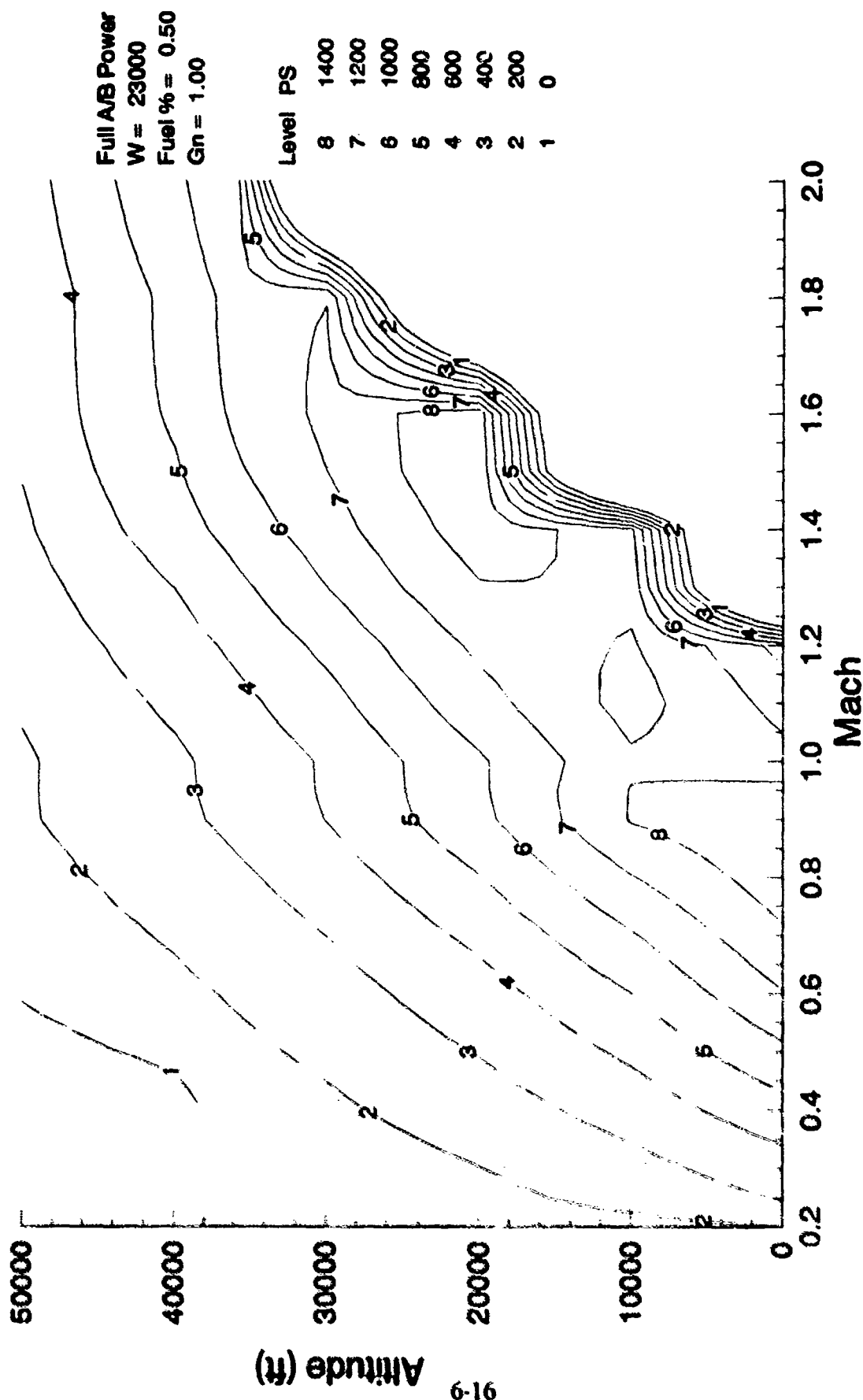


FIGURE 6-9 Specific Excess Power, $G=1.0$

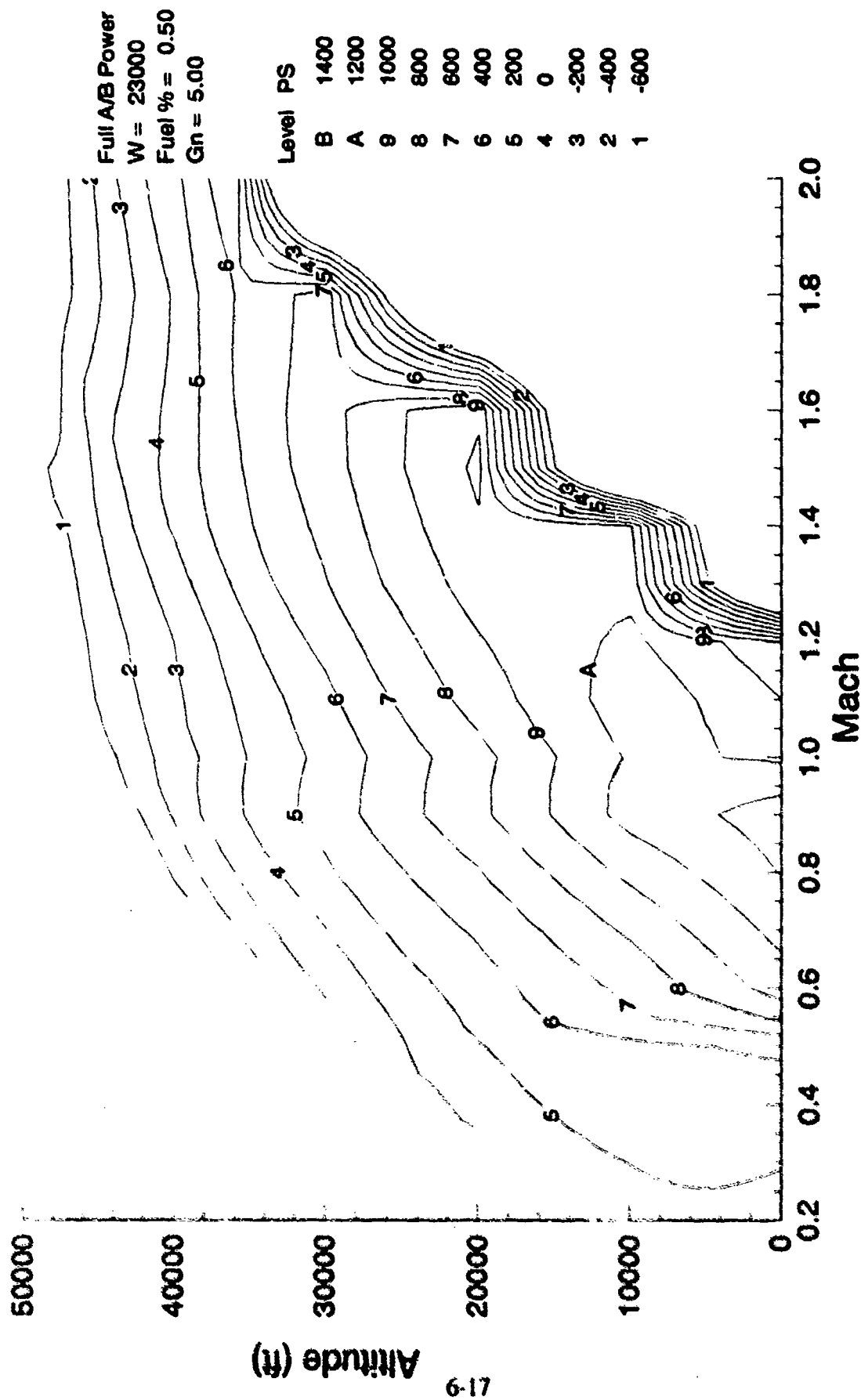


FIGURE 6-10 Specific Excess Power, $G=5.0$

solving for n results in the following relationship

$$n = \sqrt{\frac{q\pi eAR}{\frac{W}{S}} \left[\frac{T}{W} - \frac{qC_{D0}}{\frac{W}{S}} \right]} \quad (6-9)$$

Figures 6-11 to 6-13 have plotted this equation in parametric form for values of AR , " e ", and C_{D0} typical of modern aircraft. One interesting interpretation of Figure 6-12 is to note the variation of required T/W as W/S varies while keeping the maneuver capability constant. This type of chart can identify design choices for meeting maneuver specifications with either fixed or "rubber" engines. Note in Figure 6-12 that the effect of C_{D0} on the required T/W at a constant W/S is relatively small for this condition. The effects of wing planform (AR) and design technology (" e ") can also be estimated with equation (6-9). Figure 6-13 indicates similar data for supersonic flight conditions and typical fighter aircraft parameters.

In using equation (6-9) it is important to note that the thrust-to-weight, T/W , parameter is specified at the particular flight conditions under consideration. Thrust-to-weight and wing loading, W/S , are often used to characterize the performance levels and design emphasis of aircraft, high T/W and low W/S representing high performance. Since thrust varies with altitude and Mach number and wing loading varies with payload and fuel consumption; thrust to weight values are usually quoted at some reference condition such as sea level static maximum thrust and take-off gross weight. Figure 6-14 presents the variation of T/W for a typical modern fighter with both Mach number and altitude. Current high performance fighters have T/W values around 1.0 or greater at sea level reference conditions and decrease to 1/2 these values at mid altitudes and transonic speeds.

In assessing the relationships between performance requirements, typically P_s and sustained

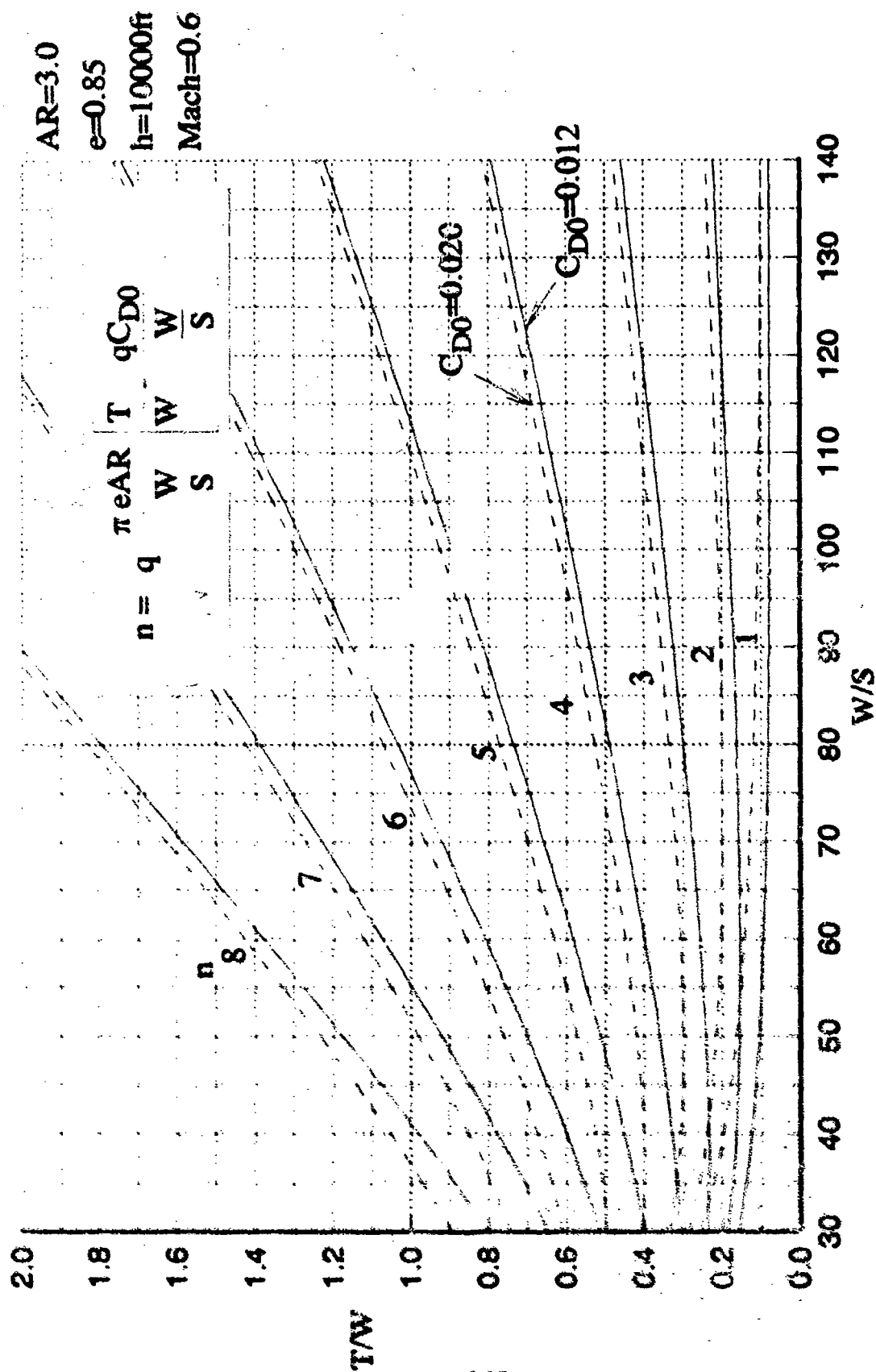


FIGURE 6-11 Maximum Sustained "G" Contours

AR=3.0
e=0.85
h=30000ft
Mach=0.9

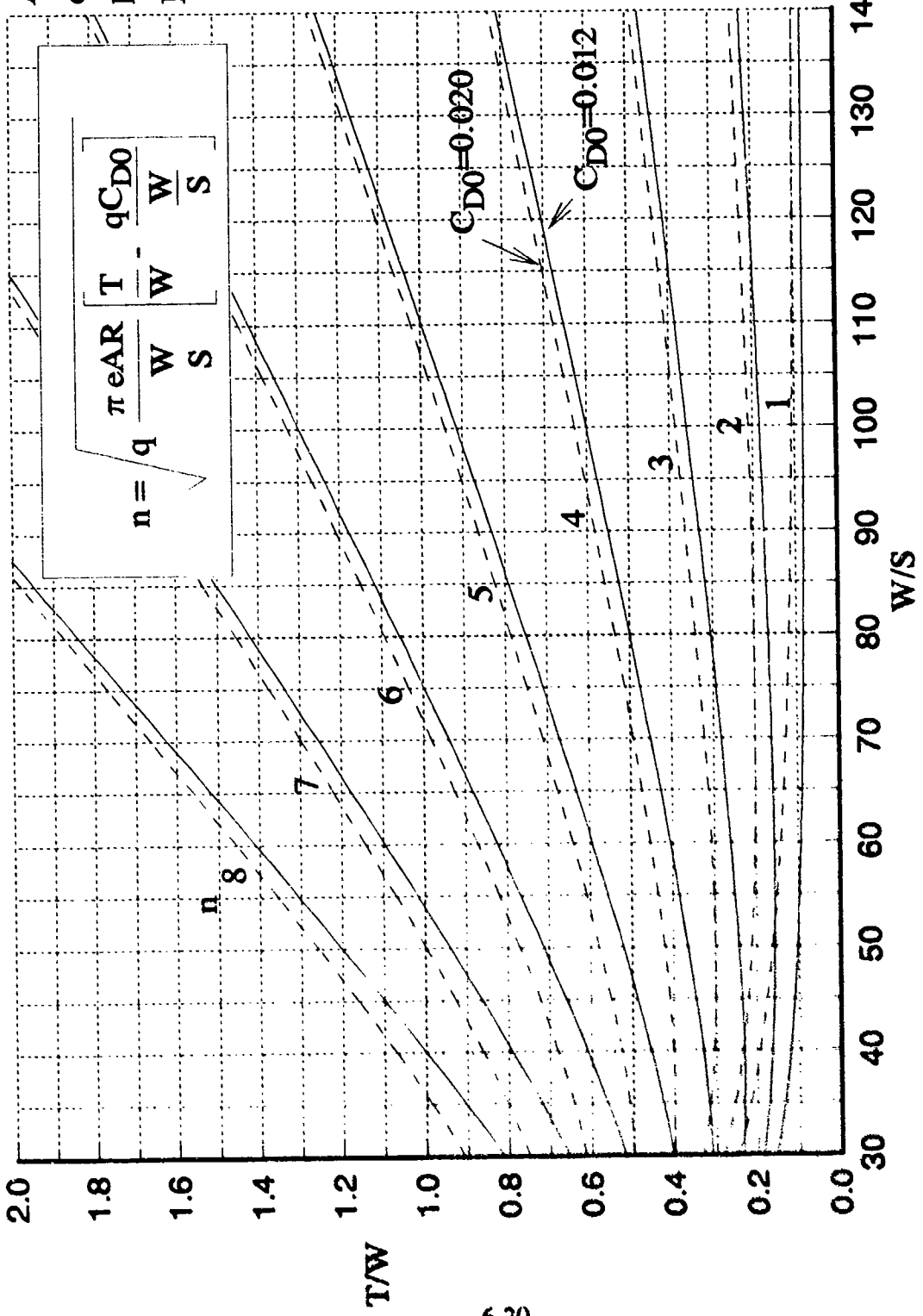


FIGURE 6-12 Maximum Sustained "G" Contours

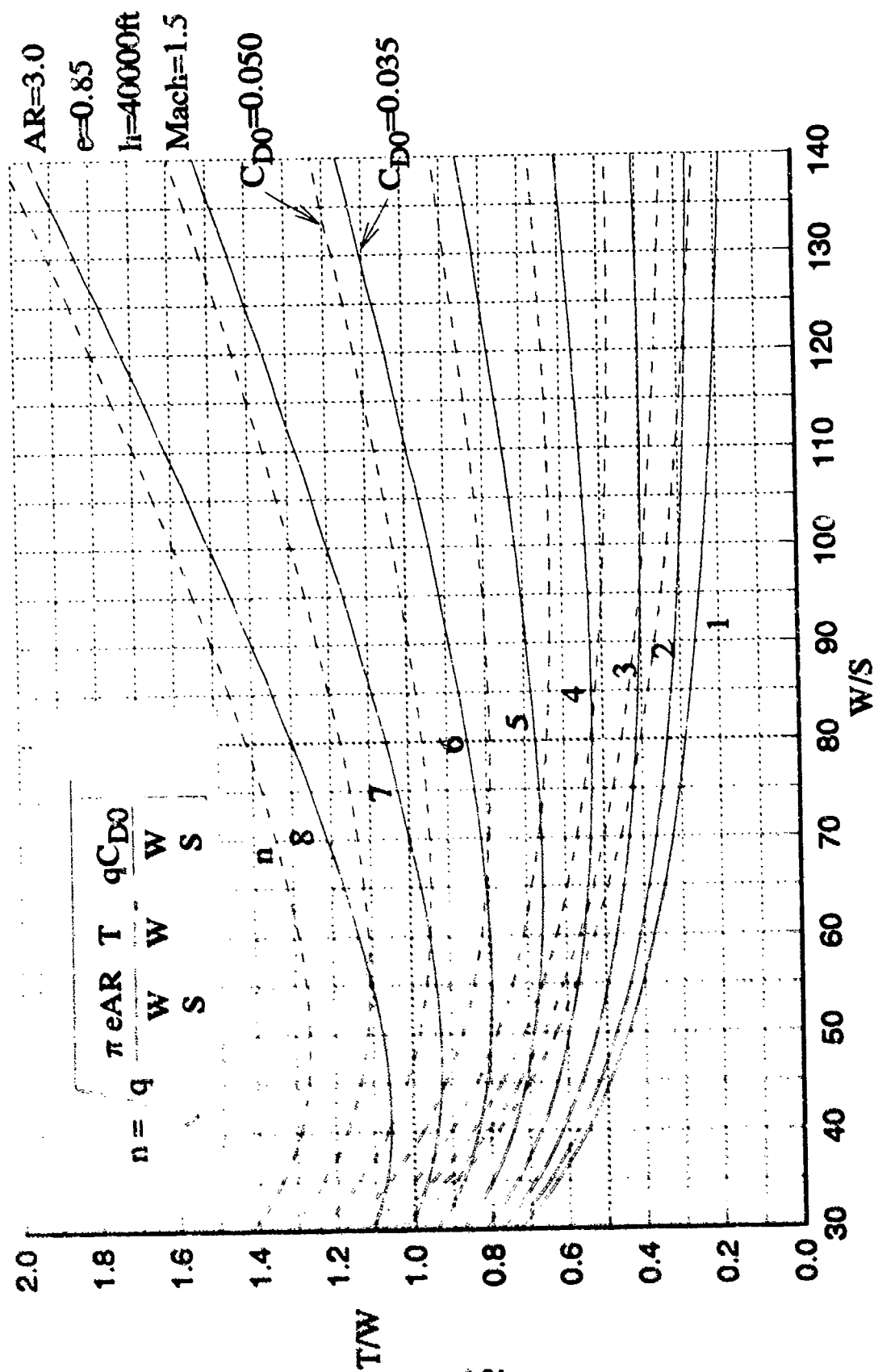


FIGURE 6-13 Maximum Sustained "G" Contours

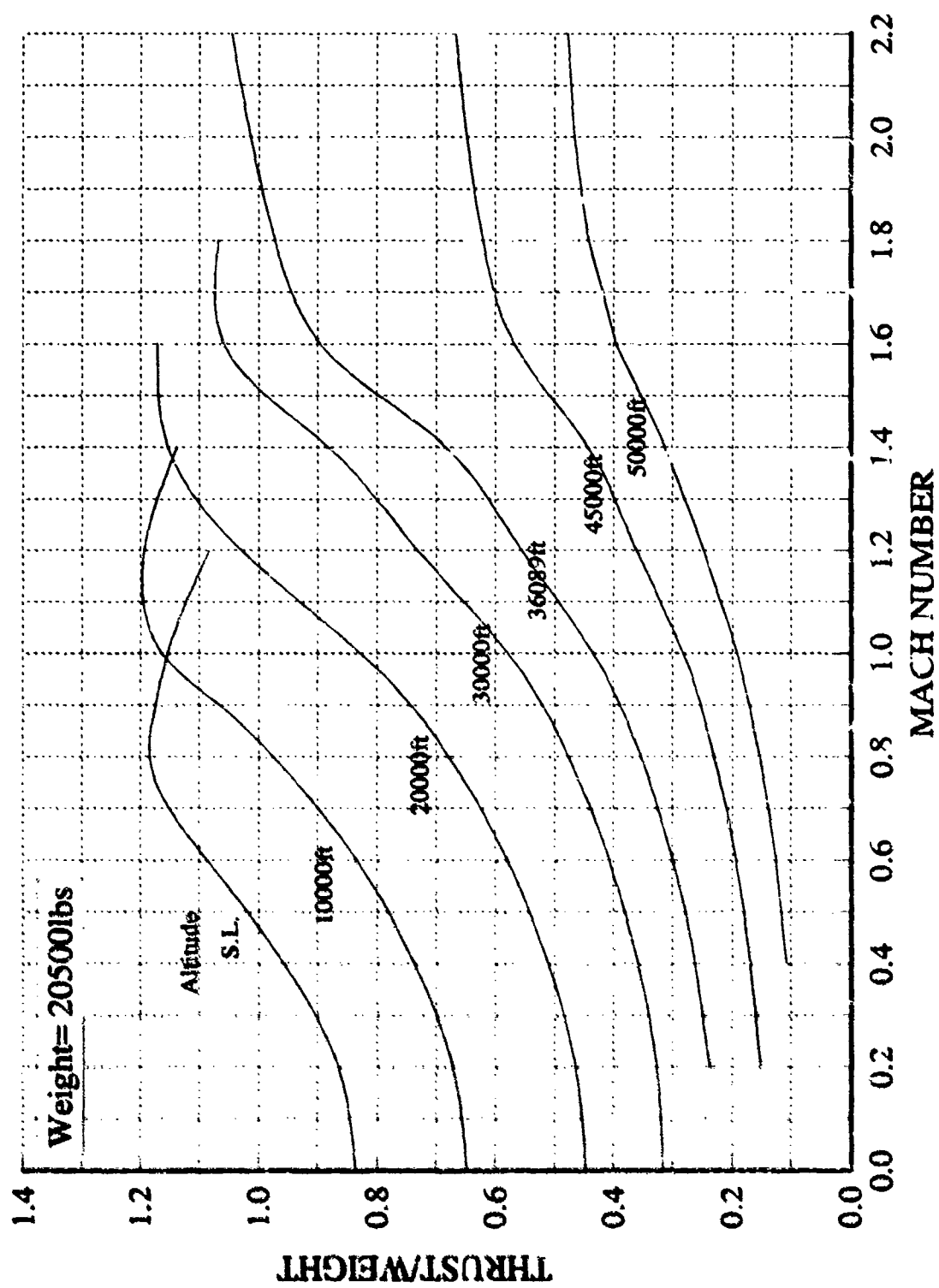


FIGURE 6-14 Thrust Variation For A Modern Fighter

g's, on aircraft design drivers such as T/W, the following observations provide some guidance.

Using the P_S equation (6-8) results in

$$P_S = V \left[\frac{T}{W} - \frac{D}{W} \right]$$

$$\frac{T}{W} = \frac{P_S}{V} \quad \text{If } D = 0$$

$$\text{or} \quad \frac{T}{W} \geq \frac{P_S}{V} \quad \text{For } D > 0$$

Given a P_S specification at some altitude and Mach number we can immediately establish a lower bound on T/W at those conditions. To obtain a better estimate consider

$$\frac{D}{W} = \frac{1}{\left(\frac{L}{D} \right)} \quad \text{If } L = W$$

if we return to the P_S relationship we have

$$\frac{T}{W} = \frac{P_S}{V} + \frac{1}{\left(\frac{L}{D} \right)}$$

The minimum value of $\frac{1}{\left(\frac{L}{D} \right)}$ results when $\frac{L}{D} = \left(\frac{L}{D} \right)_{Max}$

$$\text{so} \quad \frac{T}{W} \geq \frac{P_S}{V} + \frac{1}{\left(\frac{L}{D} \right)_{Max}}$$

At maneuver lift coefficients where $L \approx nW$, $(L/D)_{Maneuver}$ is less than $(L/D)_{Max}$ so the final estimate is

$$\frac{T}{W} \geq \frac{P_S}{V} + \frac{1}{\left(\frac{L}{D}\right)_{Man}}$$

A typical value for L/D at high speed, subsonic maneuver conditions for current fighters is 3 to 4.

The T/W 's estimated by the above procedure can be scaled back to reference conditions using propulsion data from a candidate engine (see Figure 6-14 for trends) or the following approximation when data is not available.

$$T_{ALTITUDE} = T_{SEA LEVEL} \left(\frac{\rho_{ALT}}{\rho_{SL}} \right)$$

TURN RATE

Another performance parameter often used is turn rate expressed in degrees per second and indicates how fast the pilot can "point the nose". Turn rate for sustained maneuvering is simply related to the g capability of the aircraft through the following well-known expression

$$\dot{\theta} = \frac{g}{V} \sqrt{n^2 - 1}$$

Figures 6-15 and 6-16 present parametric data for quickly converting between sustained maneuver and turn rate.

All of the expressions used or developed in this section relate to sustained maneuvering which is an idealized steady state condition. Instantaneous maneuvering is also used as a performance requirement and represents a more dynamic condition. Instantaneous turn rate or maneuver level is typically characterized by maneuvers at $C_{L MAX}$ or a structural limit for limited durations and drag levels above available thrust. These maneuvers result in negative P_S and large

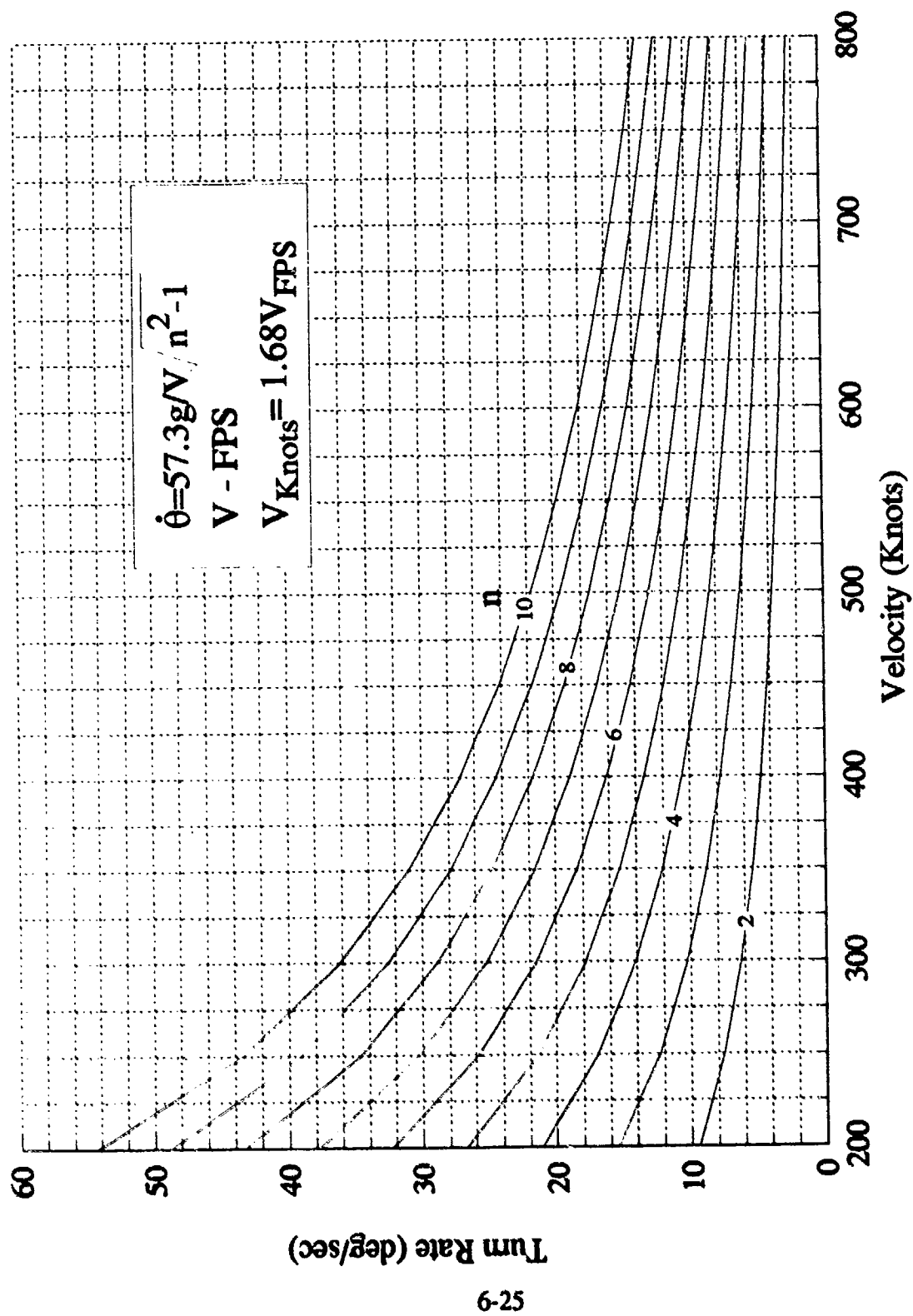


FIGURE 6-15 Aircraft Turn Rate For 200-800Knots

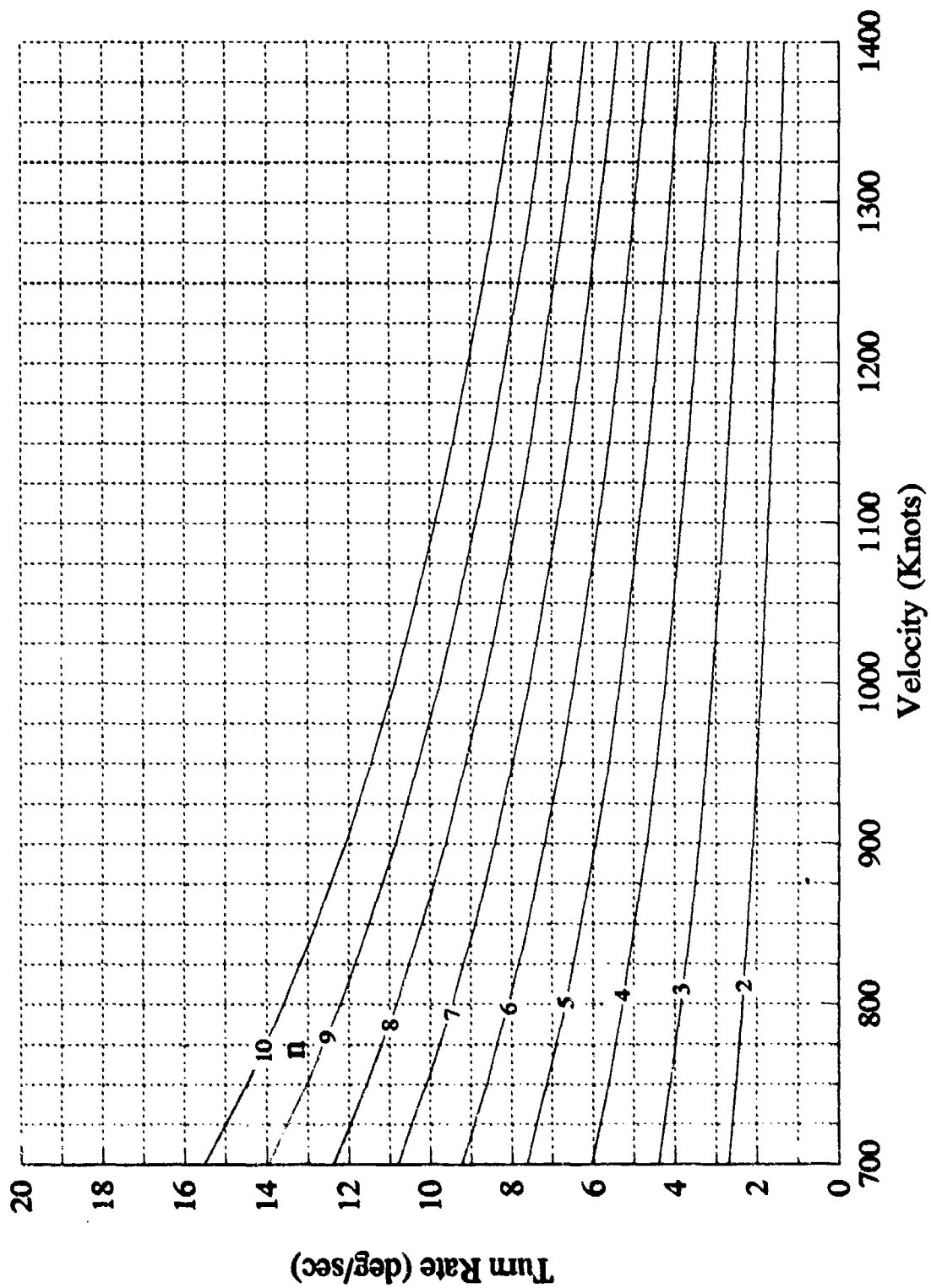


FIGURE 6-16 Aircraft Turn Rate For 700-1400Knots

changes in velocity and/or altitude, hence the name instantaneous as opposed to sustained.

LANDING

Landing performance is primarily dependent on the approach speed and the deceleration generated from braking (ignoring reverse thrust). The approach speed is normally defined as 20% above the stall velocity for $C_{L\text{ MAX}}$, which can be determined from Figure 6-1. A good braking system can provide a mean deceleration rate ($-a$) of -6 ft/sec^2 . Figure 6-17 provides the landing ground distance as a function of approach speed and deceleration and is based on the relationship:

$$\text{Distance} = \frac{V_{\text{App}}^2}{-2a}$$

Landing distance calculations normally include the horizontal distance traveled during the descent from a standard 50 foot obstacle. Figure 6-18 presents this air distance as a function of descent angle or glide slope γ , which is defined as the angle whose tangent is the ratio of vertical distance to horizontal distance and is also represented by the reciprocal of the lift to drag ratio, including power, in the approach configuration (L/D Power Approach), flaps and landing gear down, and also approximates the resulting thrust to weight ratio $\left[\frac{T-D}{W} \right]$.

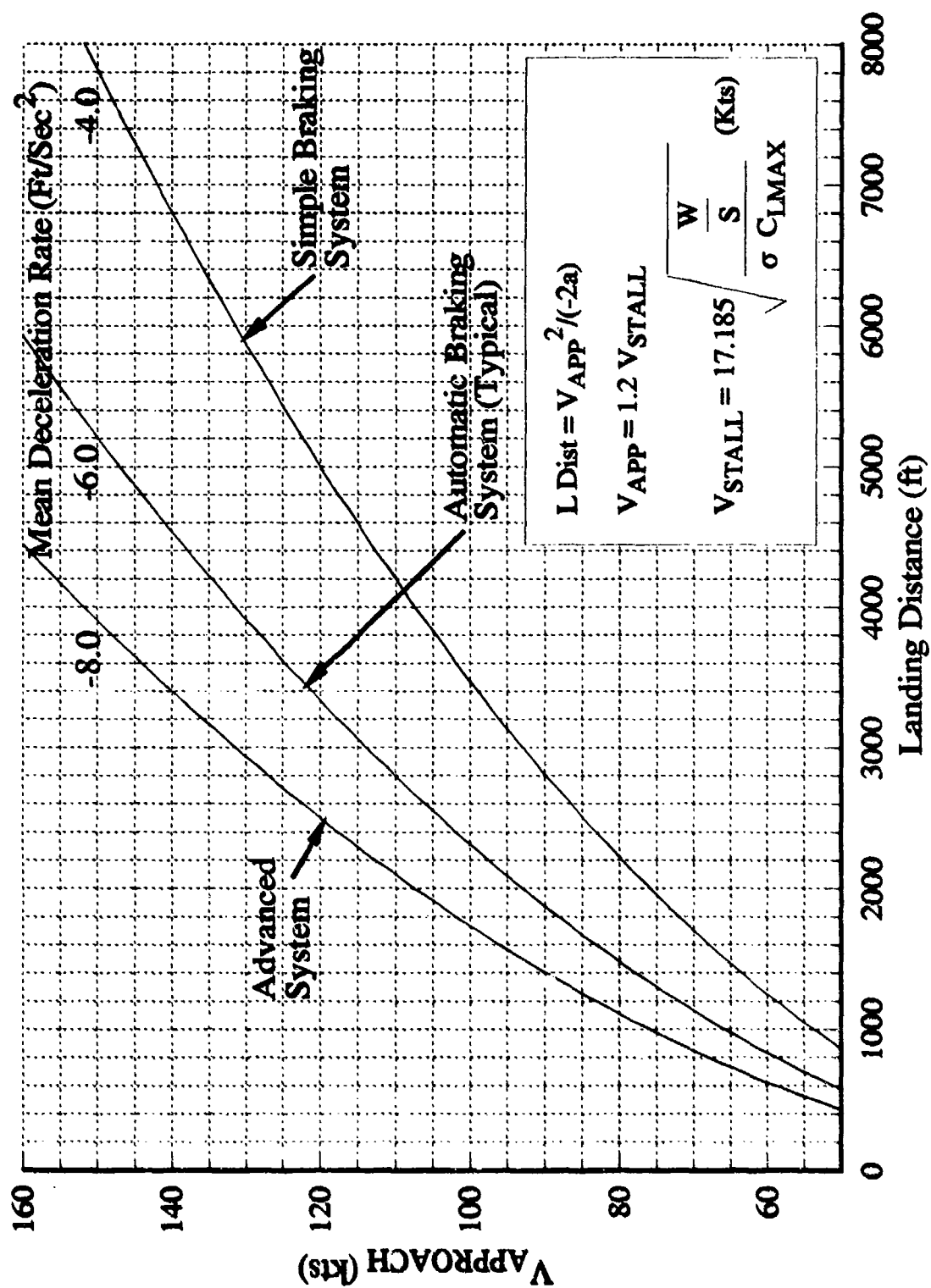


FIGURE 6-17 Landing Ground Distance

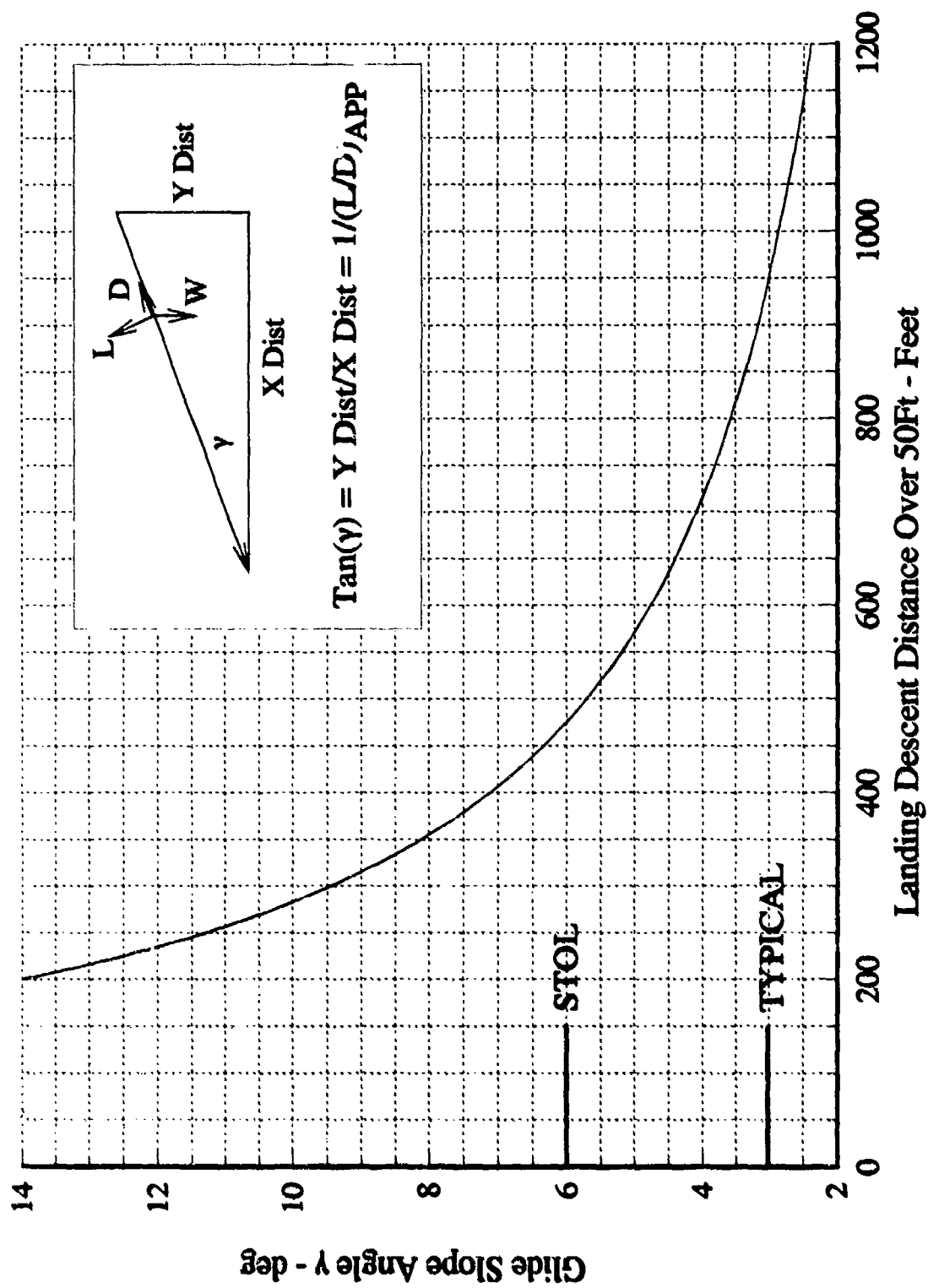


FIGURE 6-18 Descent Distance Over 50 Feet

7. PROCEDURES FOR THE FORMULATION AND ANALYSIS OF AN AIRCRAFT CONFIGURATION

This section illustrates the procedures to use for sizing and shaping an initial configuration, and to determine if it can meet the specified performance requirements. It uses many of the design charts in this report. The problem presented is only for fighters, but the procedure can also be used for transports and bombers. It is good to remember this is a starting point to defining a configuration. It is assumed the output from this procedure will be used as inputs to a more elaborate aircraft synthesis program (References 3 and 4).

Sample Problem

Performance Requirements

Max Speed: Mach= 2

Cruise Speed: Mach= 0.9

Radius: 325n.m.

Payload: 1,800lbs

Max Load Factor: 7.33g

Maneuverability:

4g's at M= 0.9/h= 30,000ft

5g's at M= 0.6/h= 10,000ft

4g's at M= 1.5/h= 40,000ft

Take-Off Distance: 3,000ft

Landing Distance: 6,000ft

Step 1 - Determine the gross take-off weight of this fighter from Figure 4-2.

$$\begin{aligned} \text{Ton-Miles} &= \frac{\text{Range} \times \text{Payload}}{2,000} \\ &= \frac{650 \times 1,800}{2,000} \\ &= 585 \\ \text{then GTOW} &= 36,000 \text{ lbs} \end{aligned}$$

Step 2 - Determine length from Figure 4-4a for a 36,000lb fighter.

$$\text{Length} = 55 \text{ ft}$$

Step 3 - Determine empty weight fraction from Figure 4-6 for a 36,000lb fighter.

$$\frac{W_{EMPTY}}{GTOW} = 0.68$$

$$\text{and } W_{EMPTY} = 24,480 \text{ lbs}$$

Step 4 - Determine fuel fraction and payload fraction from Figure 4-8 for a 36,000lb fighter.

$$\frac{W_{FUEL}}{GTOW} = 0.27$$

$$\frac{W_{FUEL} + W_{PL}}{GTOW} = 0.32 \quad \text{and} \quad \frac{W_{PL}}{GTOW} = 0.05$$

Thus:
$$\begin{aligned} \text{Fuel Weight} &= 0.27 \times 36,000 \\ &= 9,720 \text{ lbs} \end{aligned}$$

$$\begin{aligned} \text{Payload} &= 0.05 \times 36,000 \\ &= 1,800 \text{ lbs} \end{aligned}$$

Step 5 - Determine the wetted area from Figure 4-10 for a 36,000lb fighter.

$$\begin{aligned} \text{Since } W_{EMPTY} &= 24,480 \text{ lbs} \\ \text{then } S_{WET} &= 1,920 \text{ ft}^2 \end{aligned}$$

Step 6 - Estimate the internal volume from Figure 4-11 for a 36,000lb fighter, or use the relationship:

$$V = 0.0226 (S_{WET})^{1.453}$$

$$\begin{aligned} \text{Since } S_{WET} &= 1,920 \text{ ft}^2 \\ \text{then Vol} &= 1,332 \text{ ft}^3 \end{aligned}$$

Step 7 - Check estimated volume from Figure 4-12 for a 36,000lb fighter.

$$\text{Since } W_{EMPTY} = 24,480$$

$$\text{then } \frac{\rho_{EMPTY}}{\left(\frac{ULF}{3.75}\right)} = 5.8$$

$$\begin{aligned} \text{where } ULF &= 1.5 \times \text{Max Load Factor} \\ &= 1.5 \times 7.333 \\ &= 11 \end{aligned}$$

$$\begin{aligned} \text{then } \rho_{EMPTY} &= 5.8 \left(\frac{11}{3.75} \right) \\ &= 17.01 \frac{\text{lbs}}{\text{ft}^3} \end{aligned}$$

$$\begin{aligned} \text{For } V_0 &= \frac{W_{EMPTY}}{\rho_{EMPTY}} \\ &= \frac{24,480}{17.01} \\ &= 1,439 \text{ ft}^3 \end{aligned}$$

Step 8 - Average the volume from steps 6 and 7 at this point of the design.

$$\begin{aligned} \text{Hence } V &= \frac{1,332 + 1,439}{2} \\ &= 1,385 \text{ ft}^3 \end{aligned}$$

Step 9 - Re-compute the wetted area from Figure 4-11.

$$S_{WET} = 1,972 \text{ ft}^2$$

Step 10 - Determine fuselage diameter from following relation ships:

$$d = 2 \sqrt{\frac{V}{\pi K_V L}}$$

where $K_V = 0.80$ (Bombers)
 $= 0.70$ (Fighters)
 $= 0.75$ (Transports)

K_V is an empirical constant determined from many aircraft and is based on the derivation that volume can be represented by the relationship:

$$V = K_V \pi R^2 L$$

This is the volume relationship for certain bodies of revolution and ellipsoids.

For $V = 1,385 \text{ ft}^3$
 $L = 55 \text{ ft}$
 $K_V = 0.70$

$$\begin{aligned} \text{then } d &= 2 \sqrt{\frac{1,385}{(3.14)(0.70)(55)}} \\ &= 6.77 \text{ ft} \end{aligned}$$

Step 11 - Compute the fuselage fineness ratio.

$$\begin{aligned} L &= 55 \text{ ft} \\ d &= 6.77 \text{ ft} \\ \frac{L}{d} &= \frac{55}{6.77} \\ &= 8.12 \end{aligned}$$

Step 12 - Check the fuselage fineness ratio from Step 11 with the data contained in Figure 3-3. The computed value should be within the bucket of the drag rise curve at Mach= 1.0. This bucket is located between the values of 8 to 10.5. Hence, the computed value of 8.12 is a reasonable estimate. If the computed value did not fall within the drag bucket, then an average L/d value should be selected and the process reversed to estimate volume and wetted area. The fuselage may initially be represented by a sphere, right circular cone nose, a right circular cylinder for the center-body section, and a cone frustrum for the afterbody. Typical lengths of these components are:

	Fighter	Transport
Nose Section	25%L	10%L
Center Body Section	50%L	70%L
Afterbody Section	25%L	20%L

Step 13 - Estimate wing area from Figure 4-13 for a 36,000lb fighter. Assume a ratio of 4.93 for $\frac{S_{WET}}{S_{WING}}$. Which is representative of the F-16.

$$\text{Since } S_{WET} = 1,972 \text{ ft}^2$$

$$S_{WING} \approx 400 \text{ ft}^2$$

Step 14 - Determine the wing sweep back angle from Figure 4-16 for a cruise Mach number of 0.9.

$$\Lambda_{LE} = 49^\circ$$

Step 15 - Determine the wing aspect ratio from Figure 4-15.

$$AR = 3.0$$

Step 16 - Estimate the maximum L/D from Figure 5-23 at a cruise speed of Mach= 0.9. Values for fighters typically vary from 10 to 11. Select L/D= 11 representative of the F-15 and F-16. The aspect ratio may then be checked using figure 5-21 for a conventionally shaped fighter.

$$AR \approx 3.0$$

The values for aspect ratio from step 15 and 16 compare favorably and one can proceed with the evaluation.

Step 17 - Determine the wing thickness ratio from Figure 4-17 for an AR= 3 wing.

$$\frac{t}{c} = 0.055 \text{ or } 5.5\%$$

Step 18 - Compute the wing loading at take-off.

$$GTOW = 36,000 \text{ lbs}$$

$$S_{WING} = 400 \text{ ft}^2$$

$$\frac{W}{S} = 90 \frac{\text{lbs}}{\text{ft}^2}$$

Step 19 - Determine the span loading from Figure 4-14.

$$AR = 3.0$$

$$\frac{W}{S} = 90 \text{ psf}$$

$$\frac{W}{b^2} = 30 \text{ psf}$$

The span loading may also be computed from the relationship:

$$\frac{W}{b^2} = \frac{\frac{W}{S}}{AR}$$

Step 20 - Determine wing planform from Figure 4-18 for a 36,000lb fighter.

$$b = \sqrt{\frac{GTOW}{\frac{W}{b^2}}} = \sqrt{\frac{36,000}{30}} \quad (\text{from span loading equation})$$

$$= 34.6$$

Assume a wing taper ratio, $\frac{C_T}{C_R} = 0.2$, which is representative for a fighter.

$$C_R = \frac{2S}{b(1+\lambda)} \quad \text{By rearranging equation from Figure 4-18}$$

$$C_R = 19.30\text{ft}$$

$$\text{then } C_T = 3.86\text{ft}$$

A wing planform can now be generated to reflect a wing, $\Lambda_{LE} = 49^\circ$, $C_R = 19.30\text{ft}$, $C_T = 3.86\text{ft}$, and $b = 34.6\text{ft}$.

Step 21 - Determine the size of the horizontal tail using Figure 4-19 and a preliminary 3 view drawing to estimate l_{HT} for a fighter.

$$\text{Since } \bar{c} = \frac{2}{3} \left(C_R + C_T - \frac{C_R C_T}{C_R + C_T} \right)$$

$$= 13.3\text{ft}$$

$$\text{and } \bar{c}S_W = 13.3 \times 400$$

$$= 5,320\text{ft}^3$$

$$\text{then } l_{HT}S_{HT} = 1,450\text{ft}^3$$

$$\text{and } S_{HT} = \frac{1,450}{l_{HT}}$$

If a value for l_{HT} can not be determined, assume the horizontal tail area is 20% of the wing area. This is a nominal value and satisfactory for this stage of the design cycle.

- Step 22 - Determine the size of the vertical tail using Figure 4-20 and a preliminary 3-view drawing to estimate l_{VT} for a fighter.

$$\begin{aligned} bS_W &= 34.6 \times 400 \\ &= 13,840 \text{ ft}^3 \end{aligned}$$

$$\text{then } l_{VT} S_{VT} = 1,070 \text{ ft}^3$$

$$\text{and } S_{VT} = \frac{1,070}{l_{VT}}$$

If a value for l_{VT} can not be determined, assume the vertical is 20% of the wing area. This is a nominal value and satisfactory for this stage of the design cycle.

- Step 23 - Determine the subsonic zero lift drag, C_{D0} , from figure 5-10. Based on other fighter aircraft assume an equivalent skin friction coefficient of 0.004.

$$\begin{aligned} \text{For } S_{WET} &= 1,972 \text{ ft}^2 \\ f &= C_{fe} S_{WET} = C_{D0} S_{REF} \\ f &= 0.004 \times 1,972 \\ &= 7.89 \end{aligned}$$

$$\begin{aligned} \text{then } C_{D0} &= \frac{f}{S_{REF}} \\ &= \frac{7.89}{400} \\ &= 0.0197 \end{aligned}$$

- Step 24 - Determine wing efficiency factor from Figure 5-8.

$$\text{For } AR = 3.0, e = 0.85$$

Step 25 - Determine the maximum lift-to-drag ratio from Figure 5-19 or using the following relationship:

$$\frac{L}{D}_{MAX} = \frac{1}{2\sqrt{C_{D0}K}}$$

$$\text{where } K = \frac{1}{\pi A Re} \\ = 0.125$$

$$\text{and } C_{D0} = 0.0197$$

$$\text{then } \frac{L}{D}_{MAX} = 10.1$$

Step 26 - Determine the transonic drag rise at $M=1.2$ from Figure 5-14.

$$\text{For } L = 55\text{ft}, d_e = 6.77\text{ft}, \frac{t}{c} = 0.055, \Lambda_{LE} = 49^\circ, \text{ then}$$

$$\left[\frac{L}{d_e} \frac{1}{t/c} \frac{\Lambda_{LE}}{57.3} \right]^{\frac{1}{2}} = 11.24$$

$$\text{and from Fig 5-14 } C_{D0 M=1.2} = 2.15 C_{D0 SUBSONIC} \\ = 2.15(0.0197) \\ = 0.042$$

Step 27 - Determine the zero lift drag at Mach 2 from Figure 5-15. Based on other fighter aircraft assume a supersonic equivalent skin friction coefficient of 0.008.

$$\text{For } S_{WET} = 1,972\text{ft}^2 \\ f = 0.008 \cdot 1,972 = 15.77$$

$$\text{and } C_{D0} = \frac{15.77}{400} \\ = 0.039$$

Step 28 - Determine the subsonic lift curve slope from Figure 5-17

For $\Lambda_{LE} = 49^\circ$, $C_R = 19.30ft$, $C_T = 3.86ft$, and $b = 34.6ft$

then $\Lambda_{1/4c} = 42^\circ$ and $AR = 3.0$ and from Fig 5-17

$$\begin{aligned} C_{L\alpha} &= 3.2 \frac{1}{rad} \\ &= 0.056 \frac{1}{deg} \end{aligned}$$

Step 29 - Determine the optimum lift coefficient for cruise flight from the relationships on page 5-29:

$$\begin{aligned} C_{L\ OPT} &= \sqrt{\frac{C_{D0}}{K}} \quad \text{where } K = 0.125 \text{ from step 25} \\ &= \sqrt{\frac{0.0197}{0.125}} \\ &= 0.397 \end{aligned}$$

Step 30 - Determine the $\frac{T}{W}$ ratio for this postulated fighter from figure 3-4. The $\frac{T}{W}$ required at take-off for a highly agile fighter for the maneuverability specified will approach current inventory aircraft. For a $\frac{W}{S} = 90$, assume a minimum requirement of $\frac{T}{W} = 1.0$. This value may have to be iterated if our aircraft does not meet the specified maneuverability goals.

Step 31 - Determine the maximum lift coefficient from figure 6-1.

For $\Lambda_{LE} = 49^\circ$; $C_{L\ MAX} = 1.5$

Step 32 - Determine the take-off distance from Figures 6-4.

For $\Lambda_{LE} = 49^\circ$, $C_{L_{MAX}} = 1.5$, and $\frac{W}{S} = 90 \text{ psf}$

$V_{TO} = 155 \text{ knots}$ from figure 6-3

$$\text{then } \frac{\left(\frac{W}{S}\right)}{\sigma C_{LTO} \left(\frac{T}{W}\right)} = 80$$

where we assume $\frac{T}{W} = 1.0$

and $C_{LTO} = 1.125$ ($C_{LTO} = 75\% C_{LMAX}$)

Take-Off Distance = 1,200 ft

Step 33 - Determine the approximate cruise range at Mach 0.9 and 30,000 ft from Figure 6-7 or the relationship:

$$R = \frac{2.3 V \left(\frac{L}{D}\right)}{SFC} \text{Log} \frac{W_{INITIAL}}{W_{FINAL}}$$

$$R = \frac{1320 M \left(\frac{L}{D}\right)}{SFC} \text{Log} \frac{W_{INITIAL}}{W_{FINAL}}$$

$$\begin{aligned} \text{where } \frac{W_{INITIAL}}{W_{FINAL}} &= \frac{GTOW - 30\%(W_{FUEL})}{GTOW - 70\%(W_{FUEL})} \\ &= \frac{36,000 - (0.3)(9,730)}{36,000 - (0.7)(9,730)} \\ &\approx 1.133 \end{aligned}$$

and $SFC = 1.0$ at $M = 0.9$; $L/D \approx 10.1$; $W_{FUEL} = 9,730 \text{ lbs}$

then $R = 651 \text{ n.m.}$

Step 34 - Determine the sustained "g" capability from Figure 6-12 at Mach 0.9 and 30,000ft or the relationship.

$$n = \sqrt{q \frac{\pi e AR}{W} \left[\frac{T}{W} - \frac{q C_{D0}}{W} \right]}$$

Assume: $\frac{T}{W} = 0.52$ (from Figure 6-14)

$\frac{W}{S} = 77 \text{ psf}$ (50% Fuel load)

$q = 360 \text{ psf}$

$C_{D0} = 0.0197$

$e = 0.85$

$AR = 3.0$

then $n = 4.0g's$

Step 35 - Determine the sustained "g" capability at Mach 0.6 and 10,000ft from Figure 6-11.

Assume: $\frac{T}{W} = 0.84$; $C_{D0} = 0.0197$

$\frac{W}{S} = 77 \text{ psf}$

$q = 367 \text{ psf}$

then $n = 5.34g's$

Step 36 - Determine the sustained "g" capability at Mach 1.5 and 40,000ft from Figure 6-13.

Assume: $\frac{T}{W} = 0.65$; $C_{D0} = 0.041$

$\frac{W}{S} = 77 \text{ psf}$

$q = 616 \text{ psf}$

then $n = 4.54g's$

Step 37 - Determine the turn rate capability at $M=0.6$ and 10,000ft from Figure 6-15.

$$\begin{aligned} V &= Ma \\ &= 0.6(1,073) \\ &= 644 \frac{\text{ft}}{\text{sec}} = 383 \text{ knots} \end{aligned}$$

$$\dot{\theta} = 15.0 \frac{\text{deg}}{\text{sec}} \text{ for } n = 5.34 g's$$

Step 38 - Determine the turn rate capability at $M=1.5$ and 40,000ft from Figure 6-16.

$$\begin{aligned} V &= 1.5(971) \\ &= 1,457 \frac{\text{ft}}{\text{sec}} = 863 \text{ knots} \end{aligned}$$

$$\dot{\theta} = 5.6 \frac{\text{deg}}{\text{sec}} \text{ for } n = 4.54 g's$$

Step 39 - Determine the landing distance from figure 6-2, 6-17 and 6-18. Assume a landing fuel fraction of 10% (for reserves).

$$W_{\text{LAND}} = 36,000 - 0.90(9,720) = 27,252 \text{ lbs}$$

$$\text{then } \frac{W}{S} = \frac{27,252}{400} = 68 \text{ and } C_{L_{\text{MAX}}} = 1.5 \text{ from step 31}$$

$$V_{\text{STALL}} = 116 \text{ knots from Figure 6-2}$$

$$V_{\text{APP}} = 139 \text{ knots from Figure 6-17}$$

$$\text{Landing Ground Distance} = 4500 \text{ feet}$$

assume a typical glide angle of 3° then

$$\text{Landing descent over 50ft} = 950 \text{ feet}$$

$$\text{Total Landing Distance} = 5450 \text{ feet}$$

This completes the preliminary aerodynamic and performance characteristics. The preliminary performance indicates the conceptual aircraft can meet the initial specified goals. The next step is to input the configuration into an aircraft synthesis program and conduct parametric trade-off analysis and sensitivity evaluations to arrive at a more optimum configuration.

8. CONCLUSIONS

This report provides design data and procedures to initially formulate and analyze an aircraft configuration. It is based on an array of data from past military aircraft. Many convenient charts are included to rapidly define pertinent features of a configuration, and to evaluate their impact on the lift and drag characteristics.

The design data and procedures can be used to perform the following tasks:

- Size and shape initial fighter and transport configurations.
- Estimate gross-take-off weight, empty weight and fuel weight.
- Define fuselage fineness ratio and wing geometry.
- Size horizontal and vertical tails
- Estimate aircraft wetted area and volume
- Determine pertinent aircraft configuration parameters such as wing loading, span loading and thrust loading.
- Predict the drag characteristics at subsonic, transonic and supersonic speeds
- Predict lift curve slope across Mach range
- Estimate maximum lift-to-drag ratio
- Assess performance capability of conceptual aircraft

9. REFERENCES

1. Nicolai, Leland M., "Fundamentals of Aircraft Design", METS, Inc, San Diego, CA, 1984.
2. Raymer, Daniel P., "Aircraft Design-A Conceptual Approach" AIAA, Washington D.C., 1989.
3. Rinn, S. "CASP Preliminary Sizing Program Wright Laboratory, Wright-Patterson AFB, Ohio, 1989.
4. Hollowell, S. et al, "Interactive Design and Analysis System", N.A. 82-467, Rockwell International, Los Angeles CA, 1982.
5. Schemensky, R.T., "Development of an Empirically Based Computer Program to Predict The Aerodynamic Characteristics of Aircraft," AFFDL-TR-73-144, Wright- Patterson AFB, Ohio 1973.
6. Ellison, D.E., "USAF Stability and Control Handbook, (DATCOM)", Air Force Flight Dynamics Laboratory, Wright-Patterson AFB, Ohio, Revised 1976.
7. Perkins, Courtland D. and Hage, Robert E., Airplane "Performance, Stability and Control," John Wiley & Sons Inc, September 1954.
8. Wood, K.D., "Aircraft Design", Johnson Publishing Co., Boulder, Colorado, 1966.
9. Roskam, J., "Airplane Design", Parts I to VIII, Roskam Aviation & Engineering Corp., Ottawa, Kansas, 1989.
10. Genston, W., "The Encyclopedia of World Air Power," Crescent Book, Crown Publishers, Inc., 1986.
11. Taylor, U.W.R., "Janes All The World Aircraft," Janes Publishing Co, London, England, 1984.
12. Aviation Week & Space Technology, "1992 Aerospace Forecast," Vol, 136, No. 11, New York, N.Y. March 16, 1992.
13. Coming, Gerald, "Airplane Design", Edwards Brothers, Inc, Ann Arbor, Michigan, 1953.
14. Caddell, W.E., "On the Use of Aircraft Density In Preliminary Design", SAWE Paper No. 813, 5 May 1969.
15. Abbot, I.H., "Theory of Wing Sections," Dover Publications, Inc., 1959.

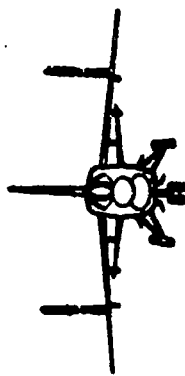
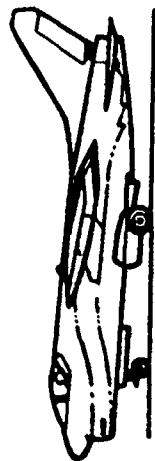
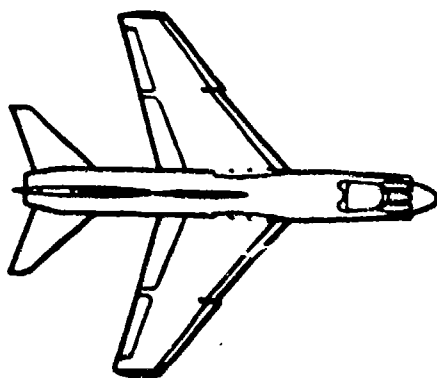
16. Abbot, I.W., "Characteristics of Wing Sections," NACA TR 824, 1945.
17. Jones, R.T., "Properties of Low Aspect Ratio Wings", NACA TR-835, 1946.
18. Johnson, M.E., "Design and Analysis of Maneuver Wing Flaps at Supersonic Speeds," NASA CR-3939, 1985.
19. Hoerner, S.F., Fluid Dynamic Drag," Midland Park, New Jersey, 1965.
20. Ely, W.E. et al, "Prediction of Aircraft Drag Due to Lift," Air Force Flight Dynamics Laboratory, AFFDL-TR-71-84, Wright-Patterson AFB, Ohio, June 1971.
21. Gollos, W.W., "Transonic and Supersonic Pressure Drag for a Family of Parabolic Type Fuselages at Zero Angle of Attack," Rand RM 982, 1952.
22. Morris, D.N., "A Summary of the Supersonic Pressure Drag of Bodies of Revolution", Journal of Aeronautical Sciences, Vol, 28, July 1961.
23. Nelson & Welsh, "Application of the Transonic & Supersonic Area Rule to the Prediction of Wave Drag," NASA TN D-446, September 1960.
24. Mirels, H., "Aerodynamics of Slender Wings and Wing Body Combinations Having Swept Trailing Edges", NACA TN-3105, 1954.
25. Hall, C.F., "Lift, Drag and Pitching Moment of Low Aspect Ratio Wings," NACA RM A53A30, 1958.
26. Carlson, H.W. and Mann, M.J., "Survey and Analysis of Research on Supersonic Drag-Due-To-Lift Minimization with Recommendations for Wing Design," NASA Tech Paper 3202, 1992.
27. Harris, R., "An Analysis and Correlation of Aircraft Wave Drag," NASA TM X-947, 1964.
28. May, F. and Widdison, C.A., "STOL High Lift Design Study" AFFDL TR-71-26, Wright Patterson AFB, Ohio, April, 1971.
29. Bonner, E. and Gingrich, P., "Supersonic Cruise/Transonic Maneuver Wing Section Development Study," AFWAL-TR-80-3047, Wright Patterson AFB, Ohio 1979.
30. Carlson, H. and Miller, D., "Numerical Methods for the Design and Analysis of Wings at Supersonic Speeds," NASA TN D-7713, 1947.

31. Miller, D., "Supersonic Wing Design Concepts Employing Non-Linear Flows," 14th ICAS Proceedings, 1984.
32. Miller, D. and Schemensky, R., "Design Study Results of a Supersonic Cruise Fighter Wing", AIAA Paper 79-0062 1979.
33. Etkins, Bernard, "Dynamics of Atmospheric Flight," John Wiley & Sons, 1972.
34. Rutowski, E.S., "Energy Approach to the General Aircraft Performance Problem," Journal of Aeronautical Sciences, March 1954.
35. Bryson, A.E. and Desai, M.N. "Energy State Approximation in Performance Optimization of Supersonic Aircraft", Journal of Aircraft, Vol. 6, November 1969.

APPENDIX A

Representative Operational and Advanced Configurations

This appendix is composed of 3-view drawings of several current and advanced military aircraft. Each drawing contains the wing area, span, length gross take-off weight and maximum speed. It is to illustrate the size and shape of aircraft configurations based on specific performance requirements.

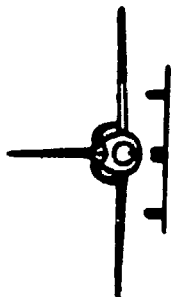
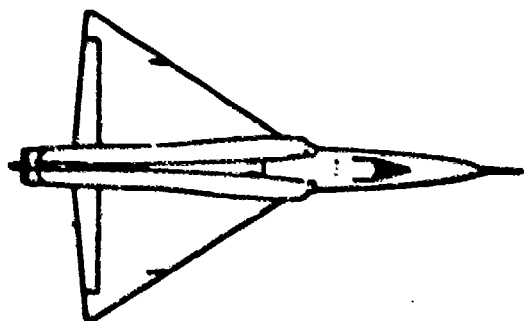


A-7D

Wing Area-----357 sq ft
 Span-----38.7 ft
 Vmax-----570 kts (0.88 M#)

Length-----46.1 ft
 TOGW-----39300 lbs

FIGURE A-1 A-7D Fighter Configuration



F-106A

Wing Area-----697.8 sq ft

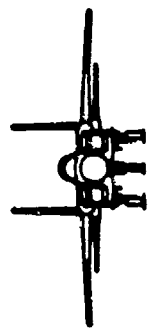
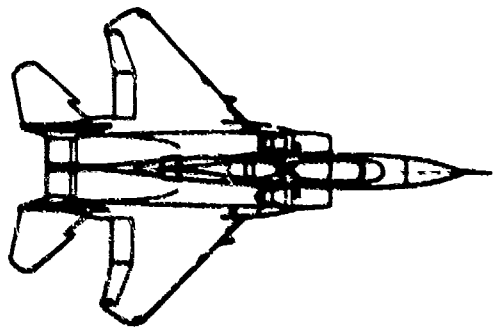
Span-----38.3 ft

Vmax-----1153 kts (2.0 M#)

Length-----70.7 ft

TOGW-----36700 lbs

FIGURE A-2 F-106 Fighter Configuration

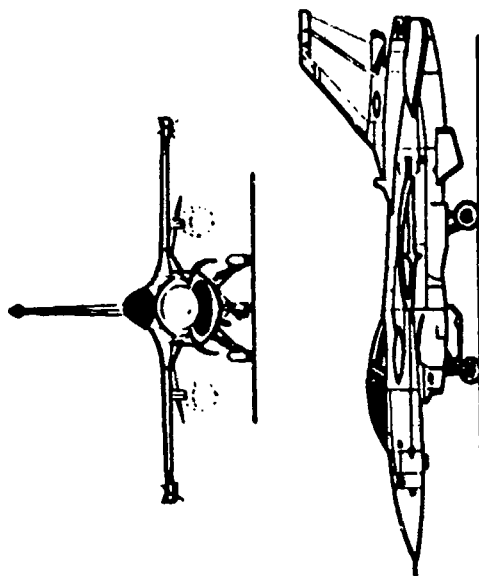
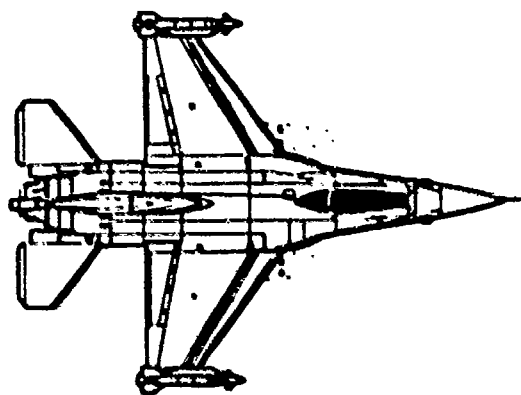


F-15

Wing Area-----608 sq ft
 Span-----42.8 ft
 Vmax-----1400 kts (2.5 M#)

Length-----63.7 ft
 TOGW-----40000 lbs

FIGURE A-3 F-15 Fighter Configuration

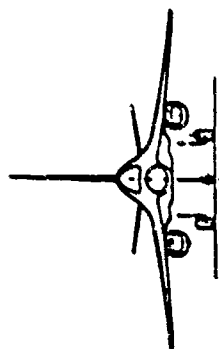
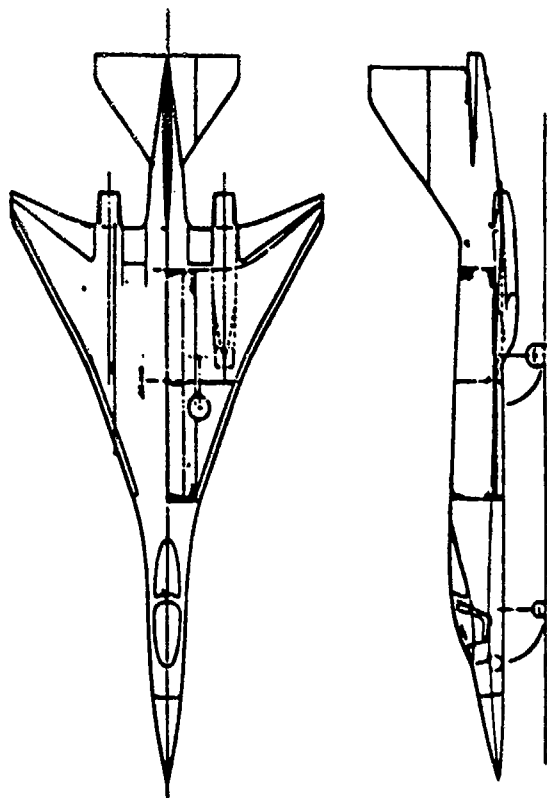


F-16C

Wing Area-----300 sq ft
 Span-----32.8 ft
 Vmax-----1170 kts (2.0 M#)

Length-----49.3 ft
 TOGW-----32000 lbs

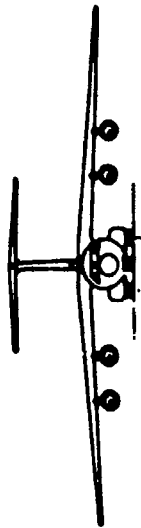
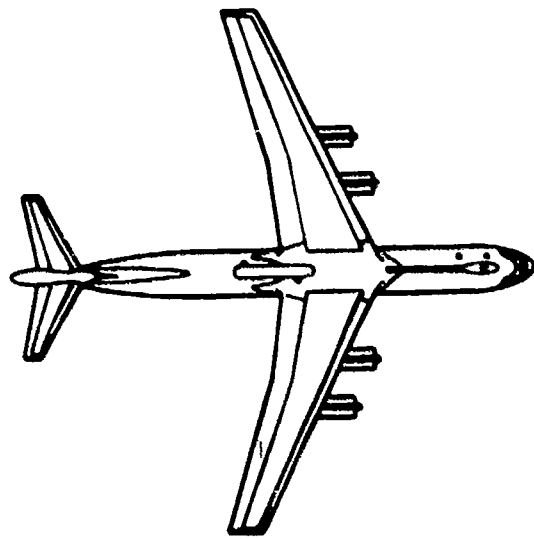
FIGURE A-4 F-16 Fighter Configuration



Advanced Fighter

Wing Area-----	655 sq ft	Length-----	77.5 ft
Span-----	36.2 ft	TOGW-----	50000 lbs
Vmax-----	1400 kts (2.5 M#)		

FIGURE A-5 Advanced Supersonic Fighter Configuration

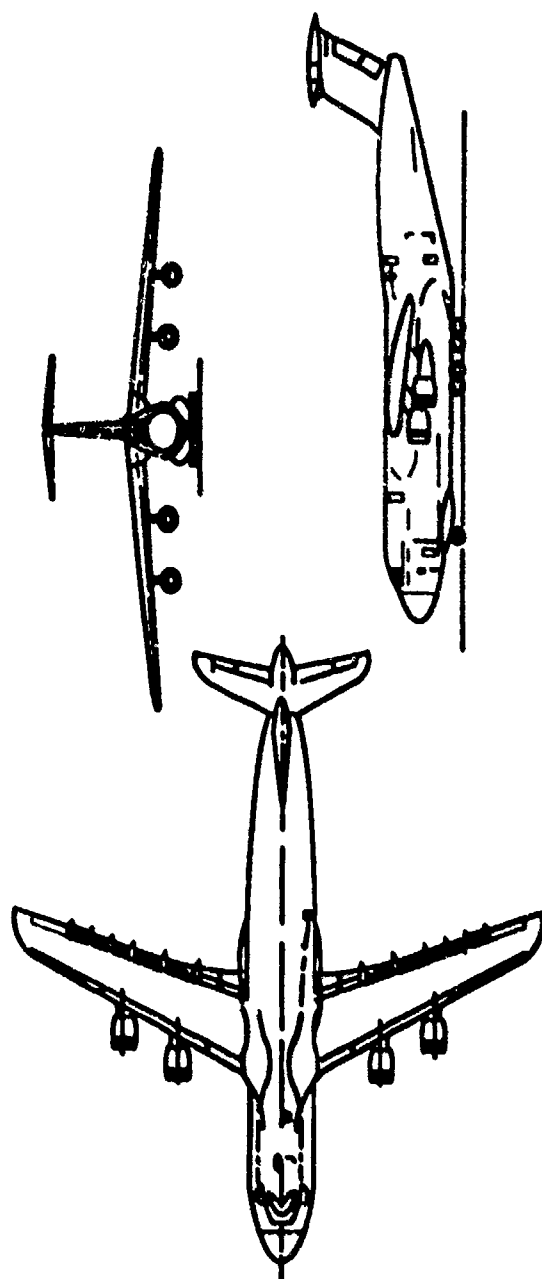


C-141B

Wing Area-----3228 sq ft
Span-----160 ft
Vmax-----493 kts (0.82M#)

Length-----168.4 ft
TOGW-----296000 lbs

FIGURE A-6 C-141 Transport Configuration

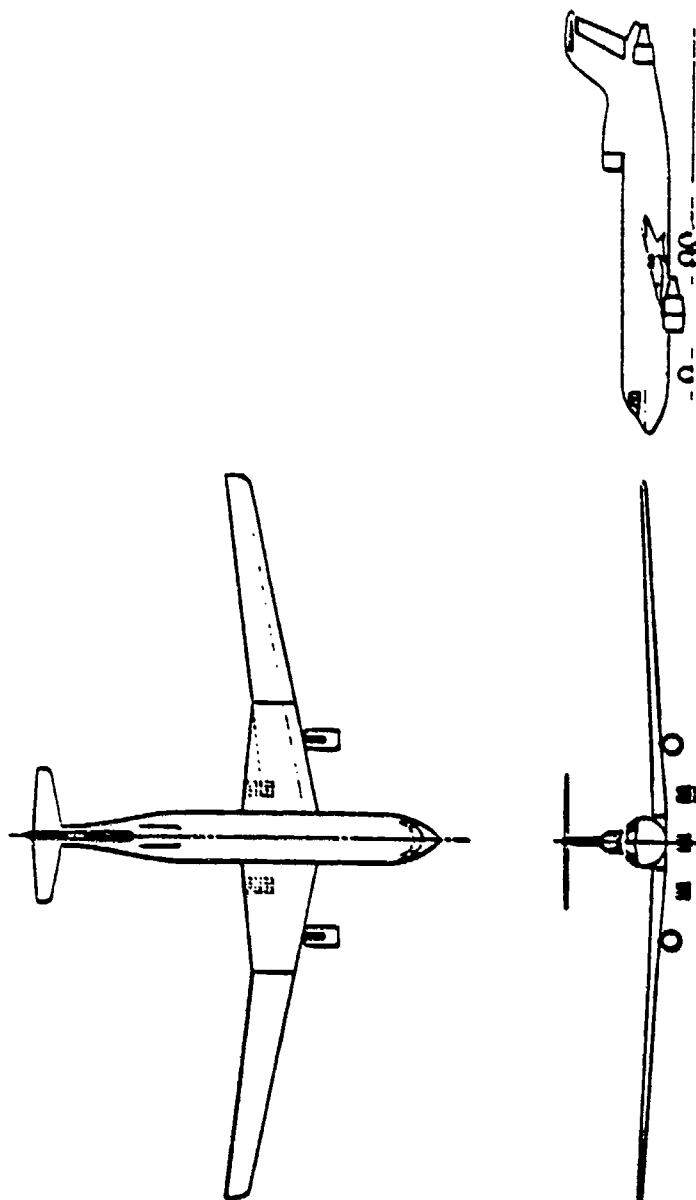


C - 5B

Wing Area-----6200 sq ft
 Length-----247.8 ft
 Vmax-----495 kts (0.82 M#)

Span-----222.7 ft
 TOGW-----767,000 lbs

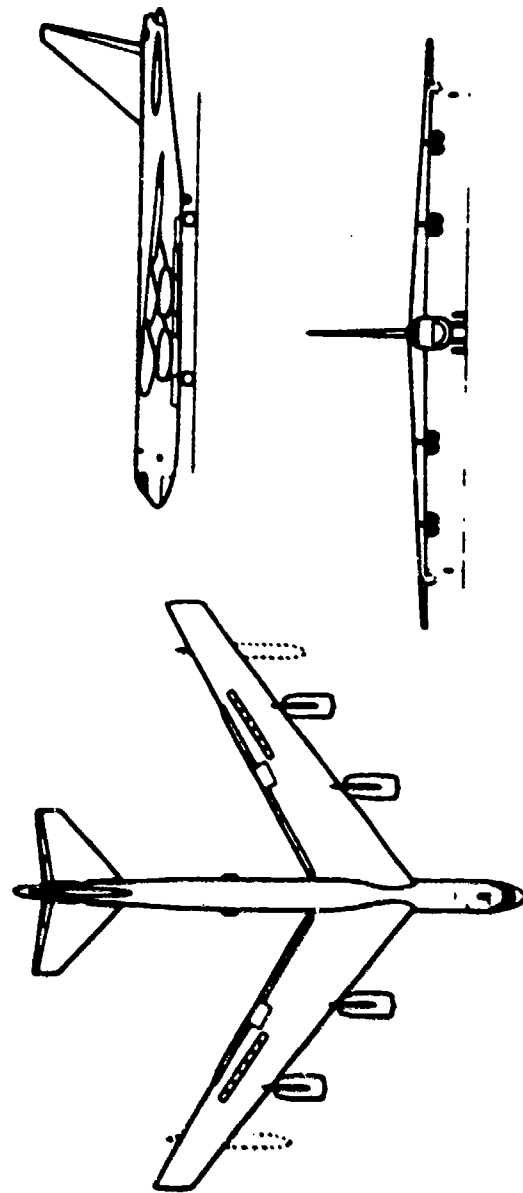
FIGURE A-7 C-5 Transport Configuration



Advanced Transport

Wing Area-----	1900 sq ft	Length-----	102 ft
Span-----	175 ft	TOGW-----	168000 lbs
Vmax-----	436 kts (0.75 M#)		

FIGURE A-8 Advanced Transport Configuration



B-52F

Wing Area-----	4000 sq ft	Length-----	156.5 ft
Span-----	185 ft	TOGW-----	450000 lbs
Vmax-----	550 kts (0.90 M#)		

FIGURE A-9 B-52 Bomber Configuration

APPENDIX B VOLUME AND AREA RELATIONSHIPS

This appendix provides a number of mathematical equations to compute the volume and wetted area of several simple shapes. They can be quickly used to check the volume and area of defined configurations.

1. Sears-Haack Body

$$V = \frac{3}{16} \pi^2 R^2 L$$

$$S_{WET} = 1.867 \sqrt{LV} = 1.27 dL$$

2. Ellipsoid

$$V = \frac{2}{3} \pi R^2 L$$

3. Von Karman Ogive

$$V = \frac{1}{2} \pi R^2 L$$

4. Prolate Spheroid

$$V = \frac{4}{3} \pi a b^2 \quad \text{where:} \quad \begin{array}{l} a = \text{major axis} \\ b = \text{minor axis} \end{array}$$

5. Sphere

$$V = \frac{4}{3} \pi R^3$$

$$S_{WET} = 4 \pi R^2$$

6. **Right Cone**

$$V = \frac{\pi}{3} R^2 L$$

$$S_{WET} = \pi R \sqrt{R^2 + L^2} \quad (\text{Curved Surface})$$

7. **Right Cylinder**

$$V = \pi R^2 L$$

$$S_{WET} = 2\pi R L \quad (\text{Curved Surface})$$

8. **Cone Frustrum**

$$V = \frac{\pi L}{3} (R_1^2 + R_1 R_2 + R_2^2)$$

$$S_{WET} = \pi (R_1 + R_2) \sqrt{L^2 + (R_1 - R_2)^2} \quad (\text{Curved Surface})$$

Where: R_1 = Radius of Base
 R_2 = Radius of Top
 L = Length

9. **Formulas for Sears-Haack body of revolution shapes, volume and drag**

The factor d/L is the fineness ratio, diameter/length.

Case I: Given length, given volume

$$\left(\frac{r}{r_0} \right)^2 = \left(\sqrt{1-x^2} \right)^3$$

$$\text{Volume} = \frac{3}{16} \pi^2 L r_0^2$$

$$C_D = \frac{9}{8} \pi^2 \left(\frac{d}{L} \right)^2$$

Case II: Given length, given diameter

$$\left(\frac{r}{r_0}\right)^2 = \sqrt{1-x^2} - x^2 \cosh^{-1}\left(\frac{1}{x}\right)$$

$$Volume = \frac{1}{6} \pi^2 L r_0^2$$

$$C_D = \pi^2 \left(\frac{d}{L}\right)^2$$

Case III: Given diameter, given volume

$$\left(\frac{r}{r_0}\right)^2 = 3\sqrt{1-x^2} - 2\left(\sqrt{1-x^2}\right)^3 - 3x^2 \cosh^{-1}\left(\frac{1}{x}\right)$$

$$Volume = \frac{1}{8} \pi^2 L r_0^2$$

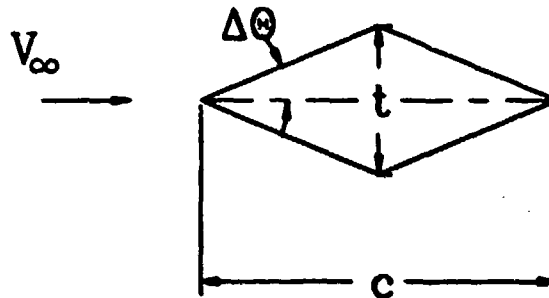
$$C_D = \frac{3}{2} \pi^2 \left(\frac{d}{L}\right)^2$$

APPENDIX C WINGS IN SUPERSONIC FLOW

Based on linear, two dimensional (2-D) supersonic flow theory (References 5 and 6), the pressure coefficient in supersonic flow can be related to the flow turning angle, $\Delta\theta$, such that

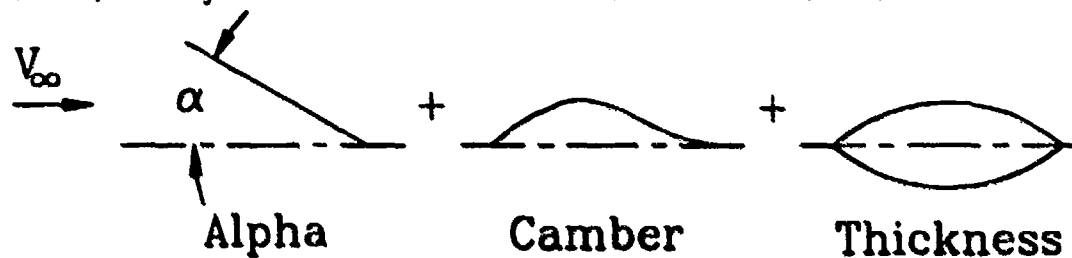
$$C_P = \frac{\pm 2\Delta\theta}{\sqrt{M^2 - 1}} \quad (C-1)$$

where $\Delta\theta$ is illustrated in sketch A.



SKETCH A

A 2-D airfoil at angle of attack can be represented by a flat plate at angle of attack, a mean camber line, and a symmetric thickness distribution as indicated in sketch B below.



SKETCH B

Integration of the pressure from equation (C-1) in the drag direction yields

$$C_{D_{WAVE}} = \frac{C_L^2 \sqrt{M^2 - 1}}{4} + \frac{4}{\sqrt{M^2 - 1}} [K_2 + K_3] \quad (C-2)$$

for the three components of alpha, camber, and thickness respectively. The second part of this

equation is the profile wave drag due to camber and thickness. The minimum profile drag occurs for a symmetrical wedge shape, and results in $K_2 = 0$ and $K_3 = (t/c)^2$ so that

$$C_{D_{WAVE}} = \frac{C_L^2 \sqrt{M^2 - 1}}{4} + \frac{4}{\sqrt{M^2 - 1}} \left(\frac{t}{c} \right)^2 \quad (C-3)$$

The first term is the wave drag due to lift and is somewhat similar to subsonic induced drag. The second term is the wave drag due to thickness and indicates the extreme importance of keeping wings thin on supersonic aircraft. The dependence on Mach number is also indicated in the equations.

The wave drag due to lift term from equation C-3 can be expressed as

$$C_{D_{WAVE}} = K C_L^2 \quad \text{where } K = \frac{1}{C_{L_\alpha}} \text{ for } M > 1$$

The above expression is often used as an asymptotic limit for wings at higher Mach numbers.

Integration of the pressure in equation C-1 in the lift direction yields

$$C_L = \frac{4\alpha}{\sqrt{M^2 - 1}} \quad (C-4)$$

or

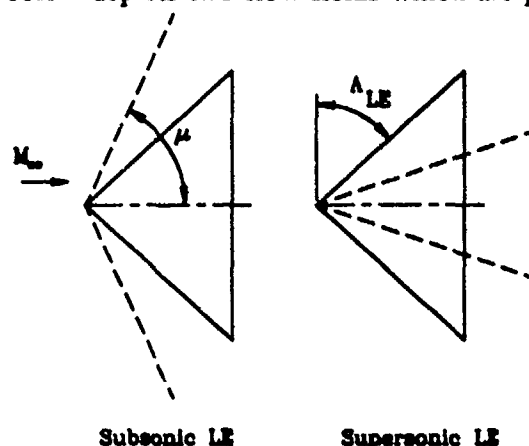
$$\frac{dC_L}{d\alpha} = C_{L_\alpha} = \frac{4}{\sqrt{M^2 - 1}} = \frac{4}{\beta}$$

If we ignore friction drag we can combine the equation for C_L and C_D , form C_L/C_D , differentiate and establish the maximum (L/D) ratio for a 2-D wedge

$$\left(\frac{L}{D} \right)_{MAX} = \frac{1}{2 \left(\frac{t}{c} \right)^2} \quad (C-5)$$

which once again indicates the importance of thin shapes at supersonic speeds.

The drag relationship developed in equations C-2 and C-3 apply to 2-D airfoils in supersonic flow. For a 3-D wing with sweepback a slightly more complicated flow field requires additional considerations. Sketch C below depicts two flow fields which are possible



SKETCH C

In sketch C μ is the Mach angle $\mu = \sin^{-1} \frac{1}{M_\infty}$ and Λ_{LE} is the wing leading edge sweep. Wings with subsonic leading edges have chordwise pressure distributions similar to subsonic wings, whereas wings with supersonic leading edges have loadings predicted by equation C-1. The equation for determining which condition exists is

$$\begin{aligned} \sqrt{M^2 - 1} \cot \Lambda_{LE} &\geq 1 && \text{SUPERSONIC} \\ \sqrt{M^2 - 1} \cot \Lambda_{LE} &< 1 && \text{SUBSONIC} \end{aligned} \quad (C-6)$$

with $\beta = \sqrt{M^2 - 1}$ and $\epsilon = 90^\circ - \Lambda_{LE}$ this is sometimes written as

$$\begin{aligned} \beta \tan \epsilon &\geq 1 && \text{SUPERSONIC} \\ \beta \tan \epsilon &< 1 && \text{SUBSONIC} \end{aligned}$$

The wave drag of uncambered and untwisted trapezoidal wings can be estimated by

$$C_{D_{WAVE}} = \frac{K}{\beta} \left(\frac{t}{c} \right)^2 \quad \text{FOR } \beta \cot \Lambda_{LE} \geq 1$$

$$= K \tan \epsilon \left(\frac{t}{c} \right)^2 \quad \text{FOR } \beta \cot \Lambda_{LE} < 1$$

with

$K = 16/3$ for biconvex airfoils

$K = 4$ for double wedge airfoils

Note that the upper expression is identical to the 2-D wedge shape in equation C-3.

The above expressions are for ballpark estimates only and do not capture many of the finer details that determine wing wave drag. Leading edge bluntness, aspect ratio, camber and location of maximum thickness are all important parameters which can significantly effect wing wave drag.

Referring to Figure C-1 the following observations are made. Above $\beta \cot \Lambda_{LE} \geq 1$ where the wing leading edge is supersonic the drag is shown to be a strong function of the chordwise location of maximum thickness, "b" in Figure C-1, and approaches the (2-D) symmetric wedge value given by equation C3 ($C_L = 0$) at higher Mach numbers. The curve is altered between $\beta \cot \Lambda_{LE} > 1$ and an abscissa value that represents the sweep of line of the maximum thickness. For example, for $b=0.3$ this value $\beta \cot \Lambda_{LE} = 0.7$ which represents where the sweep angle Λ_{uc} becomes subsonic in an analogous manner to the leading edge. At lower Mach numbers the location of optimum chordwise thickness reverses and minimum drag is represented by more forward thickness distributions characteristic of subsonic flows.

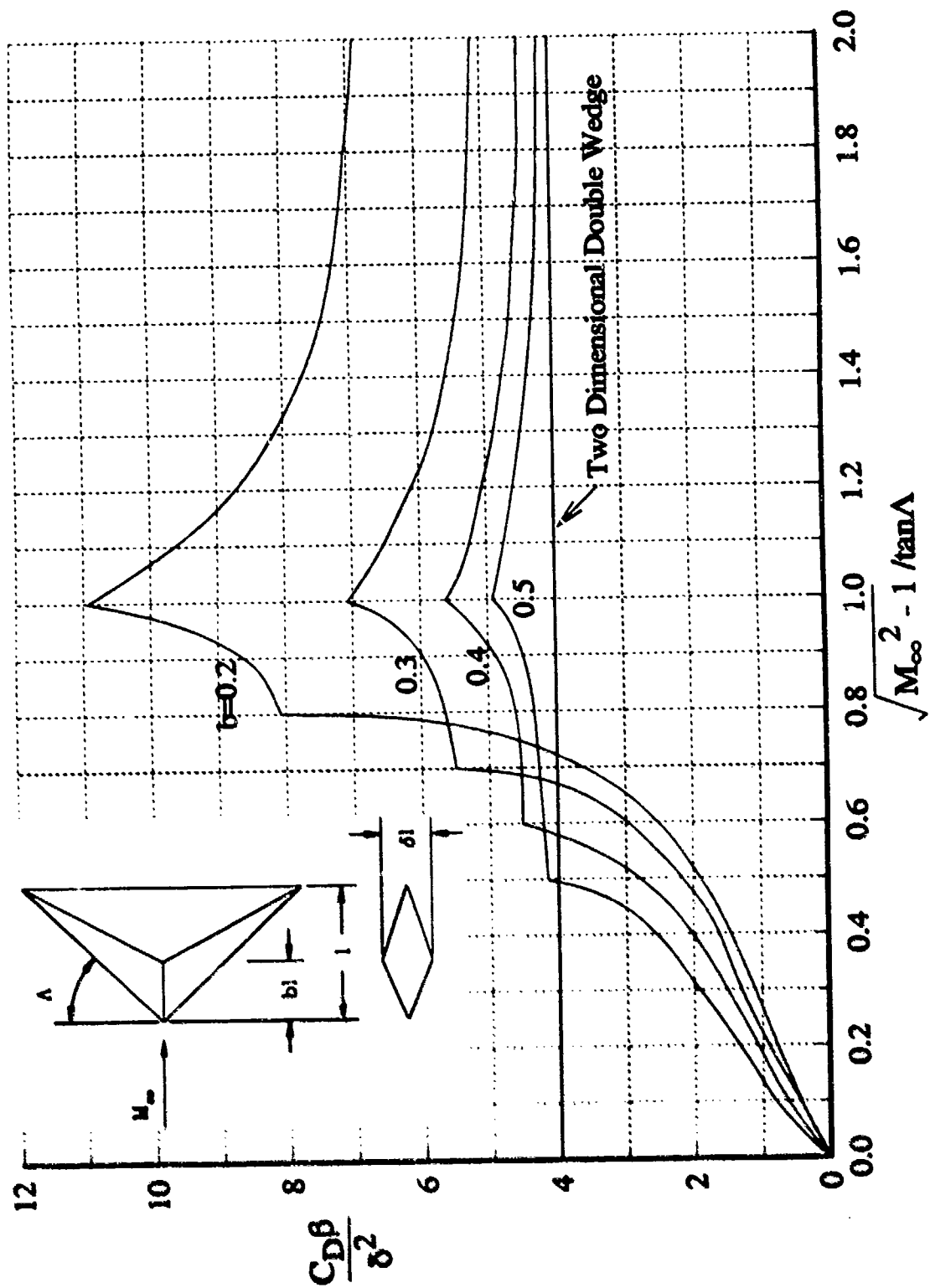


FIGURE C-1 Arrowhead Wings With Double-Wedge at Zero incidence